FACULTY OF TECHNOLOGY

CONSEQUENCE MODELLING OF A HYDROGEN EXPLOSION IN A COMPRESSOR SHELTER

Jaana Larionova

DEGREE PROGRAMME IN PROCESS ENGINEERING

Master's Thesis

November 2019

FACULTY OF TECHNOLOGY

CONSEQUENCE MODELLING OF A HYDROGEN EXPLOSION IN A COMPRESSOR SHELTER

Jaana Larionova

Supervisors: D.Sc. (Tech.) Juha Ahola
D.Sc. (Mech.) Johanna Vaittinen
M.Sc. (Eng.) Amélie Majorin
M.Sc. (Eng.) Irmeli Vauhkonen

DEGREE PROGRAMME IN PROCESS ENGINEERING
Master's Thesis
November 2019

TIIVISTELMÄ
OPINNÄYTETYÖSTÄ Oulun yliopisto Teknillinen tiedekunta

Koulutusohjelma (kandidaatintyö, diplomityö) Prosessitekniikka		Pääaineopintojen ala (lisensiaatintyö)	
Tekijä Larionova, Jaana		Työn ohjaaja yliopistolla Ahola Juha, TkT	
Työn nimi Consequence modelling of a hydrogen explosion in a compressor shelter			
Opintosuunta Teollinen tuotantotalous	Työn laji Diplomityö	Aika Marraskuu 2019	Sivumäärä 100 s., 4 liitettä

Tiivistelmä

Tämän työn tarkoituksena oli mallintaa FLACS-ohjelmistolla kompressorihallissa tapahtuva merkittävä vetyvuoto ja sen jälkisyttymisestä aiheutuvat ylipainevaikutukset. Mallintaminen suoritettiin yhteensä kolmelle eri tapaukselle: Model1 mallinnusalue kattoi kompressorihallin ja ympäröivän ympäristön ilman prosessilaitteita ja rakennuksia, Model2 mallinnusalue kattoi kompressorihallin lisäksi dieseltuotetta tuottavan yksikön sekä keskusvalvomorakennuksen ja Model3 alue kattoi kompressorihallista 100 metrin säteen sisällä olevan prosessialueen. Jokaisessa tapauksessa oli sama mallinnuspinta-ala, laskentaverkko sekä lähtötiedot/parametrit.

Ensiksi mallinnettiin vetyvuoto (dispersiosimulointi), jossa tarkasteltiin kahden eri Pasquill sääolosuhteen (2F ja 5D) ja kolmen eri tuulensuunnan vaikutusta kaasupilven muodostukseen ja leviämiseen kompressorihallissa ja sen ympäristössä. Saatujen tulosten perusteella valittiin jokaisen mallin kohdalla se dispersioskenaario, jossa muodostui suurin (syttymiskelpoisen pilven massa ja tilavuus) syttymiskelpoinen kaasupilvi. Seuraavaksi tälle kaasupilvelle simuloitiin vetykaasun räjähdysskenaario. Räjähdyssimuloinnissa selvitettiin merkittävimmät ylipainevaikutukset sekä paineimpulssit ja syttymispisteiden vaikutusta muodostuviin ylipaineisiin. Räjähdyksen ylipainevaikutuksia ja impulssia monitoroitiin mallinnusalueen eri kohdissa (mm. läheinen prosessialue ja keskusvalvomorakennus). Näissä määritettiin maksimiylipaineet ja paineimpulssit, joita mitattiin eri kohdin mallinnusaluetta. Räjähdyssimuloinnissa käytettiin stoikiometrista kaasupilveä, joka perustui konservatiiviseen Q8 pilven tilavuuteen. Räjähdyssimulointeja tehtiin myös Q9-pilvillä, joka on vähemmän konservatiivinen pilvityyppi FLACS työkalussa. Räjähdyssimuloinneista kunkin tapauksen kohdalla ääritapausskenaarioksi valittiin se tapaus, jossa muodostui suurimmat ylipainevaikutukset sekä paineimpulssit.

Työssä käytetyn FLACS-ohjelman avulla osoitettiin, että syttymispisteiden sijainnin ja estetiheyden lisäksi myös syttymiskelpoisen pilven massalla on merkittävä vaikutus kaasupilviräjähdyksen ylipainevaikutuksen suuruuteen. Maksimiylipaineet mitattiin kompressorihallissa mallinnusskenaarioissa Model2 (4.4 bar(g)) ja Model3 (3.7 bar(g)). Paineimpulssit olivat näissä tapauksissa 4770 Pas (Model2) ja 4400 Pas (Model3). Syttymiskelpoisen pilven massa ja tilavuus olivat 140 kg ja 7500 m^3 (Model2) sekä 138 kg ja 7400 m^3 (Model3). Valvomorakennukseen kohdistuvat maksimiarvot mitattiin mallinnusskenaariossa Model1 (0.5 bar(g) ja 1650 Pas), jossa syttymiskelpoisen pilven massa ja tilavuus olivat 160 kg ja 8200 m^3.

Tämä työ osoitti, että ekvivalenttisen stoikiometrisen pilven valinnalla (Q8 ja Q9) on erittäin merkittävä vaikutus ääritapausskenaarion valinnassa, sillä ääritapausskenaario vaihteli pilvestä riippuen. Vetykaasupilviräjähdys kompressorihallissa voi aiheuttaa suuronnettomuuden, joka aiheuttaa vakavia henkilövahinkoja, merkittäviä laite- ja rakennevaurioita, tuotannon keskeytymisen sekä huomattavia taloudellisia tappioita.

Avainsanat: Kaasupilviräjähdys, VCE, Vety, FLACS, Dispersiosimulointi, Kompressorihalli, Q8, Q9.

Muita tietoja

ABSTRACT
FOR THESIS

University of Oulu Faculty of Technology

Degree Programme (Bachelor's Thesis, Master's Thesis) Degree programme in process engineering		Major Subject (Licentiate Thesis)	
Author Larionova, Jaana		Thesis Supervisor Ahola Juha, D.Sc (Tech.)	
Title of Thesis Consequence modelling of a hydrogen explosion in a compressor shelter			
Major Subject Industrial Engineering	Type of Thesis Master's Thesis	Submission Date November 2019	Number of Pages 100 p., 4 App.

Abstract

The aim of this study was to model the overpressure effects of a vapour cloud explosion from a significant hydrogen leakage in a compressor shelter. Modelling was performed with the FLACS software for three different cases: Model1, Model2 and Model3. Model1 covered only the compressor shelter, and its surroundings without process equipment and buildings. Model2 included the compressor shelter, surrounding diesel producing unit and a control building. Model3 included the process area with a radius of 100 metres from the compressor shelter. Each model had the same modelling area, computational mesh (grid), and scenario settings in FLACS.

The hydrogen leakage was modelled (dispersion simulation) to examine the effects of two Pasquill weather conditions (2F and 5D) and three different wind directions on the formation and dispersion of a vapour cloud. Based on the results, the worst case dispersion scenario was chosen for each model. The dispersion scenario with the largest flammable vapour cloud (volume and mass) was chosen. Explosion simulations were performed with an equivalent stoichiometric gas cloud based on the volume of the conservative Q8 cloud. Explosion simulations were also run with Q9 clouds which are less conservative than Q8 clouds. The worst case scenario was selected for each case based on the highest overpressure and pressure impulse. Build up overpressures and pressure impulses were measured with monitor points located at several places throughout the model (e.g. nearby process area and control building). The locations of the monitor points remained the same in each model.

The FLACS software used in this study showed that not only the location of the ignition points and volume of the blockage ratio but also the mass of a flammable vapour cloud have a significant effect on the magnitude of the explosion overpressures and pressure impulses. The maximum overpressures were measured in the compressor shelter in Model2 (4.4 bar(g)) and Model3 (3.7 bar(g)) with pressure impulses of 4770 Pas (Model2) and 4400 Pas (Model3). The masses of the flammable vapour clouds were 140 kg in Model2 (cloud volume 7500 m^3) and 138 kg in Model3 (cloud volume 7400 m^3). The maximum values measured at the control building were in Model1 (0.5 bar(g) and 1650 Pas) where the mass and volume of the flammable vapour cloud were 160 kg and 8200 m^3.

This work also showed that the choice of an equivalent stoichiometric gas cloud has a very significant influence on worst case scenario selection since overpressures and pressure impulses varied according to the cloud volume (significantly higher overpressure effects in Q8 cloud than in Q9 cloud). A hydrogen vapour cloud explosion in a compressor shelter can cause a major accident with severe personal injuries, major equipment and structural damage, production interruption and significant financial damage.

Keywords: Vapour cloud explosion, VCE, FLACS, Dispersion simulation, compressor shelter, Q8, Q9

Additional Information

ACKNOWLEDGEMENTS

This Master's Thesis has been implemented between January and August 2019 at Neste Engineering Solutions in the department of Process Design. The purpose of this work was to model a hydrogen leakage and subsequent vapour cloud explosion in the compressor shelter using the FLACS CFD tool. In addition, the effect of a volumetric blockage ratio on the resulting explosion overpressures and pressure impulses was examined.

I want to thank my supervisor from the University D. Sc. Juha Ahola for the feedbacks and guiding my work. From Neste Engineering Solutions, I want to thank Project HSE Manager M. Sc. Amelie Majorin for efficient guidance and for the support during this work. I want especially thank Process Modelling Manager D. Sc. Johanna Vaittinen for the support particularly during modelling and for guidance. My big compliments to Manager, Project HSE Management, M. Sc. Irmeli Vauhkonen for an interesting and unique opportunity and for the guidance and support during this work. A modelling of a hydrogen leakage and a vapour cloud explosion with the FLACS CFD tool during the spring and summer of 2019 provided me with valuable experience and knowledge in modelling and HSE aspects. I would also like to thank my superior M. Sc. Hannu Relander for the support and System Manager Mikko Hanski for creating the 3D modelling area. Also big compliments to Chief Training Engineer and FLACS Commercial Product Manager Franz Zdravistch for the FLACS 1 course, and for assisting with the modelling, and Gexcon technical support for the quick and comprehensive help with the modelling.

My greatest compliments go to my parents and my sister for always believing in me and supporting me throughout my study. In particular, I want to thank my mom for the support and encourage through the most difficult times. Big compliments to my lovely 'Prosen Tiput' for the unforgettable and laugh-filled moments at the university and free time. Your support and encouragement, as well as the meetings of the 'munkkikerho', have been the best part of my study time. I also want to thank 'Neitoset' for the support and unforgettable domestic travels. Finally, it is my turn to graduate as a Master of Science (M. Sc.) in Engineering.

TABLE OF CONTENTS

SYMBOLS AND ABBREVIATIONS

L	Characteristic dimension of the geometry
$\dot{m}$	Mass flow rate
P	Pressure
Re	Reynolds number
u	Flow velocity
ν	Kinematic viscosity of the fluid
AIT	Auto ignition temperature
CV	Control Volume
FLAMkg	Mass of a flammable vapour cloud
LFL	Lower flammability limit
MIE	Minimum ignition energy
Q8	Equivalent stoichiometric vapour cloud (for enclosed situations)
Q9	Equivalent stoichiometric vapour cloud (for well-vented situations)
UFL	Upper flammability limit
VCE	Vapour cloud explosion

1 INTRODUCTION

In the chemical and petrochemical industries flammable liquids and gases are constantly processed and thus a risk of an explosion exists. Explosion Consequences caused by flammable vapour clouds are generally destructive and pose a high risk in particular in industrial areas. (Pekalski *et al.* 2005) The severity of a vapour cloud explosion (VCE) varies depending on e.g. a fuel, a mass of a flammable vapour cloud and a degree of congestion and confinement in the area of a vapour cloud. An explosion in an open space does not cause similar overpressures as an explosion occurring in a partly confined area. Worst case scenarios are developed to illustrate the existing hazard, evaluate the possible consequences and to highlight preventive measures. One way has been to use modelling programmes that predict overpressures generated by explosions. (Bjerkedvedt *et al.* 1997)

The most dangerous vapour cloud explosions occur in the partly confined or confined areas where the overpressures can rise to very high measures only in a few milliseconds. Modelling of partly confined areas has been challenging as the objects in the area cause turbulence. Turbulence is generally a very complex phenomenon that cannot be modelled by all software. Programmes suitable for modelling those areas are generally very expensive and require a lot of computing power. (Bjerkedvedt *et al.* 1997)

In the offshore industry it has already been a long-standing practice to model vapour cloud explosions in different areas using Computation Fluid Dynamics (CFD) based modelling software. CFD modelling programmes use numerical methods and algorithms to analyse problems involving fluid flows. One of the commonly used CFD software used in safety analyses is FLACS developed by the Norwegian company GexCon. FLACS is used to model dispersions, fires and explosions in both open and confined geometries. It is widely used in the oil, gas and process industries. It has a 3D feature that enables more accurate predictions of the consequences. (Bjerkedvedt *et al.* 1997)

The main objective of this study was to model partly confined hydrogen vapour cloud explosions in three different models with different volume blockage ratios. The modelling was done with FLACS v10.8 software. The preparation of a 3D CAD model was made with MicroStation v8i and it was imported to FLACS. Simulations were run for dispersions and consequently for vapour cloud explosions. With dispersion simulations, the objectives were to estimate

1. Formed volume of flammable vapour cloud from the flange leak
2. Masses of the flammable material in formed vapour clouds;

and with vapour cloud explosion simulations to estimate

1. Overpressure peaks
2. Pressure impulse peaks.

The same case has previously been modelled with PHAST. Software used in Neste Engineering Solutions Oy. PHAST is based on analytical methods. It has certain limitations that do not make it suitable for simulating partly confined or confined explosions with high reliability. The results obtained from FLACS and PHAST are not compared in this study. This study focuses on the simulation results of FLACS.

This study has a theoretical (chapters 1 to 4) and practical part (chapters 5 to 7). The theoretical part starts with an introduction of a partly confined vapour cloud explosion. The basic concepts and terminology for this study are explained in chapter 2 and chapter 3 introduces VCEs and review some real cases of hydrogen explosion indidents. The FLACS and PHAST are presented in chapter 4. The modelling settings for the FLACS simulations are explained in chapter 5, and in chapter 6 the results are shown and discussed. The summary of this study with further recommendations is presented in chapter 7.

2 BASIC CONCEPTS OF THE STUDY

In order to fully understand this study, the essential terms in the context of consequence modelling are explained in this chapter. Although the following terminology is commonly used in science as well as in everyday life, there still is a big risk to mix the terms with each other and mislead the reader.

To emphasize the importance of terminology, Keller *et al.* (2014) have pointed out that *"Terminology that is not precisely defined and universally understood can lead to inappropriate and confusing code development"*. In other words, in the worst cases the risk can be misinterpreted, misunderstood and analysed wrongly which can lead to incident situations and ultimately serious accidents.

2.1 Combustion

Combustion is a chemical reaction between a fuel and an oxidant where chemical energy is produced and new reaction products are formed (Helmenstine 2017). During combustion the weak bindings of molecules break and new strong bindings are formed. As a consequence excess binding energy is released that is also known as chemical energy. (Raiko *et al.* 1995) The nature of combustion and the release of chemical energy depend on the quantity of fuel involved in the phenomenon, the composition of fuel, and the amount of energy transferred. (Mannan 2012)

The velocity of a combustion reaction (the rate of an energy release) is measured with a *burning rate*. It measures the velocity of the flame front (thin reaction zone) proceeding to the unburned mixture immediately ahead of it. Burning rates are determined by the transfer processes (e.g. heat and mass transfer) within the flame front and it describes the amount of fuel consumed in combustion per unit time [kg/s]. (Bjerketvedt *et al.* 1997; Lautkaski 1997) Burning rates can be classified into laminar and turbulent burning rates.

- The *laminar burning rate* is the rate at which the laminar (planar) combustion wave proceeds relative to the unburned gas mixture ahead of it (Crowl 2003). The laminar burning rate of a flammable vapour cloud is considered as a fuel reactivity measure. The faster the burning rate the more reactive the flammable vapour cloud becomes. (Zalosh 2016)
- The *turbulent burn rate* exceeds the burning rate measured under laminar conditions to a level that depends on the scale and intensity of turbulence (eddies) of unburned gas. (Crowl 2003)

2.2 Explosion

An *explosion* is a sudden and violent release of energy leading to a rapid increase in pressure (Lautkaski 1997). The explosion can be either physical or chemical.

- A *physical explosion* is caused by the sudden release of mechanical energy (e.g. the release of the compressed gas) and it does not involve a chemical reaction. Physical explosions can be for example a vessel breakage where mechanical energy is released. (Crowl 2003)
- A *chemical explosion* requires a chemical exothermic reaction which may be for example a combustion reaction. It can occur in the gas, liquid or solid phases. (Crowl 2003)

In this study, the investigated explosion (vapour cloud explosion, described in more detail in chapter 3) is a chemical explosion that occurs due to a combustion reaction. It may occur if the substance is considered as a flammable material (see section 2.3) and certain conditions are fulfilled. The intensity of an explosion is significantly affected by for example a fuel, a mass of a flammable vapour cloud and a degree of congestion.

2.2.1 Release rate of a flammable material

A *Release rate* of a flammable material is the velocity of released flammable material from the leakage point. The higher the velocity of released fuel the easier it will ignite immediately as an ignition source is present. (Javidi *et al.* 2015) This is due to the fact

that a higher velocity of a release rate leads faster to the formation of a flammable vapour cloud.

2.2.2 Delay time of ignition

The velocity of a fuel release may affect the *delay time of ignition*. The delay time of ignition is a significant factor since the leakage must take some time to form a flammable vapour cloud. If the ignition occurs too soon, a flash fire may occur instead of a VCE. Therefore, the release rate of a flammable material significantly influences the formation of a VCE. (Javidi *et al.* 2015)

2.3 Flammable material

The main properties of a flammable material are the flammability limits, a minimum ignition level (MIE) and an auto ignition temperature (AIT). An explosion (in this context a chemical explosion) can occur for substances that have certain properties which make the materials react in the exothermic reactions. (Crowl 2003)

2.3.1 Flammability limits

The *flammability limits* are one of the major parameters for a flammable vapour cloud. The flammability limits are the volumetric concentration of the material in the vapour cloud and are expressed as a percentage in the vapour cloud. If a substance has a lower flammability limit (LFL) and upper flammability limit (UFL) then it is flammable. The determination of flammability limits is not unambiguous; Crowl (2003) mentions the following for the determination of flammability limits: *"From a practical stand point, the American Society for Testing and Fuels (ASTM) defines a fuel mixture with air as flammable if the pressure increase during the combustion process is more than 7% of the initial pressure"*. If the pressure increase is lower than 7 per cent, the mixture is not flammable.

When the substance concentration is near the flammability limits the burning rate is low. (Lautkaski 1997; Bjerketvedt *et al.* 1997) The flammability limits vary depending on the substance as shown in Table 1 for some highly flammable materials.

Table 1. The flammability limits of some hydrocarbons, ammonia and hydrogen in air. (adapted from Lautkaski 1997)

Flammable material	LFL [vol%]	UFL [vol%]
Hydrogen	4	75
Ammonia	15	28
Acetylene	2.5	80
Methane	5	15
Ethane	3	12.5
Propane	2.2	9.5
Butane	1.9	8.5

2.3.2 Minimum ignition energy (MIE)

Minimum ignition energy (MIE) describes the minimum energy that is required to initiate the combustion. The lower the MIE value, the easier chemical ignites. (Javidi *et al.* 2015) Table 1 lists MIE values for some hydrocarbons, ammonia and hydrogen in air.

2.3.3 Auto ignition temperature (AIT)

Auto ignition temperature (AIT) is the minimum temperature required for a flammable material to spontaneously ignite in ambient atmosphere without an external source of ignition. The fuel is highly flammable when its AIT value is low. (Javidi *et al.* 2015) Table 2 lists AIT values for some hydrocarbons, ammonia and hydrogen in air.

Table 2. Values of MIE and AIT for hydrocarbons, ammonia and hydrogen in air. (adapted from Lautkaski 1997)

Flammable material	MIE [mJ]	AIT [K]
Hydrogen	0.02	847
Ammonia	680	924
Acetylene	0.02	578
Methane	0.29	813
Ethane	0.24	788
Propane	0.25	723
Butane	0.25	678

2.4 Blast Wave

In general, a *blast wave* is the air wave caused by an explosion (Lautkaski 1997). It is observed as a significant pressure increase. The blast wave is a mechanical energy which is formed from chemical energy due to the expansion of gaseous fuel products. This is caused by the reaction stoichiometry (higher molar amount) and thermal expansion. (Ponchaut *et al.* 2016; Casal 2008) Blast waves can be divided into a *shock wave*, a *pressure wave*, and a *rarefaction wave*.

- A shock wave is an overpressure that reaches the peak value instantly (known as detonation). The pressures occurring in the shock waves of explosions can be determined as a *side-on and reflected pressures*. Side-on pressure is a static pressure which is behind the shock wave, while reflected pressure is a stagnation pressure which is the quantity when the shock wave hits an object, for example a wall. (Bjerketvedt *et al.* 1997)
- A pressure wave is an overpressure that reaches the peak value gradually (known as deflagration). (Bjerketvedt *et al.* 1997)
- A rarefaction wave is the gradual decay of the overpressure. (Bjerketvedt *et al.* 1997)

2.4.1 Overpressure

The formed overpressure is affected by the combustion and expansion of gases. During combustion, the pressure is increasing while in gas expansion it is decreasing. The shape of the blast wave (i.e. shock wave and pressure wave) depends on the explosion. (Casal 2008)

During the positive phase (as the pressure increases in combustion), the blast wave may collide with objects, resulting in a transient pressure on the object surface. In some cases, the overpressure is reflected from the object and forms a local reflected wave. This reflected overpressure will vary between two or several times the overpressure of the blast wave. (Casal 2008)

Even though the peak overpressure of the blast wave causes destructive effects, another destructive effect is caused by the *dynamic pressure*. The dynamic pressure consists of air movements caused by the blast wave and is proportional to the square of the velocity in the air and the density of air behind the blast wave. When the positive phase of the pressure curve of a reflected pressure or pressure in a closed system is over the object is affected by a blast wind associated with the negative phase. (Casal 2008) Table 3 lists the overpressure (blast wave) effects on people, structures and equipment.

Table 3. The effects of overpressures on people, structures and equipment. (adapted from LaChance *et al*. 2011; Casal 2008)

Overpressure (bar(g))	Description of damage
Direct effects on people	
0.14	Threshold for eardrum rupture
0.35-0.60	50% probability of eardrum rupture
0.70-1.03	90% probability of eardrum rupture
0.83-1.03	Threshold for lung haemorrhage
1.38-1.72	50% probability of fatality from lung haemorrhage
2.07-2.41	90% probability of fatality from lung haemorrhage
0.48	Threshold of internal injuries by blast
4.83-13.79	Immediate blast fatalities
Indirect effects on people	
0.1-0.2	People knocked down by pressure wave
0.14	Possible fatality by being projected against obstacles
0.55-1.1	People standing up will be thrown a distance
0.07-0.14	Threshold of skin lacerations by missiles
0.28-0.35	50% probability of fatality from missile wounds
0.48-0.69	100% probability of fatality from missile wounds
Effects on structures and equipment	
0.01	Threshold for glass breakage
0.03-0.035	Minor structural damages
0.05	Minor damages to buildings
0.07	The roof of storage tanks collapses
0.1	Some damages of steel structures in buildings
0.15-0.2	Collapse of unreinforced concrete or cinderblock walls. Local serious damages to structures and slight damages to industrial buildings and heavy machinery
0.2-0.3	Collapse of industrial steel frame structure. Breakage of oil tanks
0.30-0.4	Many buildings collapses or are destroyed (except for concrete-reinforced buildings designed to withstand e.g. earthquakes). Displacement of pipe rack, breakage of piping
0.35-0.5	Ordinary buildings are almost completely destroyed
0.4-0.55	Collapse of pipe racks
0.5-0.55	Rail car/ tank trucks crash, 20-30 cm thick brick walls collapse
0.6	Train wagons are destroyed completely
0.7	Total destruction of buildings; heavy machinery damaged
0.5-1	Displacement of cylindrical storage tank, failure of pipes

2.4.2 Pressure impulse

Another parameter that measures the damages of a blast wave is the *pressure impulse* I_P. It is a time integral of the local pressure-time curves and its unit is Pascal-second (Pas). The pressure impulse is shown in Equation 1. (Bjerketvedt *et al.* 1997)

$$I_P = \int_{t_1}^{t_2} P\, dt \qquad (1)$$

In which

I_P is the Pressure impulse [Pas]
$t_{1\text{-}2}$ is the time interval [s]
P is the local pressure [Pa]

Figure 1 shows a blast wave curve showing both the overpressure peak and the pressure impulse areas. As simplified, the pressure impulse is the area within the blast wave curve and it determines the duration of the overpressure and its amplitude.

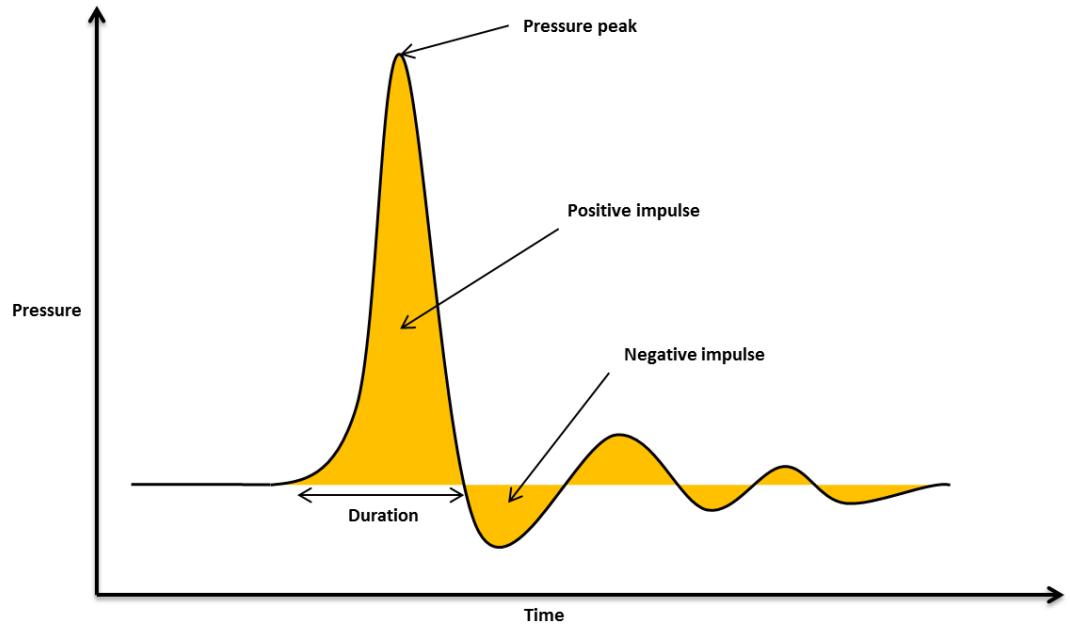

Figure 1. Overpressure (y axis) and pressure impulse (orange area) (adapted from Bjerkedvedt *et al.* 1997).

The impulse takes into account both the pressure and the duration of the pulse and may be positive and negative. Both positive and negative pressure impulses are important, but in general, a positive impulse evaluates the structural response. Positive pressure impulses take pressure and pressure pulse duration into account. The negative pressure impulse effect depends on the natural frequency of the structure. *"The negative impulse can be about 1/3 of the positive impulse phase, but this ratio depends on the layout of the geometry where the explosion occurs. The results from gas explosion analyses or experimental results are often reported as maximum pressure."* (Bjerkedvedt *et al.* 1997) Figure 2 shows the damage levels of pressure impulses together with overpressures.

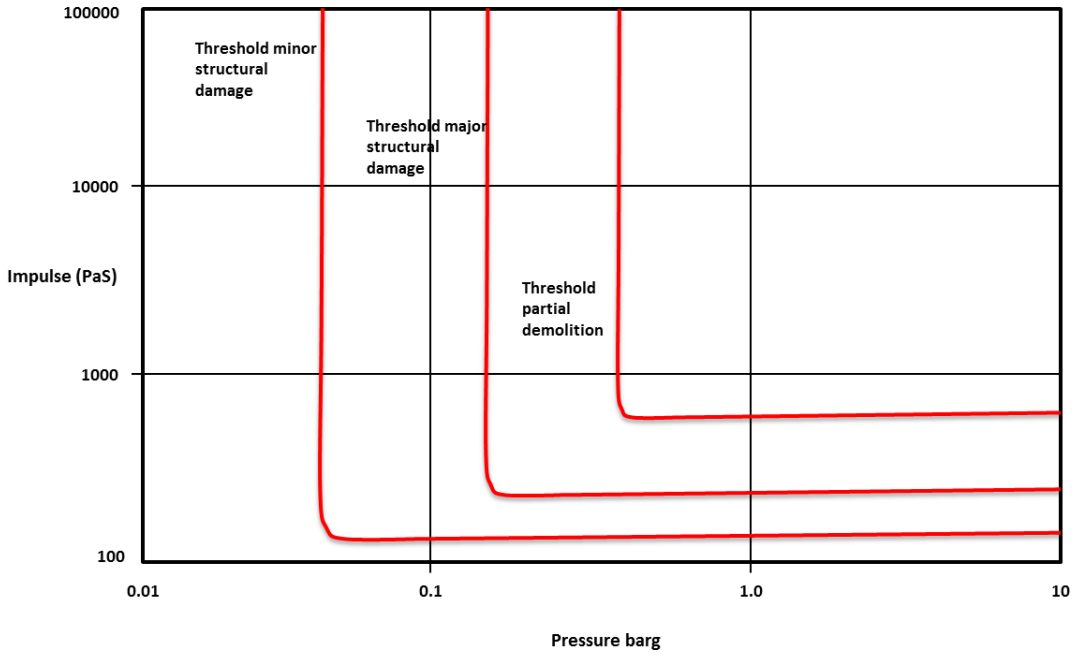

Figure 2. Damage levels to brick buildings versus the peak pressure and impulse of the blast wave from high explosives. (adapted from Bjerkedtvedt et al. 1997)

3 VAPOUR CLOUD EXPLOSION (VCE)

A VCE is one of the most significant hazards in the process industry. It is a hardly predictable event since vapour cloud can drift away and occur from a distance of the leakage point. It can be very destructive depending on the source and chemical reactivity. (Mannan 2012; Javidi *et al.* 2015) When a VCE proceeds, its negative impulse grows compared with its positive impulse (see section 2.5). This increases the negative overpressure rapidly and makes it difficult to predict the pressure of a blast wave from VCE. (Casal 2008) Despite the numerous studies and practical experiment, a VCE is still not a fully understood phenomenon. For example, the exact propagation of a VCE is still a non-predictable event. (Bjerketvedt *et al.* 1997)

Figure 3 shows the formation of flammable vapour clouds from gaseous and liquid leakage source.

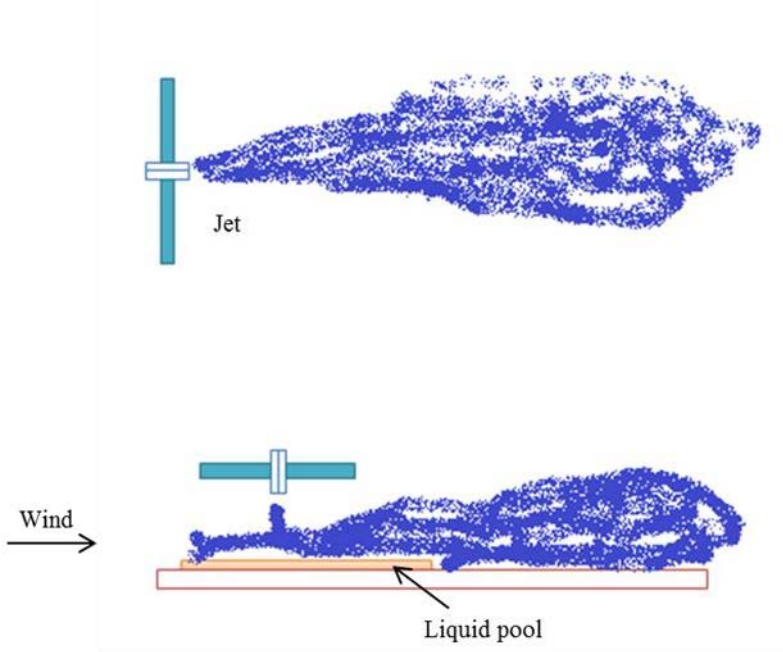

Figure 3. Jet release and evaporating pool (adapted from Bjerketvedt *et al.* 1997).

A turbulent momentum jet is formed by an undesirable gaseous leakage. In case of a liquid leakage, an evaporating pool is generated (as seen in Figure 3). (Lautkaski 1997)

In this study, the main focus is on VCE formed from a gaseous release in a partly confined area.

If a gaseous leakage occurs in a partly confined area, the jet results in a flow circulation (see figure 3). The concentration of the vapour cloud in the area increases until it reaches a steady state value determined by the gas flow rate and ventilation rate. If the formed vapour cloud is within its flammability limits and is ignited, a VCE occurs. (Laukaski 1997)

The consequences of a VCE are highly dependent for example on the surrounding environment since the concentration of a flammable vapour cloud varies between partly confined and unconfined areas. Partly confined spaces lead to more severe consequences since the burning rate increases much rapidly than in more open spaces. (Casal 2008; Bjerketvedt *et al.* 1997)

VCEs in unconfined areas usually do not cause high overpressures, and it is likely that a flash fire occurs instead of VCE. Even small obstacles can be crucial factors for the flame acceleration to increase. This was proved in 2005 in England, Buncefield oil storage terminal when a massive VCE occurred in relatively unconfined area. Figure 4 shows the Buncefield terminal area before and after the explosion and massive fire.

Figure 4. Buncefield terminal area before (upper fig.) the VCE occurred (Institution of Chemical Engineers 2017) and during the VCE occurred (lower fig.) (Denton 2015).

An overfilling protection of a gasoline tank failed and gasoline began to leak on the tank roof. Flammable vapour cloud heavier than air formed with a radius of about 250m. When the vapour cloud ignited, a strong VCE occurred, which first started as a deflagration, but as proceeding also detonation-to-deflagration transition occurred (more detailed description of explosion type in section 3.3). Due to a low degree of congestion (as seen in Figure 4), high overpressures and fast flame acceleration were unpredictable consequences. (Institution of Chemical Engineers 2017) GexCon together with Total

Petrochemicals began to investigate the accident more closely. The study found that there was a high density of vegetation (bushes and trees) in the area, which caused a significant degree of congestion and thus turbulence. The effect of trees on high overpressure and flame acceleration was simulated by FLACS, and it was found that overpressures of up to 10 bars were measured with the presence of trees, while simulations without trees showed relatively low overpressures of about 0.1 bars. (Davis *et al.* 2010)

A VCE requires different factors in order to occur. The main factors are a congested area, an ignition point, a fuel source, (Jeavidi *et al.* 2015) and the mass of a flammable material in a vapour cloud. The volumes of vapour cloud are different depending on the area, which affect the combustion reaction and thus to the burning rate. For instance, when a vapour cloud ignites in a wide-open area the generated overpressure may be negligible. Instead of an explosion, a flash fire occurs which is not as destructive as a VCE. (Tauseef *et al.* 2011; Javidi *et al.* 2015)

The delay time of ignition significantly affects whether or not an explosion occurs. If a vapour cloud is ignited shortly after its formation, a jet fire is the most likely to occur than an explosion. A delay time is required to form a large flammable vapour cloud. (Casal, 2008)

In addition to the location of an ignition source, the delay time is also affected by the factors of the flammable material itself. These factors are MIE, AIT, the release rate of a flammable material, and flammability limits, which were explained in section 2.3. Javidi *et al.* (2015) have pointed out that MIE, AIT, and release rate of a flammable material can speed up the ignition. Flammability limits, the release rate of a flammable material, and location of an ignition source can delay the ignition. When conditions are fulfilled and a vapour cloud is ignited, according to Casal (2008), *"The overall energy released will be a function of the amount of flammable substance involved in the explosion and its explosion energy, although only a relatively small part of this energy will be used to create the blast."* The VCE can be categorised into deflagration, detonation, and deflagration-to-detonation transition (DDT) depending on the intensity of the formed blast wave.

3.1 Deflagration

Deflagration is a vapour cloud explosion with less severe overpressure effects than in a detonation. Deflagrations are characterized by a blast wave that propagates at subsonic velocity (300 m/s at 0 ^{o}C). Deflagration is the most common 'explosion type' for VCEs since the volume of a vapour cloud is usually large enough that the homogeneity of a vapour cloud is not high enough for fast chemical reaction resulting in a slow energy rate. (Casal 2008; Bjerketvedt *et al.* 1997)

Deflagration starts typically as a laminar flow with a relatively low flame speed (1-10 m/s) and overpressure. The flame front propagates due to molecular heat and mass diffusion (Hansen *et al.* 2016; Mannan 2012). However, the interaction between the flow and obstacles in the surrounding area increases the flow speed (burning rate). This affects the flame front that has a cellular structure showing the peaks and troughs of the flame, also known as wrinkles. The interaction increases the wrinkles of the flame causing the higher reaction rate. Consequently, the heat and mass diffusion increases and a turbulent flow ahead of the flame front is generated where the flame speed can be in order of 100 to 1000 m/s. (Hansen *et al.* 2016; Bjerketvedt *et al.* 1997)

3.2 Detonation

A detonation is a severe explosion where the blast wave propagates through the unreacted vapour cloud at supersonic velocity. A flame front and a shock wave together propagate at supersonic velocity and generate greater overpressure than in deflagration. (Casal 2008) According to Bjerketvedt *et al.* (1997) the average burning velocity in a detonation is between 1500 and 2000 m/s and the peak pressure between 15 and 20 bars.

Compared with a deflagration a detonation requires much more energy to create a shock wave, and thus it is not likely to occur in a VCE. It is more likely that a VCE first starts as a deflagration and then proceeds into a detonation due to the formation of turbulence. This is also known as deflagration-to-detonation transition, which will be discussed in more detail in section 3.3. However, in confined spaces where the expansion area is limited, the VCE can occur directly as a detonation. (Casal, 2008)

Depending on the propagation of a VCE a detonation can occur in two different types: as a stable or an unstable detonation. A stable detonation occurs in a closed system, which has no significant variation in velocities and pressure. An unstable detonation occurs in the transition phase of a deflagration-to-detonation where there is no constant burning rate and the pressure is higher than in a stable detonation. (Zhang *et al.* 2011)

For both deflagration and detonation the pressure curves can be presented as an idealized triangle pulses. The time required for a growing overpressure is dependent on the explosion force. In general, the stronger the explosion the shorter the required time for an increase in overpressure.

Typically, the pressure growing time is from 50 to 100 milliseconds in deflagrations and a few milliseconds in detonations. (Hansen *et al.* 2016) Figure 5 presents the pressure curve for both deflagration and detonation.

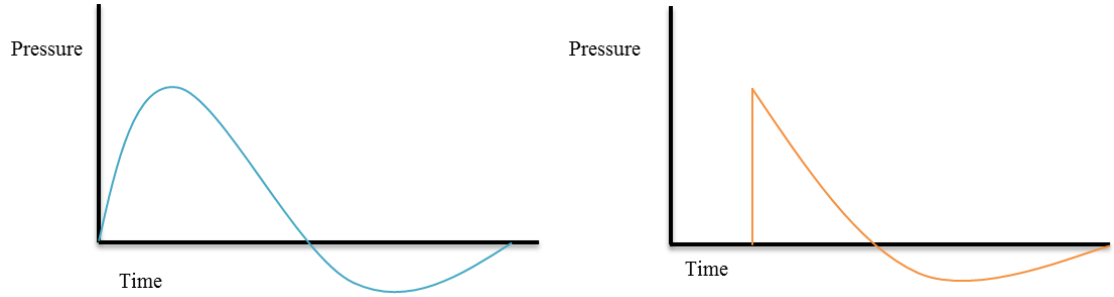

Figure 5. The blast wave curves of deflagration (left) and detonation (right) (adapted from Ponchaut *et al.* 2016)

At the beginning of the curve, the pressure is at ambient pressure, and during the explosion the overpressure increases almost instantly. The pressure increase is different for deflagrations and detonations; this is due to the chemical reaction speed. After the peak pressure, the pressure decreases less rapidly to the negative value, under-pressure, and finally increases back to the ambient value. (Casal 2008; Ponchaut *et al.* 2016) Sometimes the curve forms a slightly deformed letter *N*, known as an N wave, when the final pressure recovery appears as a second shock wave (Zalosh 2016).

In real situations, the behaviour of a blast wave can differ from the ideal blast wave curve (as seen in Figure 5) depending on the explosive fuel. In detonations, high explosives (e.g. TNT) are much more likely to follow the ideal blast wave curve. While in deflagrations, the blast wave is likely to follow the ideal blast wave curve only from the edge of the VCE. This is due to the volume of flammable material in the cloud, which is smaller in detonation and the energy release rate, which lower in deflagration. (Casal 2008)

3.3 Deflagration-to-detonation transition (DDT)

A deflagration-to-detonation transition (DDT) is a common initiating mechanism for detonations in a VCE of highly flammable materials such as hydrogen. In this type of explosions, the produced energy at the beginning in combustion is not high enough to produce a shock wave and therefore strong deflagration is generated instead. (Casal 2008) The flame front creates pressure waves which precompresses and preheats the unburned gas ahead of the flame. This generates the shock wave front and a turbulent flame brush. The formed turbulent brush strengthens the formed shock waves, makes them collide, and forms a united shock front. (Mannan 2012) DDT is a well-understood phenomenon, however the conditions for a DDT to occur are not fully understood and therefore it is a hardly predictable event. (Bjerketvedt *et al.* 1997)

3.4 VCE in partly confined area

Vapour cloud explosions may occur in areas that are partly confined. Partly confined areas are restricted for example with walls, buildings or congested obstacles. In these areas, the flame can be accelerated only in certain directions, for example through ventilations. Partly confined areas are for example rooms, congested process areas, and compressor shelters which are the particular interest of this study. In the case of buildings, overpressure escapes generally through the emergency ventilation if the constructions stand the formed overpressures and pressure impulses (seen Figure 6). (Bjerketvedt *et al.* 1997: Schiavetti *et al.* 2018)

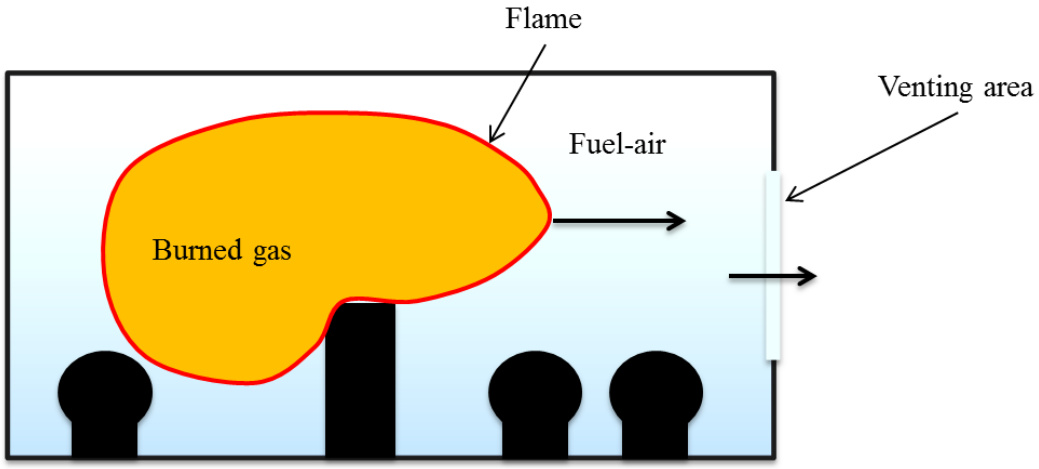

Figure 6. VCE in partly confined area (adapted from Bjerketvedt *et al.* 1997).

Due to the partly confined area and the degree of congestion caused by objects, turbulence is formed ahead of the flame, which greatly increases the pressure (see Figure 7). In some cases, the filling ratio of 30 to 50 per cent vapour cloud can cause the same explosion pressure as the 100 per cent filling ratio of vapour cloud in area that has significantly smaller degree of congestion in area due to the expansion of the burned gas. This expansion pushes the unburned vapour cloud ahead of the flame and causes the air or vapour cloud to thrust out of the room. (Bjerketvedt *et al.* 1997) As the VCE in partly confined area is studied and simulated in this study, the main parameters affecting the explosion are more thoroughly discussed in the following sections.

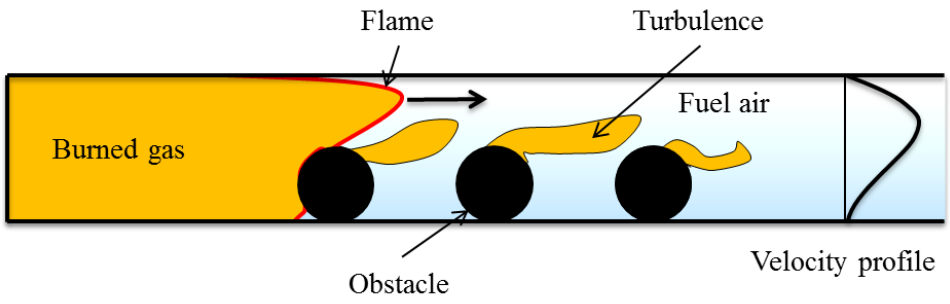

Figure 7. Effects of objects on turbulence formation (adapted from Bjerketvedt *et al.* 1997).

3.4.1 Effects of ventilation to buildings

The overpressure generated by the VCE in partly confined area is generally affected by two factors: flame, which increases pressure and ventilation, which decreases overpressure. The explosion is affected mainly by the burst of the vent and the venting of the combustion product. Activation of the venting suddenly changes the flow field in the combustion area. The interaction between the flow and the flame extension increases and the acceleration of the gases (both burned and unburned) towards the ventilation zone increases. (Schiavetti *et al.* 2018) If the venting is non-existent or too weak and an explosion occurs, considerable overpressure can be achieved even at a low combustion rate. (Lautkaski 1997; Bjeketvedt *et al.* 1997)

The location of the ignition source has a significant effect on the increasing flame acceleration, since the flame generated by the explosion flows towards the venting area. If vent openings are located at a distance from the ignition source, then the pressure increases as the flame reaches towards the vent. It should also be taken into account that there are usually objects in the rooms that increase turbulence and burning rate. (Lautkaski 1997; Bjeketvedt *et al.* 1997)

There are different types of ventilations. The best ventilation option for an explosion is open ventilation but it is not the most practical option for other factors such as the weather and fire safety. Thus, the vent openings are covered and installed to open at low pressure (in order to reduce the explosion pressure as quickly as possible). The most common vent openings are explosion relief panels, explosion relief doors, and rupture diaphragms. (Lautkaski 1997; Bjeketvedt *et al.* 1997)

Often, vent openings are designed to open at the same pressure and therefore they practically open simultaneously, allowing the venting of both unburned mixture and hot combustion products. When the flame reaches the venting area, the combustion product starts to flow through the vents, whereby the flame acceleration decreases. In addition, the volumetric flow rate of exiting vapour cloud drastically decreases due to the increased of the vented gas (Schiavetti *et al.* 2018). The velocity of the flow through the vent is increased due to the difference in supersonic velocity between the combustion

product (~900 m/s, average velocity for combustion products) and the vapour cloud (~340 m/s, average velocity for vapour cloud). Figure 8 shows the effect of early phase venting on turbulence formation. (Lautkaski 1997; Bjeketvedt *et al.* 1997)

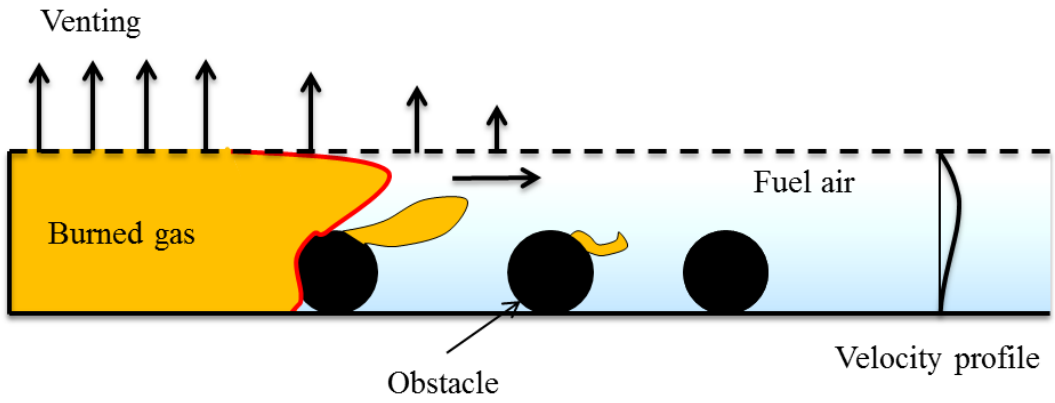

Figure 8. Early phase venting of hot combustion product (adapted from Bjerketvedt *et al.* 1997).

3.4.2 Effects of obstacles

Congestion caused by objects significantly increases flame acceleration. When the flame front reaches the obstacle, it folds (as seen in Figure 9) and thus the flame front surface area increases resulting in a higher reaction rate. As the flame advances, part of the vapour cloud is pushed forward due to obstacles generating turbulence. The number of obstacles, their arrangement and the shape of the obstacles significantly influence the formation of the flame front fold. (Lautkaski 1997; Bjerketvedt *et al.* 1997)

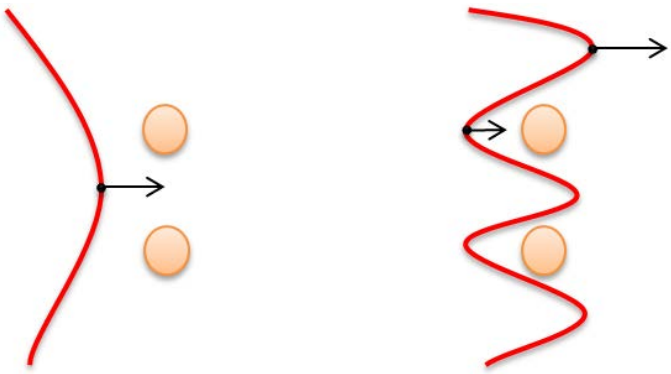

Figure 9. Flame folding caused by the objects (adapted from Lautkaski 1997).

It has been discovered that round shaped objects form less turbulence than sharp shaped objects. This is due to the turbulence intensity that is much smaller with round-shaped objects. If there are several objects in a line, the flames and burn rate will increase after each object affecting the increased turbulence formation. This significantly increases the flame acceleration. (Lautkaski 1997; Bjerketvedt *et al.* 1997)

The number of objects in relation to the flow can be estimated by the blockage ratio and the volume blockage ratio. The blockage ratio is the total area of obstacles relative to the cross section of the vessel, room or process area. It is an important parameter when estimating flame acceleration (the higher the value, the stronger the acceleration). The volume blockage ratio is the total volume of objects relative to the total volume of the room. However, the blockage ratio does not take into account the arrangement of the obstacles, which is also a very important factor in case of flame acceleration. Studies have shown that small objects in a partly confined area cause greater overpressure during an explosion than one larger object with the same blockage ratio. (Lautkaski 1997)

Figure 10 shows the effect of arrangement to the overpressure formation during an explosion.

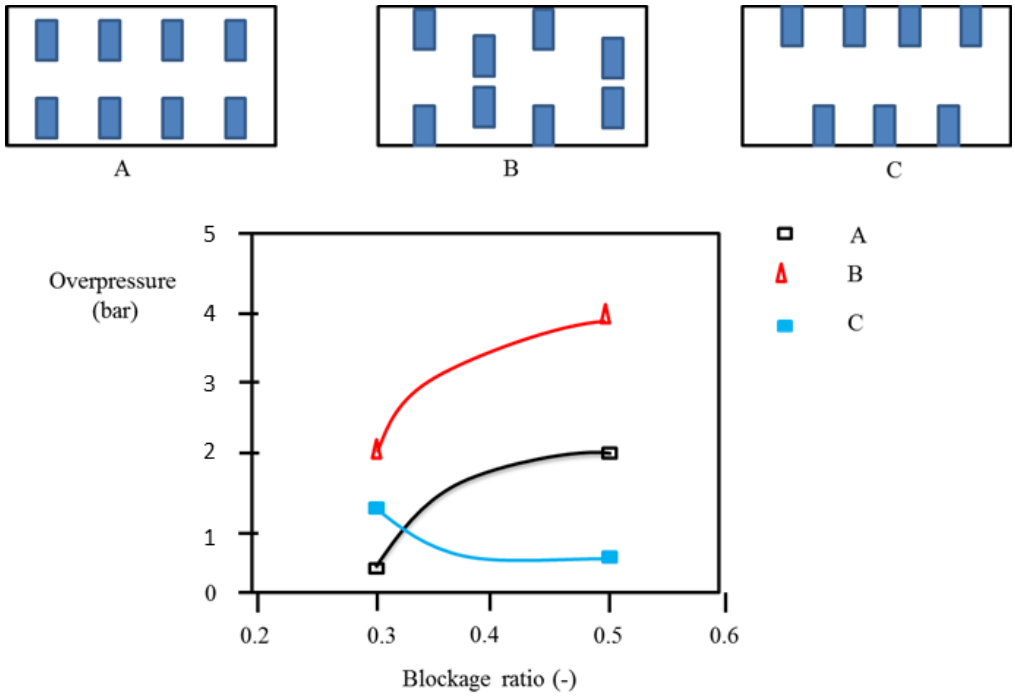

Figure 10. Influence of obstacle arrangements on flame propagation (adapted from Bjerketvedt *et al.* 1997).

As seen from Figure 10, the arrangement of objects is a very essential factor for flame acceleration. The distance between objects can decrease or increase the flame front. If the distance between two objects is sufficient, then continuous flame acceleration is not possible. If the distance is negligible, then the so-called “pocked” of unburned mixture formed between the objects is too small to cause flame acceleration. (Lautkaski 1997)

The location of vent openings must be taken into account when arranging the objects. If an explosion occurs, then the resulting flame flow will proceed towards the vents. When the flame flow progresses, the burning rate increases due to turbulence and according to how far the ignition point is from the vent openings. In order to minimize the formation of turbulence, it is the most sensible to arrange the objects in such way that their longest side or diameter is parallel to the flow direction. In addition, it is very important that objects are not arranged in the immediate vicinity of the vents, since the flame rate is at its highest value, and that objects are not placed in a queue sequentially. (Bjerketvedt *et al.* 1997; Lautkaski 1997) Figure 11 shows the better and worse arrangement of objects.

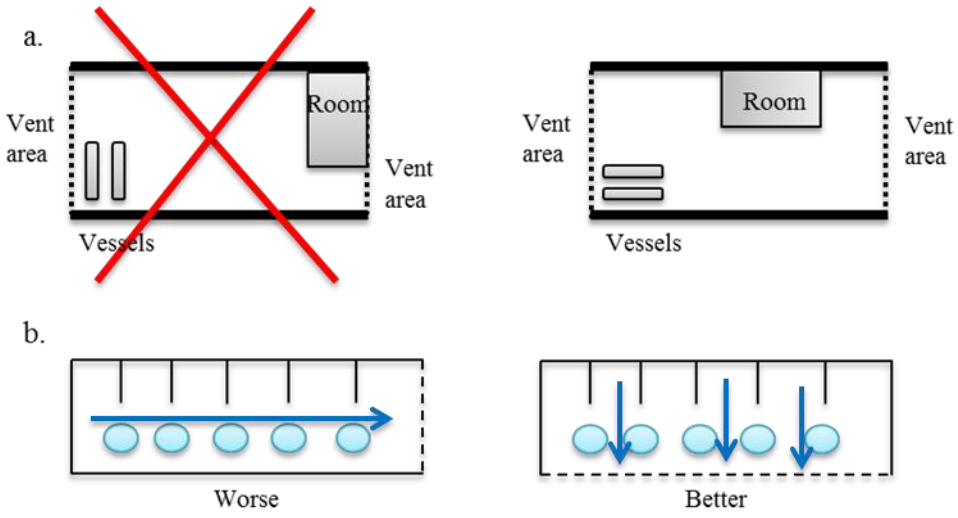

Figure 11. Better and the worse arrangement of obstacles. In option a. the different layout arrangements in a room and in b. the repeated obstacles in relation to the vent opening (adapted from Lautkaski 1997).

3.4.3 Shape of a compartment of building

Room shape effects significantly on the ventilation and this was proved by the Bauwens and Dorofeev (2014) study. The area and especially the height of a room significantly affect the overpressure peak of an explosion. The peak overpressures formed from hydrogen explosions were simulated for three rooms of different surface area with and without ventilation. During the study, the room height was changed from 8 metres to 12 metres while keeping the other room dimensions constant, the ventilation area was the same size in each room. In higher rooms, the peak pressures were lower as the overall volume of the rooms were bigger and the flame acceleration was not accelerating the same way as in the smaller rooms due to less contact of obstacles. This proves that the total volume of the room has a significant effect on the explosion behaviour. The ventilation depends on the volume of the room since the ventilation rate is determined by the volume of the room (Bauwens & Dorofeev 2014).

However, if the room is congested with objects, then the flame propagation is determined by the objects and the shape of the room is a less important factor. (Lautkaski 1997) There are three principles to apply when optimising the shape of a room (Lautkaski 1997):

1. The ignition source must be as close as possible to the venting area, in order to achieve an early phase of explosion venting.
2. The flame must propagate in spherical form as long as possible. A spherical form is usually formed when the ignition occurs in the centre of the vapour cloud. The flame propagates in spherical form only at the initial stage of an explosion before the flame front touches the walls or other obstacles and flame front begins to "wrinkle" and flame starts to accelerate.
3. The obstacles must be arranged in a way that a strong turbulence in unburned mixture and long flame front are avoided.

3.5 Review of hydrogen explosion incidents

VCE is one of the most common incidents with catastrophic consequences such as the fatalities and complete destruction of buildings. From the 1940s to the 2010s in total of 174 VCE worldwide accidents have been reported in chemical process areas. Cases have shown that VCE accidents can occur in all areas of hazardous chemical processes such as preparation, utilization, storage, and transportation. (Zhu *et al.* 2017) The biggest risk factors for most of the VCE cases have been found to be leakages and mechanical failures (Nolan 2011).

Based on Nolan (2011) all accidents are preventable. It is important that incidents are investigated by experts who then prepare a public report - a lessons learned report and create new standards. Malfunctions and mistakes leading to incidents must be learned and prevented in the future by adding the necessary security features. Since the objective of this study is the hydrogen VCE in the refinery area, the following sections briefly describe hydrogen VCE and gas explosions in chemical process plants.

3.5.1 Hydrogen VCE in the Silver Eagle Refinery, US (2009)

On the 4th of November a massive explosion and fire occurred in the Silver Eagle Refinery. The explosion damaged over 100 nearby homes. Fortunately there were no fatalities. Four workers were working near the unit when the explosion occurred. They

were blown down by the blast wave but they were not badly injured. (Exponent Failure Analysis Associates 2013)

The explosion occurred during the regeneration of the catalyst hot in which hydrogen rich gas was used. During the regeneration, the operating temperature increased approximately from 370 °C to 427 °C. A 10-inch pipe located at the bottom of the reactor in the Mobil distillate dewaxing unit suddenly ruptured completely and a relatively small amount of hydrogen rich gas (approximately 100 kg) was released. The gas was immediately ignited and exploded. The result was a pressure wave that damaged more than 100 homes. During the accident investigation, it was found that the ruptured pipe was very thin due to corrosion and that no corrosion studies had been carried out on that pipe. (Exponent Failure Analysis Associates 2013)

3.5.2 Hydrogen gas explosion in an ammonia plant, Norway (1985)

In the summer of 1985, a serious hydrogen explosion occurred at an ammonia plant in Norway. Three people were seriously injured in the accident, two of whom died later. The building where the explosion took place was completely destroyed, the windows broken down at a distance of 700 metres from the explosion, and concrete blocks of 1.2 kilogram (part of the building wall) flew up to 16 metres. According to Bjerketvedt & Mjaavatten (2015) the accident is one of the largest industrial hydrogen explosion reported.

The initial cause of the accident was the blow out of the water pump seal. The pump fed water into a tank containing hydrogen gas at a pressure of 30 bars. This pressure caused backflow of water through the pump and the failed seal. The hydrogen leaked inside a building, where the water pump was located, lasted 20 to 30 seconds and delayed ignition caused an explosion. The total weight of the leaked hydrogen was estimated to be 10 to 20 kg. The ignition source is assumed to a hot bearing. (Bjerketvedt & Mjaavatten 2015)

The main explosion was very violent and it is likely that the explosion occurred as a detonation. It is estimated that 3.5 to 7 kg of hydrogen burned in the explosion. The roof of the building rose by about 1.5 metres before it fell down. A 350-millimetre diameter

pipe with 65 to 95 per cent hydrogen gas was attached to the roof. As the roof rose to the air the hydrogen pipe burst resulting in a large about 50-metres long jet fire which lasted for 30 seconds. (Bjerketvedt & Mjaavatten 2015)

3.5.3 Hydrogen gas explosion at Danisco Sweeteners Oy, Kotka mill, Finland (2004)

In a xylose hydrogenation plant, Danisco Sweeteners Oy, an explosion occurred on the 13th of January 2004. During maintenance work, a hydrogen explosion occurred in a hydration reactor when the reactor mixer was lifted up. Three maintenance workers got burns and hearing damages and six other employees got hearing damage. The explosion caused damage also to a lightweight wall. (Aarnivuo & Vauhkonen 2004)

Four person maintenance team did the maintenance work of the reactor. Three of them were working next to the reactor and one at a lower level. At the lower level of the reactor space there were two welders working. There was also a working group of two vocational school students and a tutor on the ground level. The reactor flange and mixer were lifted and moved slightly to the side. During the transfer, the mixer bumped to a flange panel, which caused a peeling of a dried nickel catalyst from the flange and mixer. At the same time, employees saw a flash followed by an explosion. (Aarnivuo & Vauhkonen 2004)

The accident was primarily caused by the fact that the hydrogenation process was not in a safe state when the reactor maintenance was started. The instructions for preparation work were not given sufficiently. Firstly, a supervisor gave instructions orally and after that wrote them in the so called black book located in a control building. Secondly, he did not mention in the book about nitriding which is an essential phase during preparation work. The supervisor was not present during preparation and maintenance work. In addition, the supervisor made a miscalculation with the nitriding by assuming it was done. (Aarnivuo & Vauhkonen 2004) Also the change of shifts affected that the preparation work was done by several employees and the communication was not sufficient.

A flammable hydrogen-air mixture was formed at the latest when the maintenance workers opened the reactor flanges. The ignition of the hydrogen-air mixture was probably caused by a Raney nickel catalyst that glows when it is dry, or possibly due to a mechanical spark. (Aarnivuo & Vauhkonen 2004)

3.5.4 Explosion at a Finnish Chemicals Oy Äetsä mill, Finland (2005)

At a fine chemical factory, Finnish Chemicals Oy, an explosion occurred on the 31st of October 2005. A process operator was opening a blockage in a connecting pipe between a drier and a melting pan. The operator heard anomalous sounds and ran to the emergency stop device. As soon as he left the process space an explosion occurred. There was no personal injury but the operation was interrupted for a long time causing property damage. (Salomäki *et al.* 2005)

An unexpected and fierce chemical reaction caused the gas formation and pressure rise in the dryer. The discharged pressure from the dryer launched the dryer mixer and the engine through the roof. As a consequence, a fire occurred at the end of the exhaust pipe of the hydrogen line. It was seen far away. The fire was extinguished in about 20 minutes. The discharged hydrogen gas caused an explosive fire also inside the building. The discharged pressure damaged all lightweight walls inside the building. (Salomäki *et al.* 2005)

The cause of the event was the use of water to open the blockage in the connecting pipe. The use of water first led to an increase in pressure in the melting pan and then in the dryer. There were several events that contributed to the accident. The bottom valves of the dryer were open, for example, whereby a large amount of product (Sodium borohydride powder) had accumulated in the dryer. When the powder reacted with water, it caused a rapid increase in heat and pressure in the washer. Amine had accumulated in the dryer, as the exhaust pipe was fed with nitrogen and blocked. Thus the amine was not obtained from the purified dryer. When the product reacted with the carbonates and amines there was a strong gas formation that was mostly hydrogen. (Salomäki *et al.* 2005)

4 MODELLING OF PARTLY CONFINED EXPLOSIONS

Modelling and scaling of consequences are based on different methods such as analytical, experimental and computational methods (Skjord *et al.* 2018). VCEs have been studied both experimentally and by modelling. Although practical experimentation is the best way to observe a possible accident, and the result is reliable, it is time consuming, expensive and challenging to implement (certain conditions, such as the right wind velocity and direction, must be realised). Modelling tools on the other hand are more cost-effective, time-saving, and to some extent convenient compared with field experiments. (Ponchaut *et al.* 2016) Some models have been developed to predict the intensity of pressure waves but most commercial models are based on the theory of explosives where the parameters need to be adjusted to evaluate the consequences of a VCE (Dobashi *et al.* 2011). The purpose of this chapter is to explain the basics of explosion modelling as well as introduce the modelling programs PHAST (analytical modelling) used in Neste Engineering Solutions Oy and FLACS (CFD modelling) used in this study.

In general, analytical modelling is mathematical modelling. The modelling is based on a variety of collected data and it can be applied to various disciplines such as natural science, engineering, and social science. With the collected data it is possible to calculate certain features which enable to predict certain causes. (Caliri 2000) Analytical modelling is generally a cost efficient method and the modelling is relatively fast against CFD.

"Computational fluid dynamics (CFD) is a branch of fluid mechanics that uses numerical methods and algorithms to solve and analyse problems that involve fluid flow, with or without chemical reactions." (Gexcon AS 2018) CFD software can be applied to various disciplines from process industries to civil engineering and biomedical science. Despite the fact that CFD software can be used in a wide variety of disciplines and can model complex phenomena they are in general very expensive and require sufficient computing power. (Tu *et al.* 2013)

Fire and explosion phenomena are theoretically well understood; the principles of governing equations for turbulent fluid flows and chemical reactions are well known. Modelling helps better identify how a particular fire and explosion phenomenon is likely to behave and what are the potential consequences and damages. (Skjord *et al.* 2018)

4.1 Process Hazard Analysis Software (PHAST)

PHAST (Process Hazard Analysis Software) is one of the most comprehensive process industry risk analysis software based on analytical modelling. The software can be used for modelling dispersion, fires and explosions. (Pandya *et al.* 2008; Witlox 2010) PHAST is popular especially in Europe (Pöyry 2018) and it is used in versatile ways in maritime, oil and gas, and power and renewables industries (DNV GL 2019a). In Finland, the tool is used by many large companies such as Neste Engineering Solutions Oy and Pöyry Oy Finland. PHAST is tailored for consequence modelling based on standards and authority recommended methods. With PHAST, the modelling is relatively fast and cost-effective (compared with CFD models, see section 4.2 for details). (Pöyry 2018) Although PHAST is a versatile, cost-effective and relatively fast modelling program, it has limitations. PHAST is not suitable for modelling confined areas. PHAST have simple 3D feature enabling the explosion modelling but it does not have a 3D dispersion modelling.

In this study, the modelling dispersions and explosions occurred in a partly confined area (compressor shelter); whereby the PHAST is not the most suitable software (the reliability of accumulation modelling of hydrogen gas is not reached). Therefore, instead of the PHAST, it was decided to use the FLACS modelling software based on the CFD method. FLACS is specifically tailored to model industrial leakage, fire and explosion scenarios with 3D capability and can be applied to model enclosed spaces.

4.2 Flame Acceleration Simulator (FLACS)

FLACS is a CFD modelling tool tailored to safety applications. It is used to model dispersions, fires and explosions in both open and confined geometries. (Gexcon AS

2018) FLACS is widely used in the oil, gas and process industries, and the software has also been applied in the nuclear industry. FLACS has a 3D feature that enables more accurate predictions of the consequences, as FLACS takes into account, among others confinement and congestion in the geometry, ventilation and dewatering. (Gexcon 2018)

FLACS was originally developed for VCE modelling, and at a later stage, the dispersion modelling was also added to the software. With FLACS it is possible to model different dispersion and explosion flows such as the dispersions of dissolved chemicals, homogeneous gas mixtures, and suspension of solid particles. (Gant & Hoyes 2010)

In this study, a FLACS (v10.8) was chosen to model a hydrogen vapour cloud explosion. The choice was based on FLACS being able to model explosions occurring in the confined and partly confined areas. Also FLACS takes the geometry carefully into account, which is not possible with PHAST. In addition, Neste Engineering Solutions Oy was interested in testing the usability of the software in a consequence analysis. It is, however, important to take account that the preparation of a 3D CAD model for the FLACS modelling requires significant amount of time and 3D modelling expertise. Nevertheless the results obtained from FLACS give a more detailed description of the modelled area than what is obtained with PHAST. Table 4 shows a comparison of two different models.

Table 4. Comparison of two different models (PHAST vs. FLACS).

	PHAST (7.2)	FLACS (v10.8)
Applicability	Dispersion, fires and explosions	Dispersion, fires and explosions
Advantages	Simple and relatively fast modelling Cost-effective Based on standards and authority recommended methods	A 3D feature that allows to make more accurate predictions for the consequences Possible to model in open and confined geometries. Results give a more detailed description of the modelled area The results are not based on for example on the average volume blockage ratio, but on a model that takes into the account accurate geometry of the space.
Disadvantages	Not suitable for modelling confined areas A detailed description of the surrounding environment is not possible	Labour-consuming: the preparation of a 3D CAD model for the FLACS modelling requires significant amount of time and 3D modelling expertise Long simulation times Expensive software licence

5 DESCRIPTION OF THE FLACS MODELLING FOR A HYDROGEN VCE IN A COMPRESSOR SHELTER

The aim of chapter 5 is to present the method of dispersion and explosion CFD simulations done with FLACS. The selected modelling area is a compressor shelter and its surroundings located in a diesel producing unit. Objects located within a radius of 100 metres from the compressor shelter were selected for this study (see Figure 12). The selected radius covers the control building and the process area including a compressor shelter of two piston compressors and one centrifugal compressor. In this study, the dispersion modelling was modelled from one piston compressor (flange leakage) and leaked gas was assumed to be 100% hydrogen.

Figure 12. Modelling area.

5.1 Compressor shelter

The compressor shelter is a part of the unit and it protects the compressors and related equipment from various environmental factors such as wind, snow, heat and rain. It includes an operating platform as well as lifting equipment, which is generally used for maintenance. (Panchal 2014)

The design and implementation of a compressor shelter depends on the overall arrangement, operation, maintenance and safety of the compressor. The general arrangement of the compressor is provided by the vendor. Compressors can be installed either on a grade or on a table top depending on the type of compressor. The shelter has to cover the compressor and its auxiliary systems including supporting arrangements. Also, it has to accommodate the supporting structures and lifting equipment. (Piping Engineering 2018)

In this study, hydrogen dispersion and VCE modelling were done in the compressor shelter and in its immediate surroundings. The compressor shelter has a volume of 9528 m^3 and a wall material of corrugated sheet. The shelter has an opening on the east side and it is open all around from the bottom (1.2 metres) and on the top of the long sides there are ventilation gratings.

Climatic conditions affect how compressor shelters shall be built. In warm climates, where there is no significant rainfall, the compressor shelter may be partially covered. In such cases it is sufficient for the compressor shelter to have a roof and side curtains. These protect the compressors from direct sunlight and rainfall. In rainy and cold climates the building must be covered with cladding. (Piping Engineering 2018)

From a safety point of view the compressor shelter must have an easy access and exit. There must be enough space to allow the operating personnel to walk safely around the machines. They must have clear visual perception and access to, among others, valves, instruments, measurement instruments, and switches. In fully covered compressor shelters adequate ventilation must be arranged in case of hazardous gaseous leakages. Also a sufficient amount of doors and stairs must be provided in case of emergencies.

(Piping Engineering 2018) In addition, devices measuring gas concentration and fire detectors are required in compressor shelters.

Also maintenance requirements must be taken into account when compressor shelter is designed. During a maintenance removal of the main components is generally done by cranes, and therefore the design of the shelter must take into account the use of various cranes such as the EOT (Electrically operated travelling crane) or HOT crane (Hand operated travelling crane). (Piping Engineering 2018)

5.2 Properties of hydrogen

In order to fully understand the simulations of this study some general properties of hydrogen are explained in this section. Hydrogen is the lightest of all gases and it is a colourless, odourless, and highly flammable gas. Even 0.02 mJ energy is enough to ignite a hydrogen-air mixture (Lautkaski 1997) whereas for hydrocarbons MIE is higher (from 0.2 mJ and higher). (explosionsolutions 2019). The flammability limit of hydrogen is between 4 and 75.6 volume per cent in the air which is really wide in comparison with hydrocarbons. In general, a leakage of compressed high pressure hydrogen can create so much static charge that the leakage may ignite immediately. A static charge, spark, hot surface, and flame ignite hydrogen easily. (Työterveyslaitos 2017) Since hydrogen is lighter than air, it starts to rise after a while. Because of the very wide flammability limit of hydrogen, a wide flammable vapour cloud of hydrogen is formed. Flammable hydrogen vapour cloud can be formed especially in fully or partially enclosed spaces or in the congested process area. In open spaces it is more likely that hydrogen is dissipating preventing the formation of flammable vapour cloud. Hydrogen causes high pressure in case of VCE because of the fast chemical kinetics, high molecular diffusivity and its high reactivity; it burns explosively (Bjerketvedt *et al.* 1997). Table 5 shows the flammability properties of hydrogen.

Table 5 Combustion properties of hydrogen.

	Hydrogen	Reference
Minimum ignition energy (MIE)	0.02 mJ	Lautkaski 1997
Auto ignition temperature (AIT)	560 °C	Työterveyslaitos 2017
Lower Flammability limit Upper Flammability limit	LFL = 4 vol% UFL = 75.6 vol%	Työterveyslaitos 2017
Heat reaction per unit volume, Hst	3.06 MJ/m3	Lautkaski 1997
Stoichiometric fraction in air	30 vol%	HySafe 2019
Maximum burning rate	3.5 m/s	Lautkaski 1997
Maximum flame speed	28 m/s	Lautkaski 1997
Sound velocity in normal temperature and pressure (20 C, 101325 Pa)	1294 m/s	HySafe 2019

5.3 Defining the case

A hydrogen flange leak of the piston compressor and the subsequent hydrogen VCE were modelled with FLACS. In FLACS, the leakage was simulated with a dispersion scenario and the VCE was simulated with a gas explosion scenario. The work steps in this study were:

1. Creating 3D geometry with MicroStation V8i program
2. Defining dispersion scenarios with CASD pre-processor to simulate leakages where the key factor was creating the right weather conditions
3. Simulating leakage scenarios in FLACS and, based on the results, selecting worst case scenario for simulating vapour cloud explosions

4. Building vapour cloud explosion scenarios with CASD pre-processor. The purpose was to investigate the effect of different ignition point locations on the destructive nature of the explosion
5. Simulating explosion scenarios and selecting worst case scenario in each model

The scenario which caused the most significant consequences (e.g. the largest vapour cloud and highest overpressures) was selected as a worst case scenario. Certain parameters such as release rate and flange orifice size were kept constant, but weather conditions, wind directions, and ignition points varied between different scenarios. By simulating the dispersion scenarios the propagation of a vapour cloud was followed as well as the volume and mass of a flammable vapour cloud could be defined. By simulating the explosion of this vapour cloud, overpressure effects on selected monitor points could be defined.

5.3.1 Preparation of a 3D model

In this study, 3D CAD geometry was created in MicroStation v8i software and imported to the FLACS CASD pre-processor. FLACS can define the volume blockage ratio (or in other words the porosity of the objects) only for the box and cylindrical objects. In special cases, ellipsoids, truncated cones and convex polyhedrons can be also defined as an obstacle but there are certain limitations as they are *"not contributing to turbulence and drag force"*. (Gexcon AS 2018) 3D CAD geometry required large-scale editing, as part of the objects had to be edited manually to be defined by FLACS as obstacles. Figure 13 shows a modelling area made with MicroStation v8i.

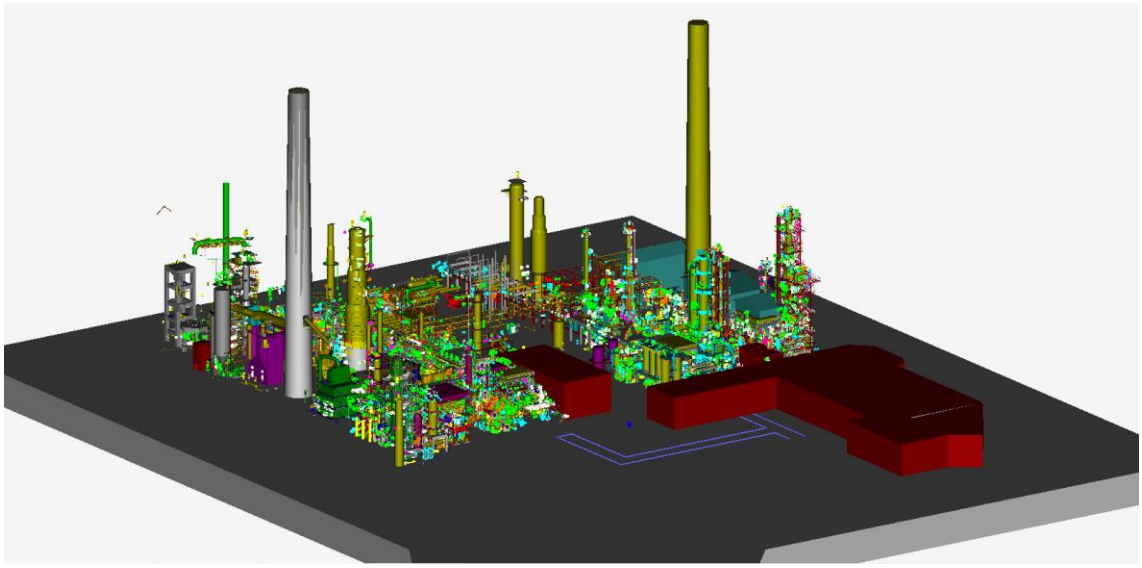

Figure 13. 3D model of the modelled case in MicroStation v8i**.**

When 3D CAD geometry was completed in MicroStation, it was then divided into smaller files in order to speed up the importing and to create three different models. The FLACS modelling was performed by using three different models in which the volume blockage ratio varied (compressor shelter, environment and terrain remained the same). The aim was to study the effects of a volume blockage ratio on dispersion and explosion overpressure. Three different models were named Model1, Model2 and Model3 and are shown in Figures 14. A modelling area of the Model1 was compressor shelter, Model2 modelling area was a diesel producing unit and control building, and Model3 modelling area was total modelling area shown in Figure 14.

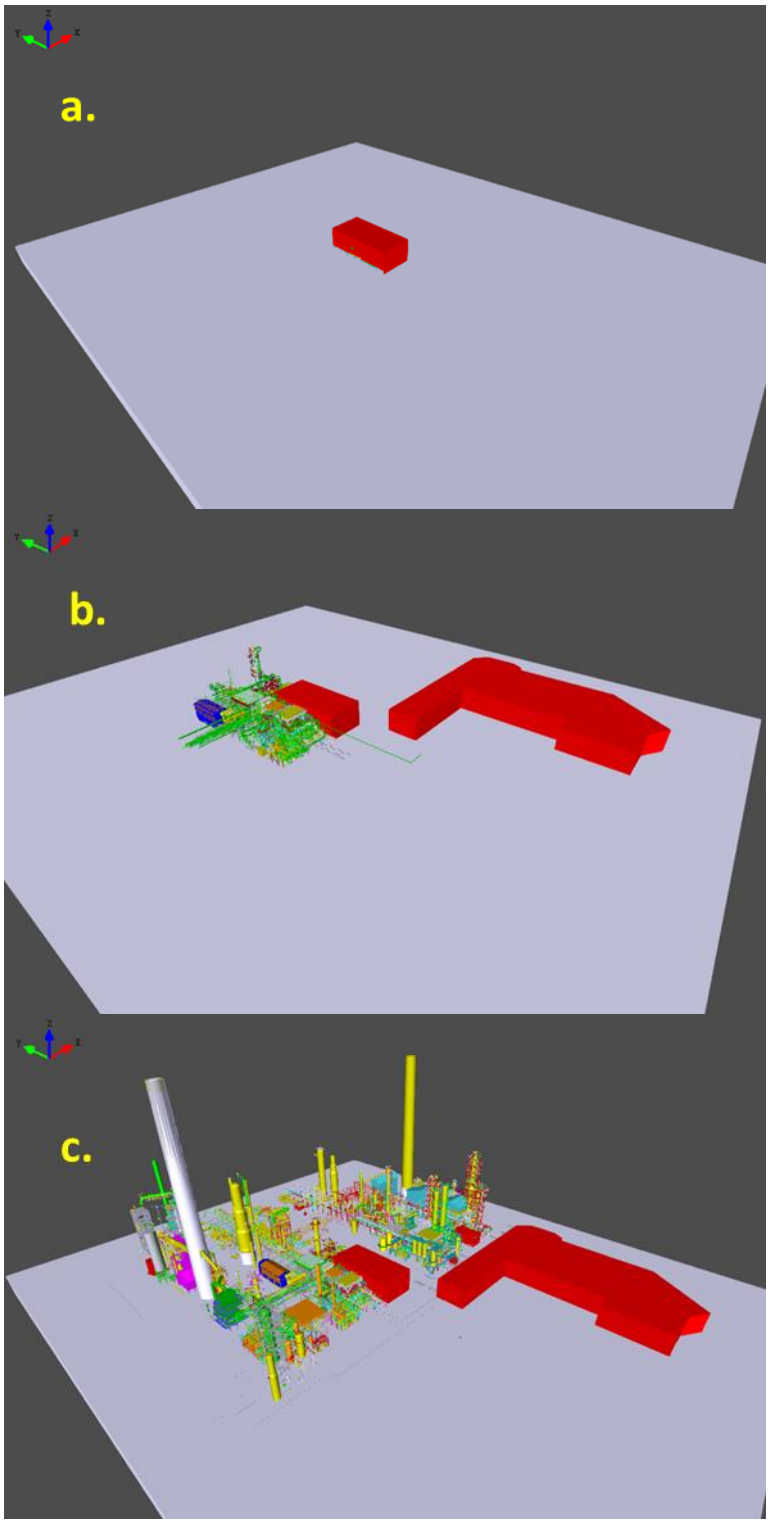

Figure 14. Three different models with a different volume blockage ratio. a) Model1 (compressor shelter), b) Model2 (diesel producing units and control building), and c) Model3 (Total modelling area).

The 3D CAD geometries were imported to a separate pre-processor program called CASD (*Computer Aided Scenario Design*) before simulations are done (Gexcon AS 2018). In this program, the aimed scenario is created (e.g. vapour cloud explosion, dispersion and ventilation, pool fire etc.). In addition, the geometry is added and computational mesh (grid) is prepared.

5.3.2 Preparation of a computational mesh and monitor points

For the iterative simulation process, the computational area must be divided into small cells; hence computational mesh has to be made. The governing equations are then solved in each and every cell to obtain predictions for the local values of hydrogen concentration and pressure (among others). For FLACS simulation, the mesh must consist of cubical and rectangular cells that are horizontally and vertically aligned in the x, y and z directions of the obstacles. The cell size of a grid is a crucial factor since it affects the accuracy of the simulation results and duration of the simulation (wall clock time). Too large cell size gives a rough indicative result, while too small cell size leads to a too long simulation and tends to over predict the results (e.g. in vapour cloud explosion simulations burning velocities are over predicted when cell size is smaller than 1 to 2 centimetres). (Gexcon AS 2018) The cell size should be selected by the relative to the geometry and domain length-scales and the leaking substance; the more reactive substance the smaller cell size should be used.

The size of the computational mesh (cell count) itself is primarily influenced by the simulation geometry. In FLACS, there must be terrain in the geometry where the bottom of the grid is placed. The grid must not exceed the boundaries of the terrain as FLACS assumes that everything outside the terrain is an empty space.

FLACS has a pre-processor porosity calculation program ‘Porcalc’ that can detect objects smaller than the cell size of mesh (e.g. pipes) as obstacles. ‘Porcalc’ has built-in information: *“Porcalc reads the grid and geometry files and assigns volume and area porosities to each rectangular grid cell”* (Gexcon AS 2018). In the simulations, the porosity field represents the local congestion and confinement which allows smaller objects to be considered as obstacles. (Gexcon AS 2018) Porcalc automatically transfers

the objects to the nearest line of mesh. This can cause unwanted flaws to the 3D geometry such as gaps between walls. For this reason, when drawing up mesh, it is important that the largest objects (such as walls, ceilings, and large process equipment) are aligned with the grid lines before using the 'Porcalc' function. For smaller objects, it is not as critical set to align with grid line unless the geometry does not have many objects. (Gexcon AS 2018)

The hexahedral mesh is created in the CASD pre-processor using the 'Quick Grid' function. First, the size of the grid (in metres) is determined by setting the minimum and maximum values for x, y, and z directions and the simulation volume was determined as 7 959 060 m^3. Minimum and maximum values determine where the grid begins and where it ends. It is possible to choose whether to use a uniform cell size in all directions, or to determine the individual cell sizes for each coordinate direction.

Creating mesh varies between different simulation scenarios. In this study, two scenarios were used: dispersion and ventilation scenario and VCE scenario. The same values of the computational mesh size (minimum and maximum values) and cell size were used for both scenario settings. The cell size was selected to be 1.5 metres, which is the recommended value for large geometries where the leakage contains a highly reactive substance (hydrogen in this study). In Appendix 1 a different cell sizes were compared and the test results showed that the cell size have a major impact on the results.

For the dispersion and ventilation scenario, the grid was modified, whereby both the cubical and the rectangular cells were present. Towards further away from the compressor shelter i.e. less interesting areas, the edge cells were strengthened to make the simulation effective enough. In addition, the grid was made denser around the leakage point; this function ensures that the leaking gas in the simulation is not initially diluted. The editing of a grid in dispersion and ventilation scenario ensures that the simulation can be done in a reasonable time and results are reliable. In a VCE scenario, it is essential that the cell size is equal in all directions and in the cubical shape. Figure 15 shows the grids for two different scenarios.

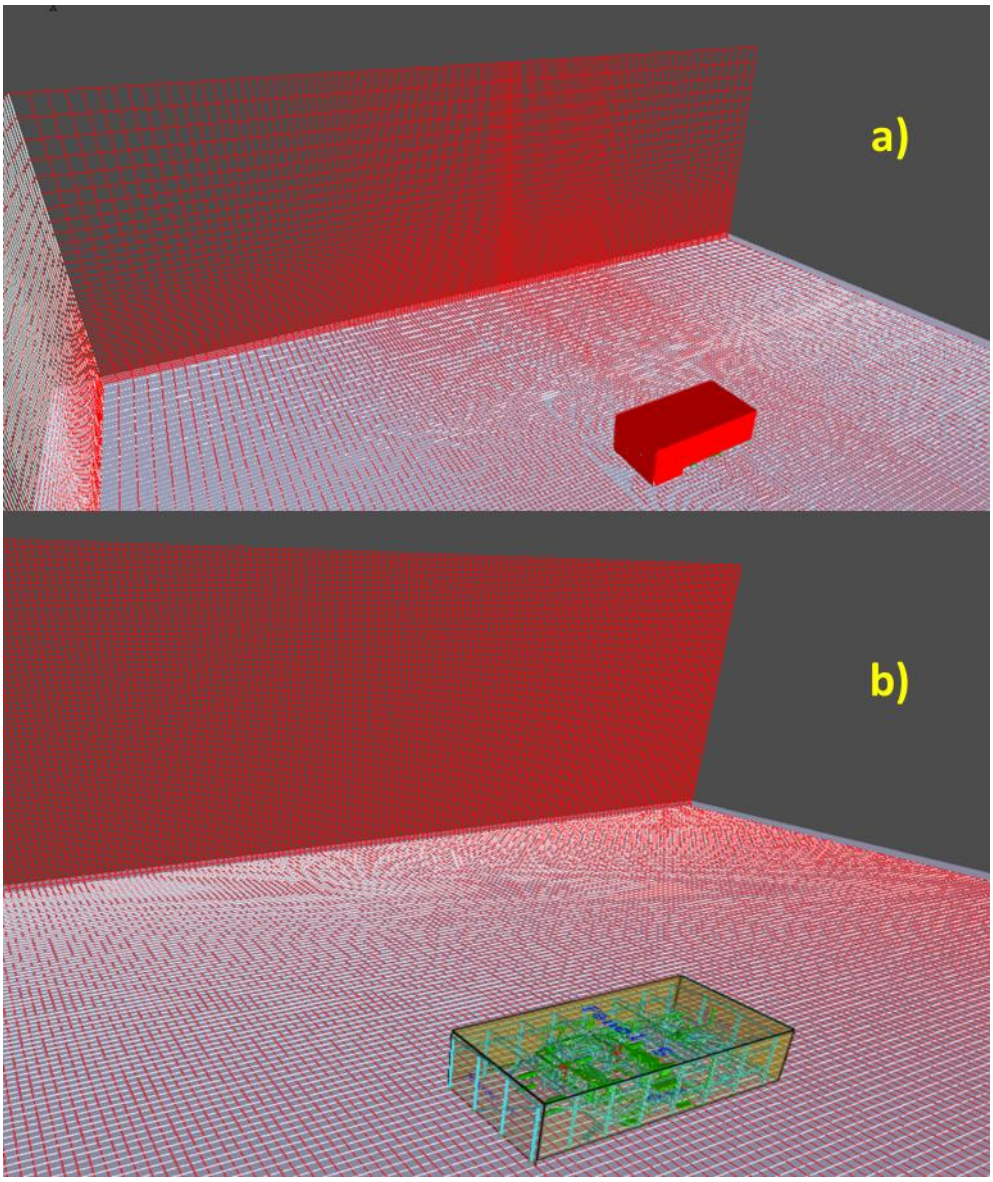

Figure 15. Grid differential in a) dispersion simulation and b) vapour cloud explosion.

The interesting variables predicted in FLACS such as pressure, temperature and volume ratio are simulated in every simulation cell, but in order to store data in specific locations monitor points must be defined by the user prior to the simulation. According to the instructions of Gexcon AS (2018), the monitor points should be placed according to the mesh and not according to geometry.

In this study, the same monitor points were used in both dispersion and gas explosion scenarios. Depending on the scenario, different variables were selected to be saved. In total 25 different monitor points were used and their locations are shown in Figure 16.

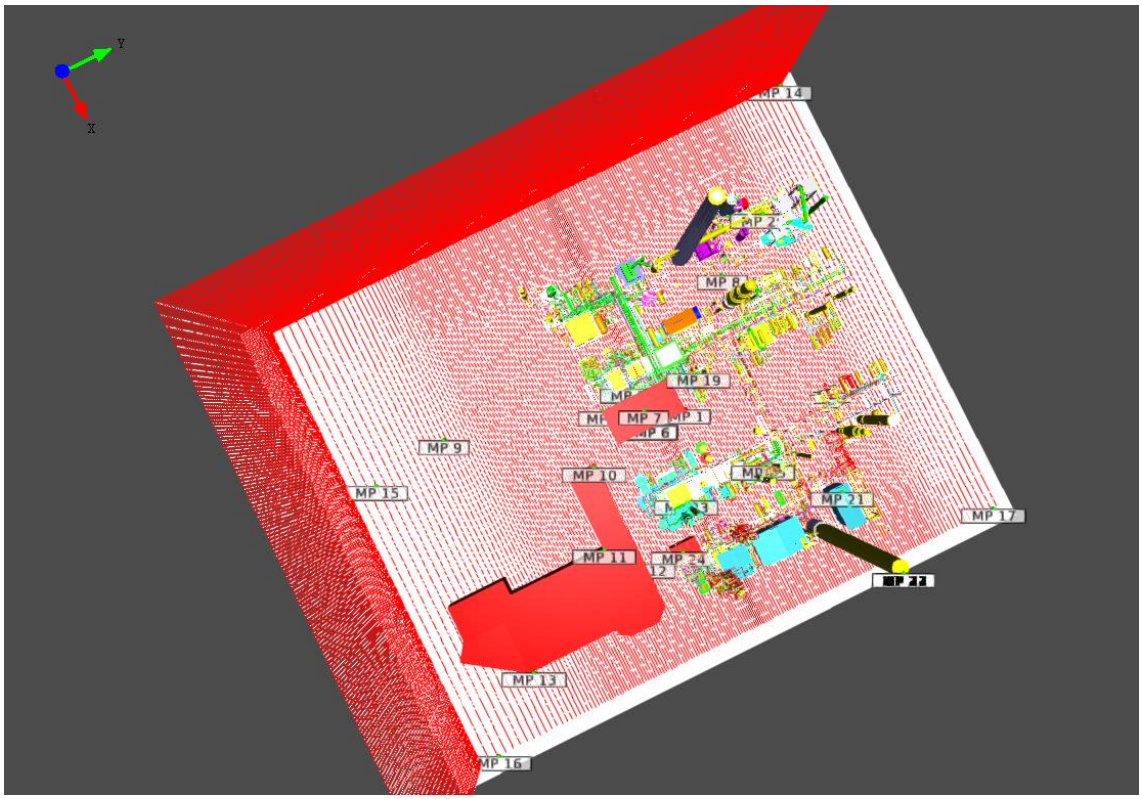

Figure 16. Location of the monitor points. The points were kept constant throughout the whole modelling work.

In order to make 2D or 3D contour plots of the desirable variables, the user defines ‘Single field 3D output’ in FLACS. The number of saved variables should be optimized with regards the file size and computer performance. Table 6 lists the saved variables used.

Table 6. Selected variables for monitor points and contour plots for two different scenarios.

Scenario	Monitor points	Contour plots
Dispersion and ventilation	Fuel mole fraction (FMOLE [m3/m3]) Pressure (P [bar(g)]) Velocity value (UVW [m/s]) Fuel mass fraction (FUEL [-])	Fuel mole fraction (FMOLE [m^3/m^3]) Velocity vector (VVEC [m/s]) Equivalence ratio (ER [-])
Vapour cloud explosion	Drag value (DRAG [Pa]) Fuel mole fraction (FMOLE [m^3/m^3]) Pressure (P [bar(g)]) Combustion product mass fraction (PROD [-]) Temperature (T [K]) Velocity value (UVW [m/s]) Fuel mass fraction (FUEL [-]) Mach number value (MACH [-]) Pressure impulse (PIMP [Pa*s]) Density (RHO [kg/m3])	Fuel mole fraction (FMOLE [m3/m3]) Pressure (P [bar(g)]) Combustion product mass fraction (PROD [-]) Velocity vector (VVEC [m/s]) Maximum pressure (PMAX [bar(g)])

5.3.3 Defining boundary conditions for the dispersion scenarios

The modelling initiated with defining boundary conditions for the hydrogen dispersion scenarios. In dispersion simulations different weather conditions (Pasquill atmospheric stability classes shown in Table 7) and wind directions were taken into account. Pasquill atmospheric stability class is a method for classifying the amount of turbulences in the atmosphere (Gexcon AS 2018).

Table 7. Pasquill stability classes.

Stability class	Type	Occurence
A	Very unstable	Weather conditions with a significant vertical mixing. Can occur during sunny days, when the ground heating causes the strong movements of an upward convected air. (Ponchaut et al. 2016)
B	Unstable	
C	Slightly unstable	
D	Neutral	Cloudy weather. Can occur both day and night time. (Ponchaut et al. 2016)
E	Slightly stable	Usually at night time. The ground cools down due to radial heat transfer to the atmosphere. As a result, stable density stratification is formed in the atmosphere and turbulence decreases. (Ponchaut et al. 2016)
F	Stable	

In this study, the 5D and 2F were chosen as weather types where numbers 5 and 2 represent wind velocities metres per seconds (m/s). The 5D weather condition represents the average atmospheric conditions in southern Finland and 2F weather condition corresponds to the most unfavourable situation spreading. Table 8 shows more detailed weather conditions for 2F and 5D in this study.

Table 8. Properties of 5D and 2F weather conditions in this study.

Parameter	Weather condition	
	5D	2F
Wind velocity	5 m/s	2 m/s
Outside-air temperature	+15 C	+ 15 C
Outside-air relative humidity	70 %	70 %
Atmospheric stability class	D (neutral)	F (stable)
	Weather condition represents the average atmospheric conditions in Southern Finland.	Weather condition corresponds to the most unfavourable situation spreading. The mixing of air with fuel is minor. It is a typical weather condition during clear nights or winter days.

South-westerly, southerly, and easterly winds were chosen as the wind directions. The South-westerly wind is a dominant wind direction in the modelled region, the southerly and easterly winds were considered as the most unfavourable directions for hydrogen spreading with respect to the surrounding process area. Total of six dispersion simulations were made for each model in which the weather conditions and wind directions varied.

With the defined atmospheric conditions and wind directions the boundary conditions of a simulation domain were determined. In dispersion simulation, the boundary conditions can be set automatically using the Wind Wizard function. This determines the wind condition type for modelling. The function determines the wind direction, wind speed, air temperature, Pasquill class, ground roughness, and boundary condition. Wind speeds were determined according to weather types by 5 m/s and 2 m/s. The temperature was selected to be 15 °C and Pasquill to neutral (D) and stable (F). Ground roughness was selected to be 1 metre, which is a common value for the area with regular large objects. The boundary condition was Nozzle formulation, which is the best suited for a porous area with many different objects (Gexcon AS 2018).

After defining the boundary conditions, the leakage was determined. FLACS simulates a leakage as a gas outlet that begins at a user-defined leakage point and spreads within the computation area. In CASD, the leakage is determined by the Leakage Wizard function, which automatically adjusts the leakage. A leakage can be defined to occur either from a specific point (within a single grid cell) or an area leakage (leakage covers multiple grid cells) (Gexcon AS 2018). In this study, the leakage was determined to occur within a single cell at the flange joint of the compressor's pressure face (1.5 metres from ground level). Table 9 lists the parameters which were used to set the leakage.

Table 9. Parameters and values for jet leakage in 'Leakage Wizard' -function.

Parameter	Jet leakage values for dispersion and ventilation simulation scenarios
Gas type	Hydrogen
Volume (equipment) [m^3]	350.0*
Pressure (equipment) [bar(g)]	115.0
Temperature (equipment) [°C]	120.0
Atmospheric temperature [°C]	15.0
Nozzle diameter [m]	0.028
Discharge coefficient [-]	0.85
Start time [s]	0.0

* The volume is based on a 15 min hydrogen leak rate.

Based on calculation done with PHAST previously, it has been shown that in the worst case situation a leakage, from the hole with a diameter of 28 millimetres, can leak at the same velocity as flow velocity. The duration of 15 minutes is an estimate during which operators are expected to notice a weakened flow and locate the leakage.

The volume of the leaking device (i.e. compressor) was calculated according to the leakage rate, the density of the leaking fuel (hydrogen) and duration as seen in Equation 2.

$$V = \frac{\dot{m}\, t}{\rho} = \frac{2.78\ \frac{kg}{s} \cdot 900\ s}{7.155\,\frac{kg}{m^3}} = 350\ m^3 \qquad (2)$$

In which

V is the volume of the equipment [m^3]
ṁ is the mass flow rate [kg/s]
t is the duration time [s]
ρ is the density [kg/m^3]

The density at the rupture point, *ρ*, was calculated by ideal gas Equation using hydrogen molar mass as seen in Equation 3

$$\rho = \frac{PM}{RT} = \frac{11601325\ \frac{N}{m^2} \cdot 2.016\,\frac{kg}{kmol}}{8314\ \frac{Nm}{Kkmol} \cdot 393.15\ K} = 7.155\ \frac{kg}{m^3} \qquad (3)$$

In which

P is the pressure [N/m^2]
M is the molar mass [kg/kmol]
R is the universal gas constant [Nm/K/kmol]
T is the temperature [K]

With input results listed in Table 9, the Leakage Wizard calculated the values of leakage output rate, which are listed in Table 10.

Table 10. Parameters and values for leakage outlet in 'Leakage Wizard' -function.

Parameter	Leakage outlet value for dispersion and ventilation simulation scenarios
Area [m^2]	0.000625
Velocity [m/s]	805.566
Mass flow [kg/s]	2.78
Relative turbulence intensity [-]	0.1
Turbulence length scale [-]	0.002822
Temperature [°C]	97.272
Start time [s]	0.0
Duration [s]	900

The total leakage area is user defined and In this study, the leakage area was determined to cover the volume inside the computational mesh (see Figure 17).

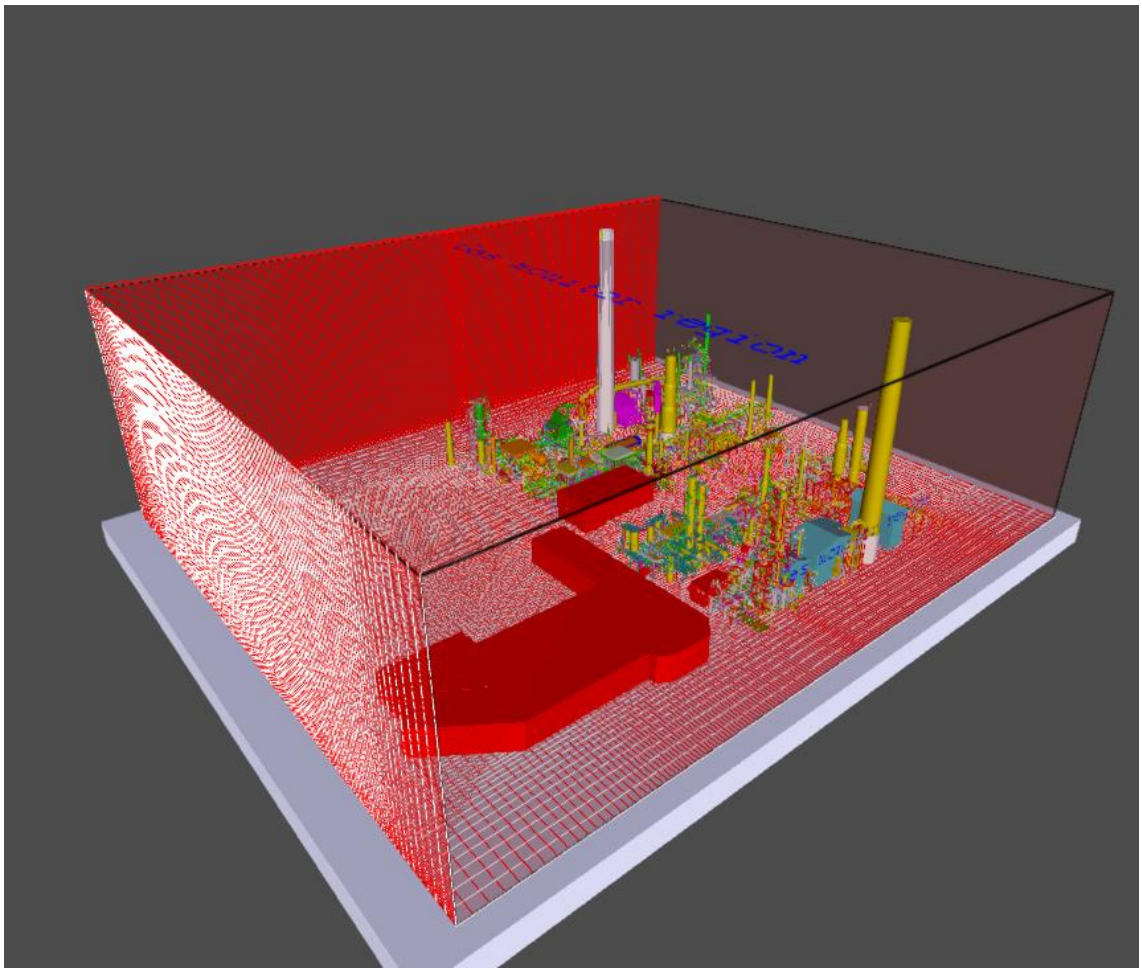

Figure 17. Total leakage area of modelling area.

In addition to leakage scenario set user defines the general simulation and output control values for the simulations. The defined parameters are the maximum simulation time (TMAX), Courant-Friedrich-Levy number based on sound velocity (CFLC), Courant-Friedrich-Levy number based on fluid flow velocity (CFLV), MODD time-step (MODD), and parameters determine how often the field plot data (NPLOT) and simulation data (DTPLOT) are written. In addition, the simulation start time (TSART), the minimum time (TMIN), the last time step, the load number and the scale can be determined separately if needed. The set parameters for simulation and output control for dispersion simulations are listed in Table 11.

Table 11. Simulation and output control values for dispersion simulations.

Property	Value for Dispersion and ventilation
TMAX	900 s
CFLC	10
CFLV	1
MODD	10
NPLOT	-1
DTPLOT	10 s

CFLC and CFLV values determine the time steps in the simulation for the sound wave (CFLC) and fluid flow (CFLV). Each time step is selected so that the sound velocity and fluid flow can proceed only a limited distance. (Gexcon AS 2018) The values CFLC 10 and CFLV 1 were used (values were automatically proposed in a FLACS Run Simulation), the higher values resulted in unstable simulation and thus too high mass residual error. Therefore the values had to be lowered to 10 and 1.

5.3.4 Defining boundary conditions for the gas explosion scenarios

Gas explosion scenarios in each model were based on the dispersion simulation scenario which gave the largest flammable stoichiometric gas cloud (more detailed discussion about the results is presented in chapter 6). The boundary conditions for gas explosion scenarios were based on the dispersion scenarios. Instead of the Nozzle formulation the boundaries based on Euler Equation were used which are commonly used in gas explosion simulations (Gexcon AS 2018).

The simulation and output control values differ in some extent from the dispersion modelling. Values for simulation and output control are shown in Table 12.

Table 12 Simulation and output control for gas explosion scenarios.

Property	Value for Vapour cloud explosion
TMAX	-1 s
CFLC	5
CFLV	0.5
MODD	1
NPLOT	25
DTPLOT	0.025 s
TMIN	1.5 s

In a gas explosion scenario, the maximum time is not usually determined (set value -1), but the simulation stops automatically when ignition occurs and either of two criteria is met (Gexcon AS 2018):

1. At least 90% of the fuel is burnt or has left the calculation area
2. At least 50% of the fuel is burnt or has left the calculation area *and* the mean pressure value is negative

In this study, the default values for CFLC and CFLV were used. The CFLC time step limit is generally a determinant factor at an early stage of the explosion when flow rates and combustion rates are still low. While the value of CFLV is generally a determinant factor after of an explosion, when flow rates and burning rates are high. (Gexcon AS 2018) Additionally, a minimum time (TMIN) was determined. In practice, the TMIN means that the simulation does not stop automatically before the set value is reached. For this work, the minimum simulation time was selected 1.5 seconds.

For the explosion scenario, flammable gas cloud was determined according to the dispersion simulations. The flammable vapour cloud was assumed to be pure hydrogen gas and in FLACS the properties of hydrogen are already defined. It is possible to identify toxic substances in the gas mixture. In this study it was assumed that no toxic substances are present.

The location and size of a formed vapour cloud were determined according to results obtained from dispersion simulations. Figures 18, 19 and 20 show the location and size of three different clouds of vapour cloud explosion simulations. A more detailed description of these vapour clouds (e.g. size, volume, and mass) is described in chapter 6.

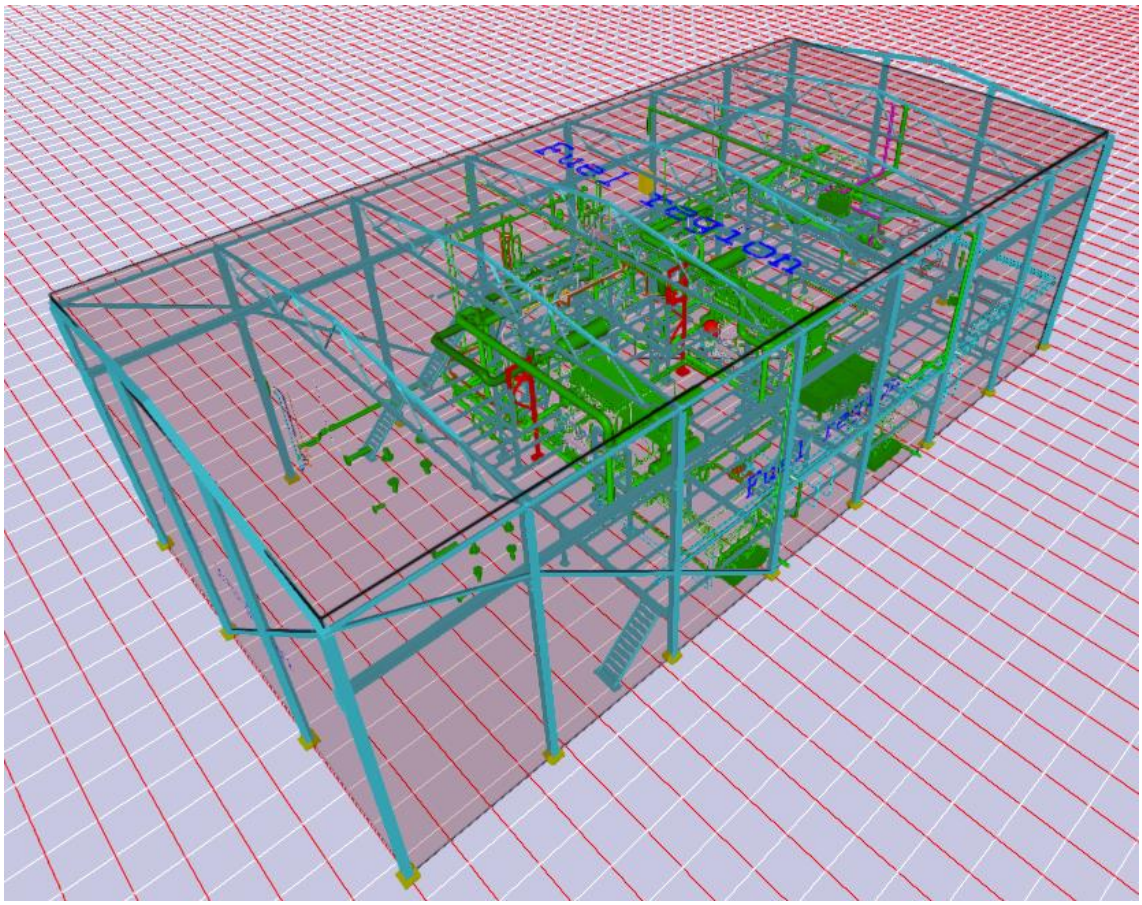

Figure 18. Volume (8200 m^3) of a hydrogen vapour cloud in Model1 (20m x 40m x 10.5m and mass of a flammable vapour cloud: 160 kg).

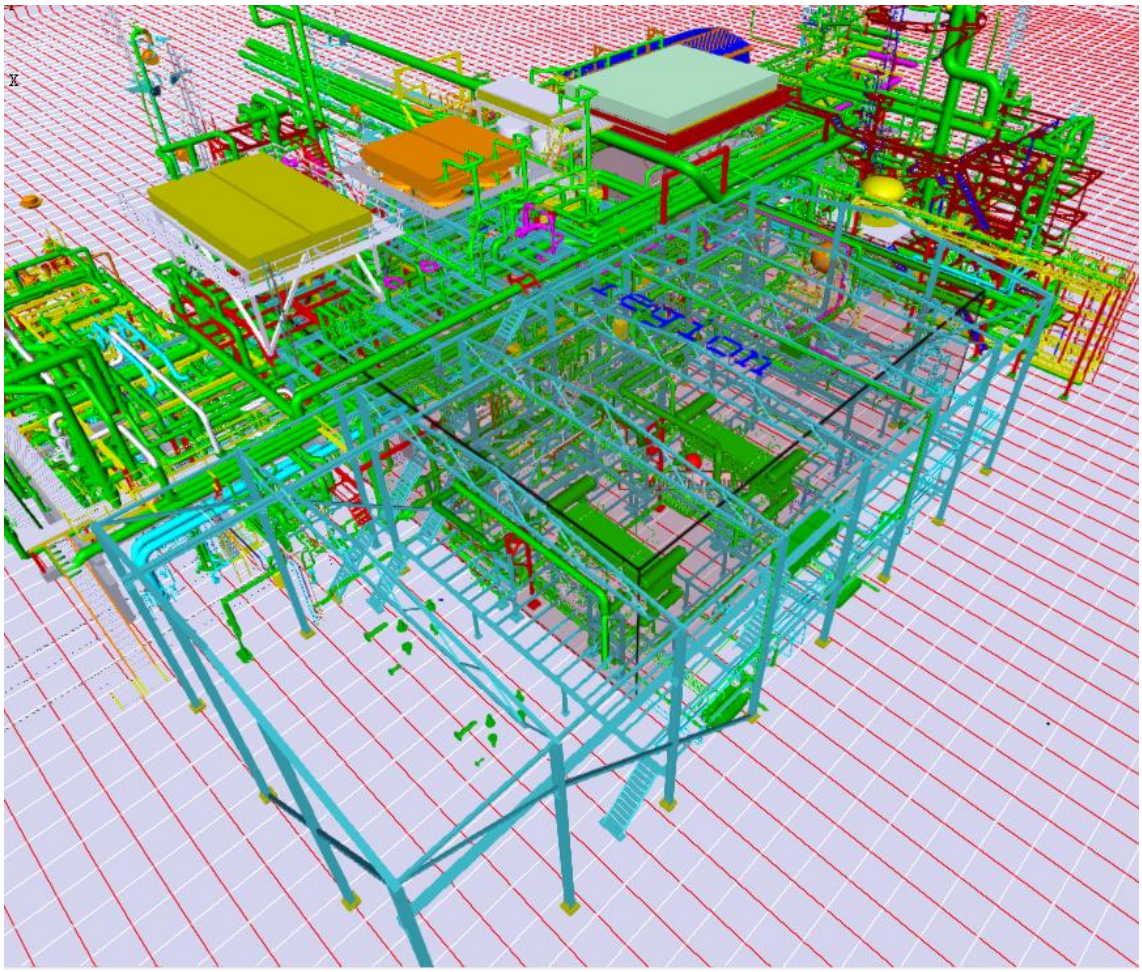

Figure 19. Volume (7500 m^3) of a hydrogen vapour cloud in Model2 (19m x 46.5m x 8.5m and mass of a flammable vapour cloud: 140 kg).

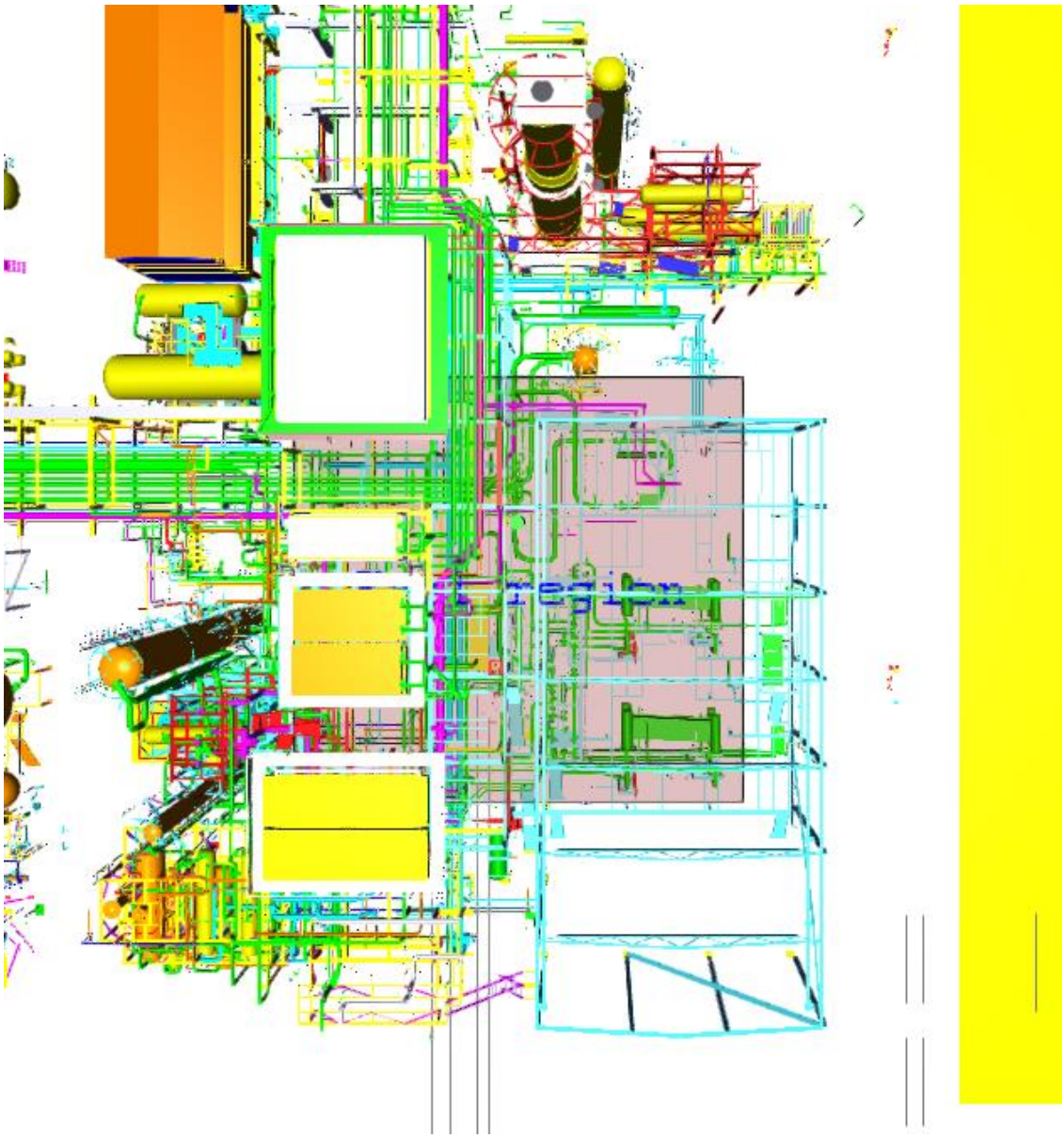

Figure 20. Volume (7400 m^3) of a hydrogen vapour cloud in Model3 (18.5m x 47.5m x 8.5m and mass of a flammable vapour cloud: 138 kg).

Additionally pressure relief panels were used to represent the walls and roof of a compressor shelter. Pressure relief panels represent the situation where the walls 'opens' during an explosion as the 'real thick walls' are assumed in FLACS to withstand the explosion. Panels were edited in a way that they represent the walls and roof of a compressor shelter, which are all the same and shelter does not have lightweight wall. In vapour cloud explosion simulation FLACS assumes, if no pressure relief panels are used, that normal walls stand up during an explosion and therefore the generated

overpressures are much higher and do not represent the realistic values. In real, the walls of compressor shelter are so light that they will not withstand in case of an explosion. This is why the thick walls were replaced with pressure relief panels.

The wall and roof of the compressor shelter consist of corrugated sheet made of stainless steel. Figure 21 shows the walls and roof of compressor shelter in MicroStation (a) and pressure relief panels (b).

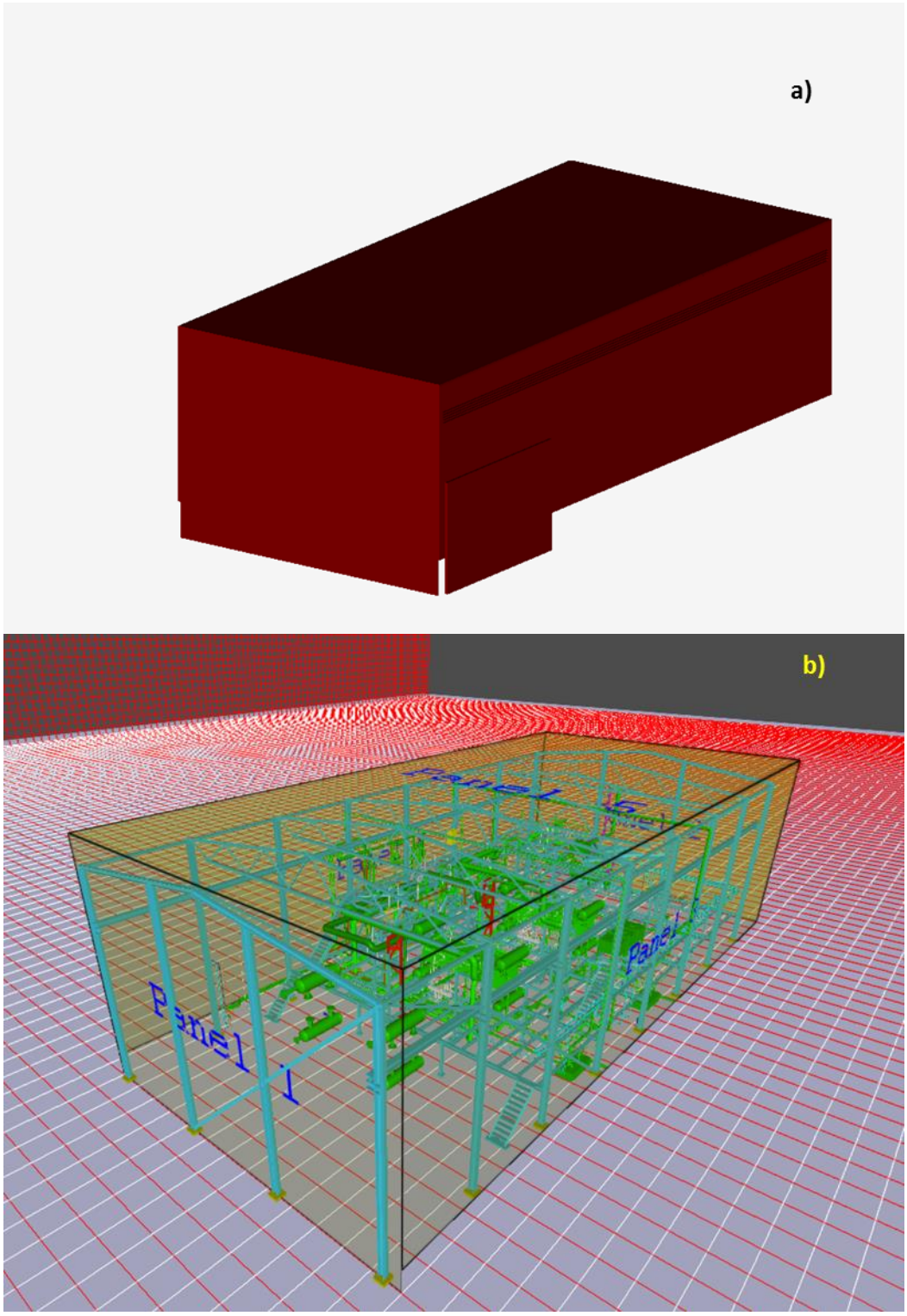

Figure 21. Walls and roof of a compressor shelter in MicroStation v8i (a) and in CASD (b). The size of the compressor shelter is 19 x 40 metres and the height is 13 metres.

The compressor shelter is open at bottom: side and back walls are 1.2 metres off the ground for ventilation. Shelter also has small (0.5 m) venting openings in the upper

walls (except the front wall). However, these vent openings did not print in CASD as the wall shape was too special shaped. Therefore it was made a conservative assumption that compressor shelter has ventilation only at the bottom. In the explosion modelling it was assumed that all the walls will fall at the same time.

In this study, the 'unspecified' active panel for walls and roof was selected. The relief panel opening pressure difference it was set to be 0.1 bar(g). The pressure value was chosen based on the effects of overpressure on structures and buildings (Casal 2008), where the effect of 0.1 bar overpressure is in some extent damage to the steel structures of the buildings. It should be pointed out that in this study panels are not represented as a precaution but their purpose is only to represent the breaking of the shelter walls and roof during an explosion. The porosity value before the explosion was determined to be zero (fully non-porous) and after the explosion one (the walls have completely yielded). Panels can be determined a weight of kilogram per square metre. If the weight of the panel is set to 0 kg/m^2, then in the simulation FLACS assumes that the wall is so light that the mass forces can completely be ignored. The weight of the panels was assumed to be 10 kg/m^2, since they are made of steel. For the panels, a dimensionless drag coefficient needs to be set Drag coefficient is used when modelling the attraction force of the panel to fluid. The value was set to 2, which is the recommended value in FLACS.

5.3.5 Running the models

When the scenario definition was ready in CASD, then the simulation was performed in a separate simulation program called FLACS Run Manager. It is possible to follow simulation results in Run Manager with simulation Plot and Log file (as seen in Figure 22). However, more detailed results can be followed in a separate pre-processor called Flowvis. In Flowvis it is possible to visualize the results for example based on graphs, 2D plots and 3D plots. The results presented in this study are done by Flowvis 5.

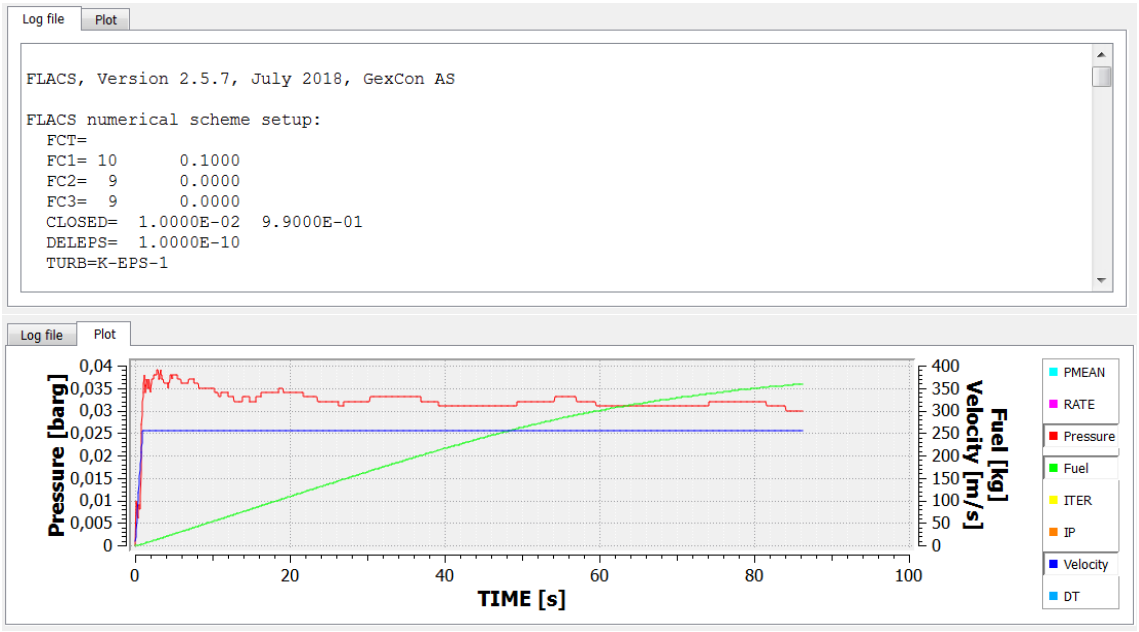

Figure 22. Log file and Plot in FLACS Simulation Run Manager.

6 RESULTS

The aim of chapter 6 is to present and discuss the results obtained from the dispersion simulations and vapour cloud explosion simulations. The purpose was to find out at which modelling conditions worst case scenario is formed.

6.1 Dispersion simulations

The criteria for the worst-case hydrogen vapour cloud in this study were the largest cloud volume between the flammability limits and the largest mass of a flammable vapour cloud. At each scenario different weather conditions were performed.

FLACS evaluates the flammable vapour cloud according to a special equivalent stoichiometric gas cloud. It is common to use stoichiometric vapour clouds in worst case scenarios but most of them are however too conservative and can lead to overestimated results. The specific equivalent stoichiometric vapour clouds, Q8 and Q9 that are used in FLACS, are less conservative options as they are smaller scaled clouds with high reactivity (compared with other conservative gas clouds). The idea is that any explosive effects of a non-homogeneous VCE can be estimated for a smaller vapour cloud which has the stoichiometric concentration. At this kind of vapour cloud the reactivity is high and VCE occurs as detonation. (Hansen *et al.* 2013)

The Q8 equivalent stoichiometric vapour cloud takes into account the volume expansion of vapour cloud. The Q8 cloud formula is shown in Equation 4 (Hansen *et al.* 2013).

$$Q8 = \frac{\Sigma\, Volume_{Fuel} \cdot E}{E_{max}} \qquad (4)$$

In which

Q8 is the equivalent stoichiometric vapour cloud [m^3]
$\Sigma Volume_{Fuel}$ is the overall flammable volumes of the grid inside the gas monitor region [m^3]
E is the volume expansion of the actual mixture
E_{max} is the maximum expansion of the mixture

Q8 is best suited for situations where the burning rate is of a little importance for the stoichiometric cloud. Such situations are for example the formation of a large vapour cloud in a fully enclosed space (ventilation is non-existent), or situations where combustion causes rapid flame speed (e.g. DDT) and the unburned gas have no time to burst into flame during combustion. (Hansen *et al.* 2013)

The Q9 cloud is a less conservative option that takes into account also the laminar burning rate. Therefore, the Q9 cloud is best suited for areas with ventilation. The Q9 cloud scales a non-homogeneous vapour cloud into a smaller stoichiometric vapour cloud that is expected to give similar explosion loads as the original cloud. The Q9 cloud formula is shown in Equation 5 (Hansen *et al.* 2013)

$$Q9 = \frac{\Sigma\, Volume_{Fuel} \cdot S \cdot E}{(S \cdot E)_{max}} \qquad (5)$$

In which

Q9 is the equivalent stoichiometric vapour cloud [m^3]
$\Sigma Volume_{Fuel}$ is the overall flammable volumes of the grid inside the gas monitor region [m^3]
S is the laminar burning velocity for the actual concentration

E is the volume expansion of the actual mixture
S_{max} is the maximum laminar burning velocity
E_{max} is the maximum expansion of the mixture

In this study, the selected stoichiometric cloud was originally Q9 because it is the recommended and mostly used cloud type by FLACS users. In addition, the compressor shelter is not an enclosed area. This was thought to have a significant effect on the laminar flame rate and for that reason the Q9 cloud was selected. However, the overpressure results of explosion simulations seemed to be too low. After examining the results more closely and discussing with Gexcon the cloud type was selected to be Q8. The comparison of these two cloud types is shown in more detailed in Appendix 2.

The more conservative Q8 cloud is better suited for the studied area since the hydrogen vapour at the flammability limits fills the compressor shelter. In addition, hydrogen is also a reactive fuel with a maximum laminar velocity of 2.85 m/s that makes it possible to form DDT. In the following sections results obtained in dispersion simulations are discussed separately.

6.1.1 Model1 - Compressor shelter

The dispersion simulation of Model1 was performed in an area where the volume blockage ratio was formed by the compressor shelter with equipment inside. Figure 23 shows the volume blockage ratio at height of 1.5 metres.

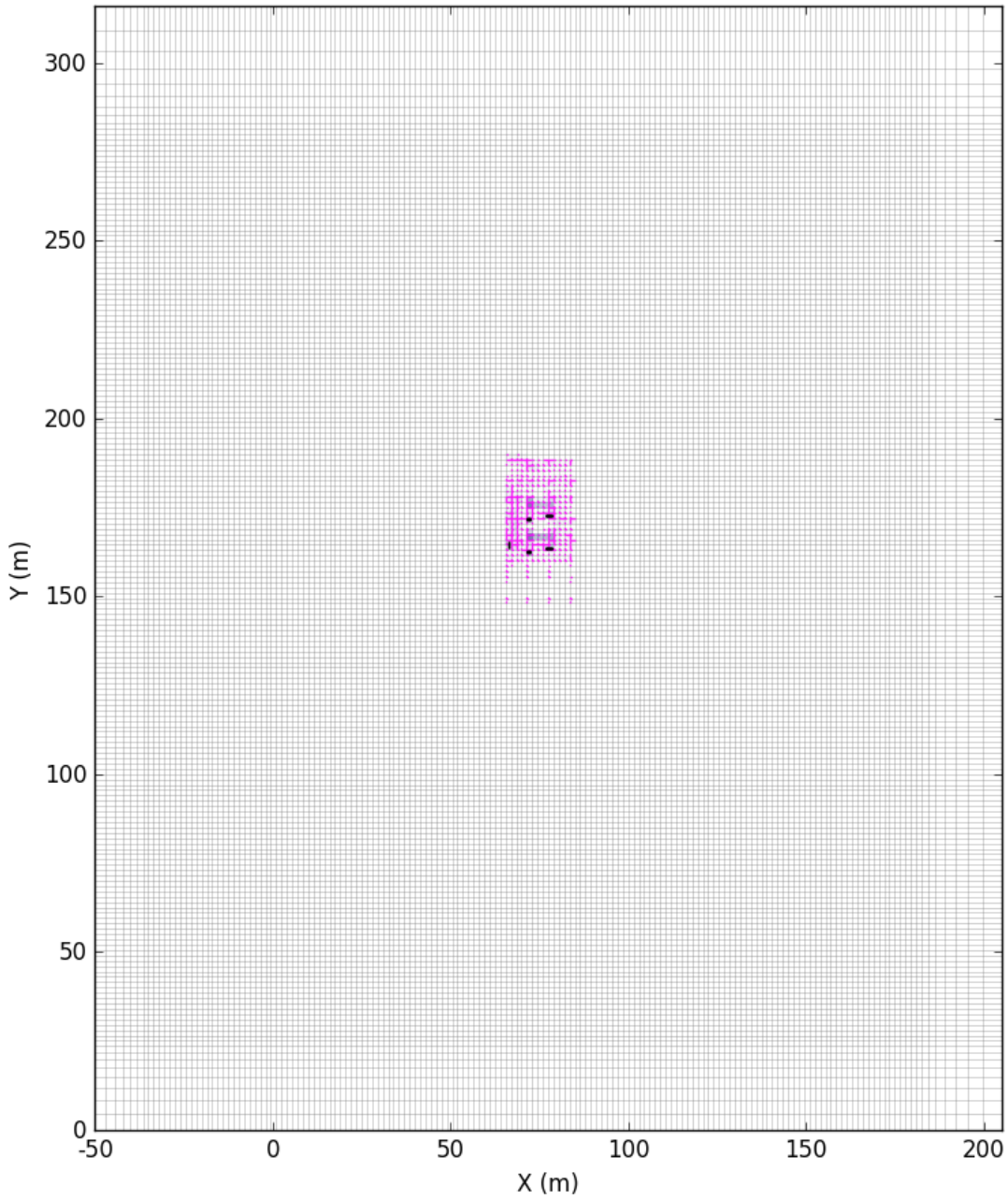

Figure 23. Volume blockage ratio (lilac) in Model1 at height of 1.5 metres.

The set duration for the dispersion simulations (15 minutes) was not reached due to the long simulation times. The simulations for all scenarios were interrupted when they had reached their steady-state conditions (maximum values for pressure, flammable material (fuel), and leakage velocity). Figure 24 shows the general log simulation results for six different scenarios.

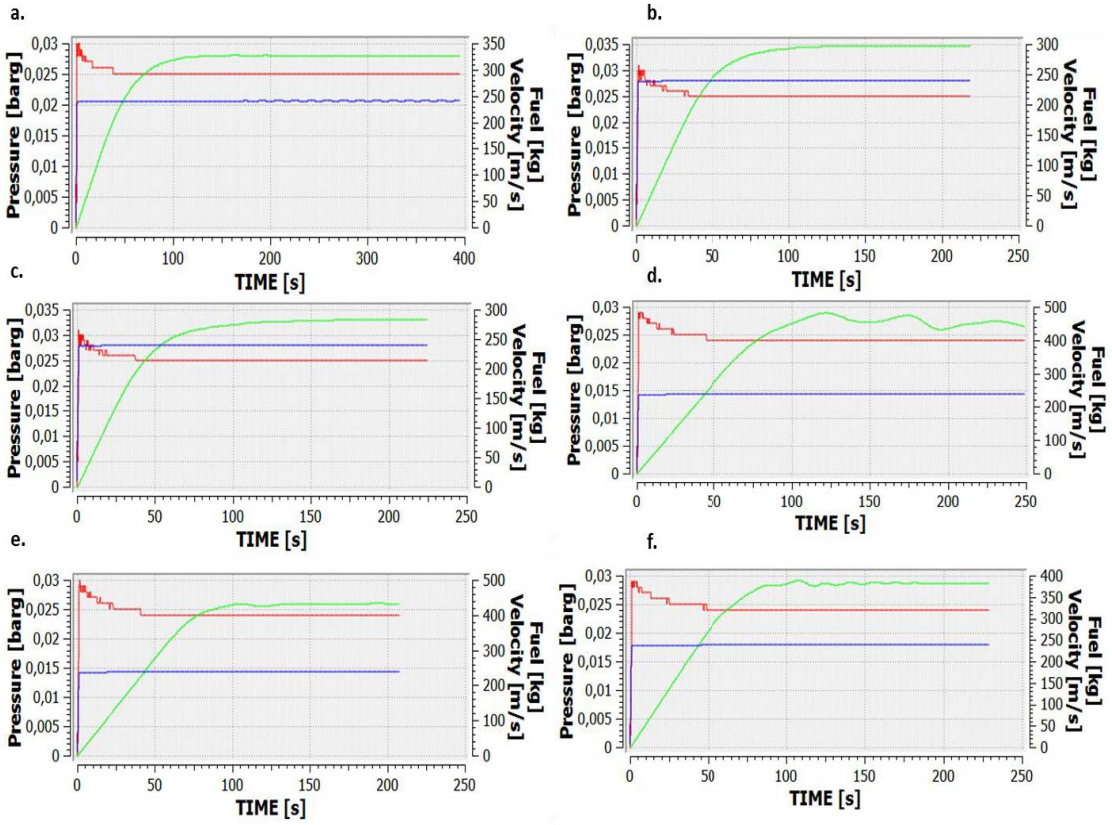

Figure 24. Dispersion simulation results in general simulation log files in different scenarios: a. 5D south-westerly wind direction, b. 5D southerly wind direction, c. 5D easterly wind direction, d. 2F south-westerly wind direction, e. 2F southerly wind direction, and f. 2F easterly wind direction. A red line describes pressure, a green line the leakage fuel amount, and blue line the leakage rate.

As can be concluded from Figure 24, the maximum leakage amounts were reached in about 150 seconds. In general, in simulation log files, the amount of fuel (green line), pressure (red line), and leakage rate (blue line) were measured. It is very important to take into account that the amount of fuel measured in a simulation log file is *"as a function of time for a standard gas monitor region (covering the same volume as the complete computational domain, i.e. the closed cube)"* the values remain the same during the simulations and they are corresponding the initial value of flammable (Gexcon AS 2018). For gas explosion simulations, the amount of fuel was measured with the mass of a flammable vapour cloud. It measures the mass of flammable material ignoring the mass of air or oxygen. The mass of a flammable vapour cloud together with the volume of the stoichiometric vapour cloud over a time, are shown in Figure 25.

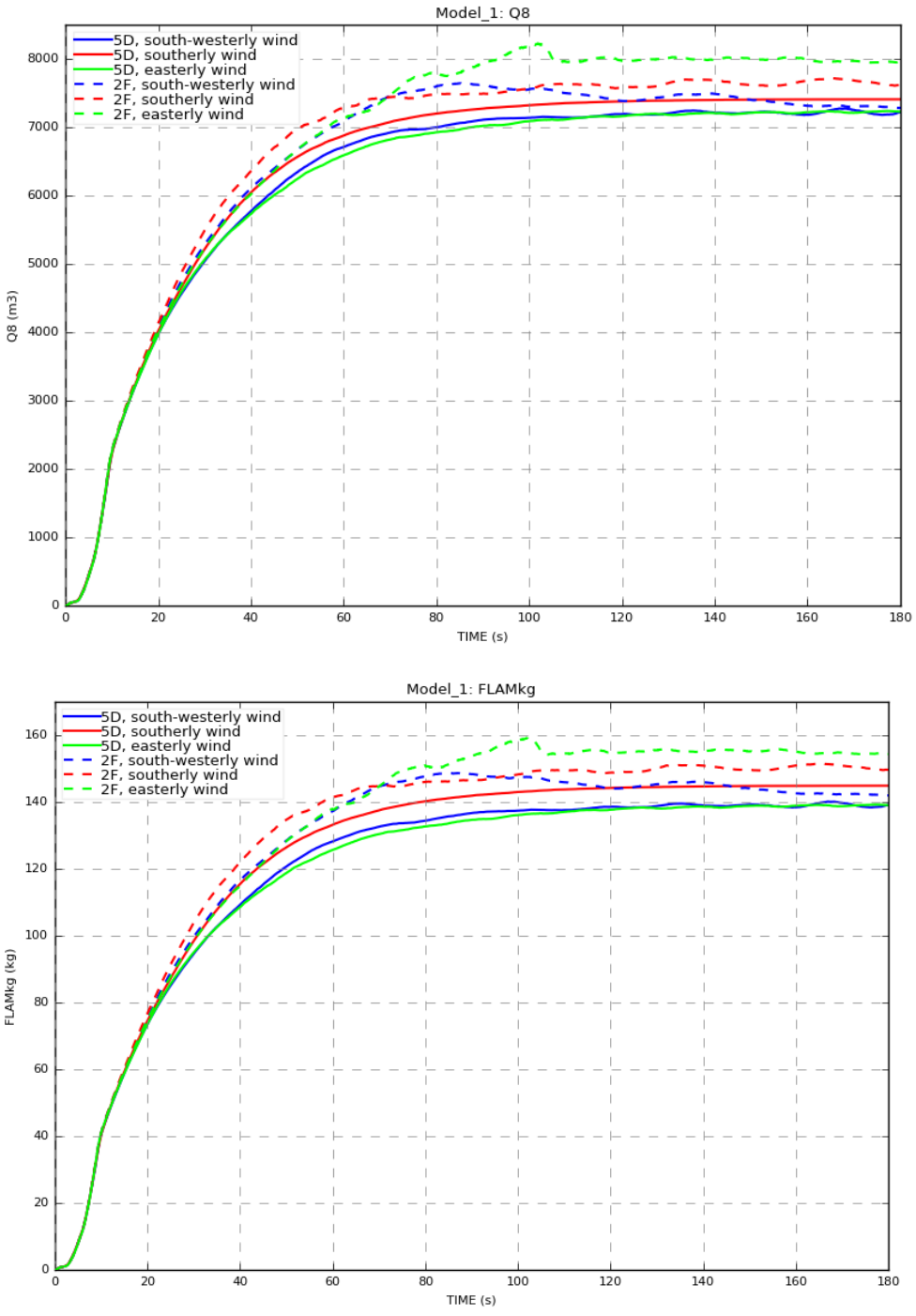

Figure 25. Volume-time plot of an equivalent stoichiometric vapour cloud (1.) and mass of a flammable vapour cloud (2.) in different scenarios.

As shown in Figure 25, both the maximum stoichiometric vapour cloud volume of 2800 m^3 (about 20m x 40m x 10,5m) and the mass of a flammable vapour cloud of 160 kg were reached in the 2F easterly wind scenario at about 100 seconds. Two results (Q8

and mass) are clearly in line with each other. Figure 26 shows the cloud dispersion range at 100 seconds at the height of 1.5 metres and presented from the side (YZ direction). The dispersion of a vapour cloud is shown in more detail in Appendix 3 which shows the volume fraction versus time. In the dispersion scenario in Model1 the highest values for Q8 and mass of a flammable vapour cloud were the biggest at the scenario of 2F easterly wind. Therefore it was chosen for further VCE simulations (described in more detail in section 6.2).

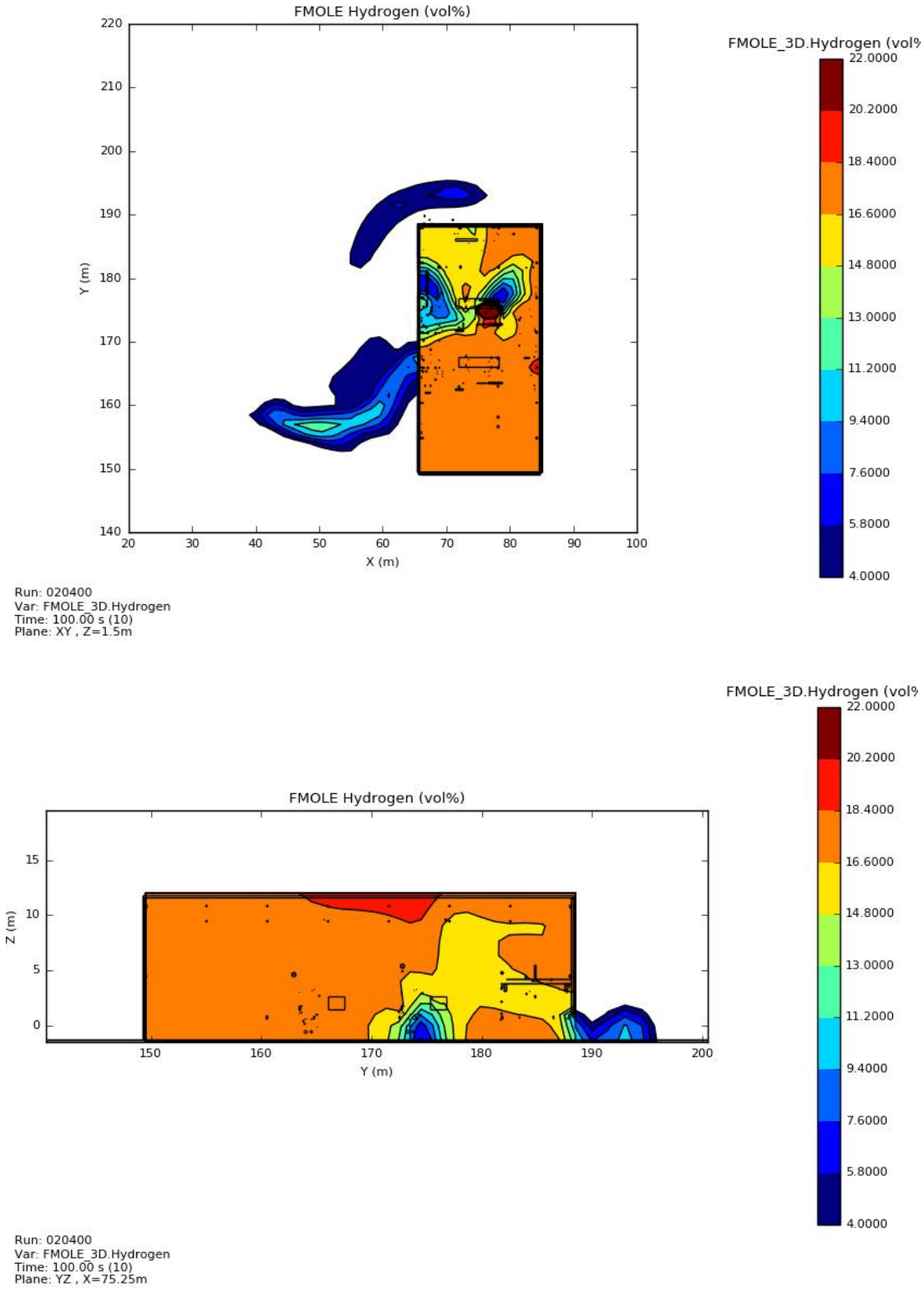

Figure 26. Hydrogen volume fraction (4-22 vol%) in the compressor shelter at 100 seconds with 2F weather condition and easterly wind direction.

6.1.2 Model2 – Diesel producing units and control building

The dispersion simulation of Model2 was performed in an area where the volume blockage ratio was formed by the diesel producing units and control building at the heights of 1.5 metres as shown in Figure 27.

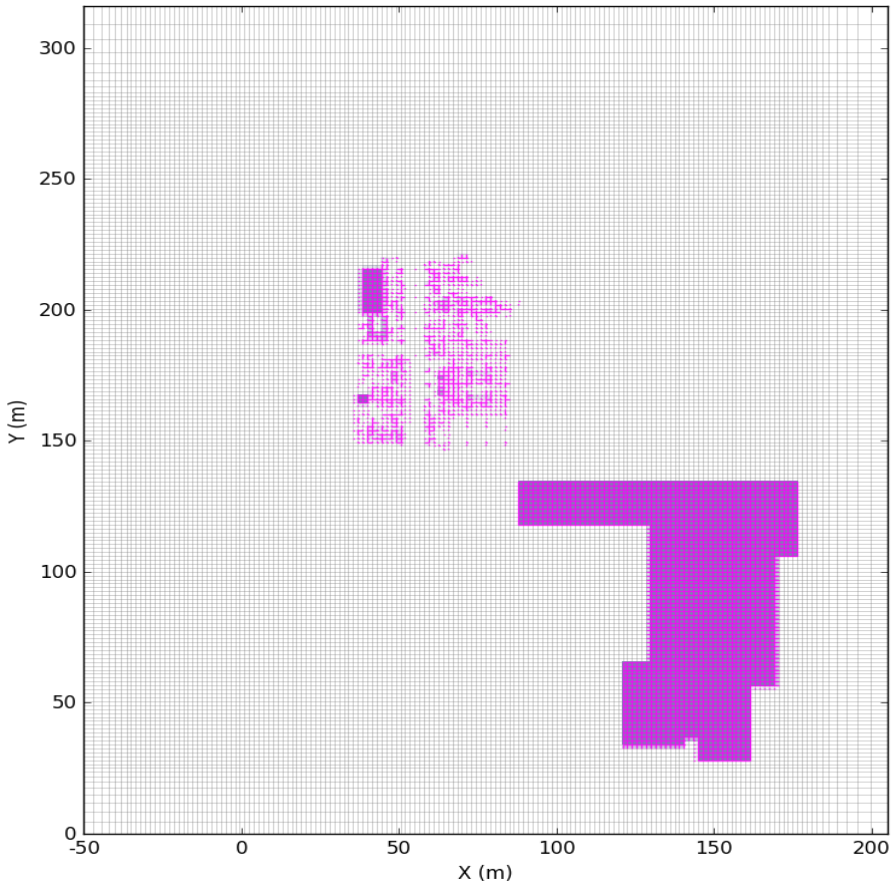

Figure 27. Volume blockage ratio (lilac) in Model2 at height of 1.5 metres.

As in Model1, the dispersion simulation set time duration (15 min) in Model2 was not reached. Dispersion simulations were initially performed under both weather conditions (2F and 5D) with a south-westerly wind direction (dominant wind direction at the refinery). Based on the results obtained, the weather type with higher values (the Q8 and mass of a flammable vapour cloud) was then selected and ran with two other wind directions. Figure 28 shows the volumes of equivalent stoichiometric vapour clouds and flammable masses for the 5D different leakage scenarios and the 2F scenario.

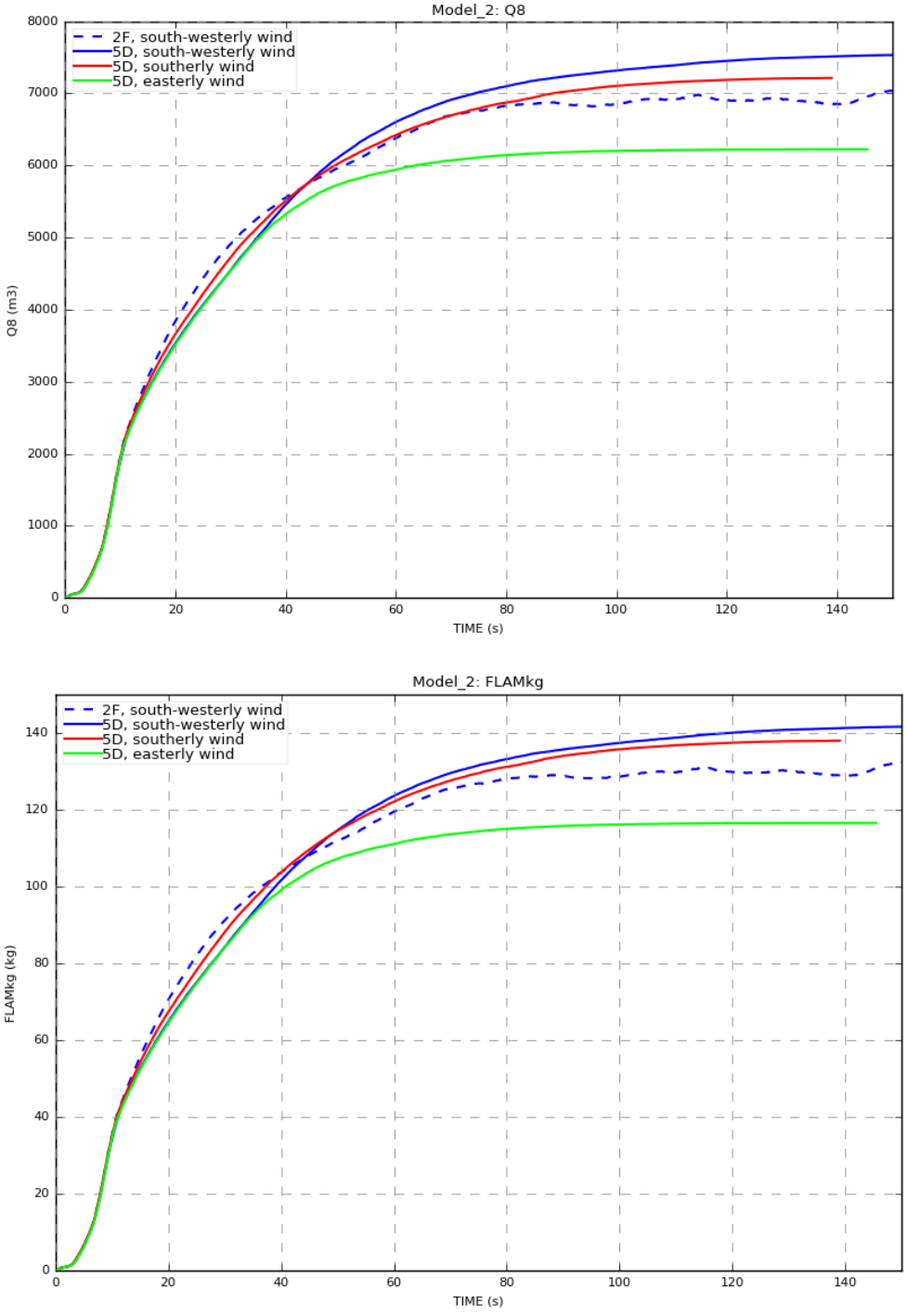

Figure 28. Volume-time plot of an equivalent stoichiometric vapour cloud (1.) and mass of a flammable vapour cloud (2.) in different scenarios.

As in Model1, Model2 shows that the volume curves of the stoichiometric vapour cloud follow the mass curves of the flammable vapour cloud. Figure 28 shows that worst case scenario is the 5D south-westerly wind scenario with a stoichiometric volume of about 7500 m^3 (about 19 m x 46.5 m x 8.5 m) and a flammable vapour cloud mass of about 140 kg which was reached in 130 seconds. This (5D) can be explained by the fact that a higher wind velocity blows more hydrogen gas into the process area where it is not easily evaporated but captured (if compared with Model1). The stoichiometric cloud volume of Model2 is smaller than for Model1. This is due to the volume blockage ratio, which is lower for Model1 and therefore the vapour cloud is slightly more spread out than in Model2. When looking at hydrogen in the volumetric fraction amount state (Figure 29) it is found that also the concentrations are lower for models.

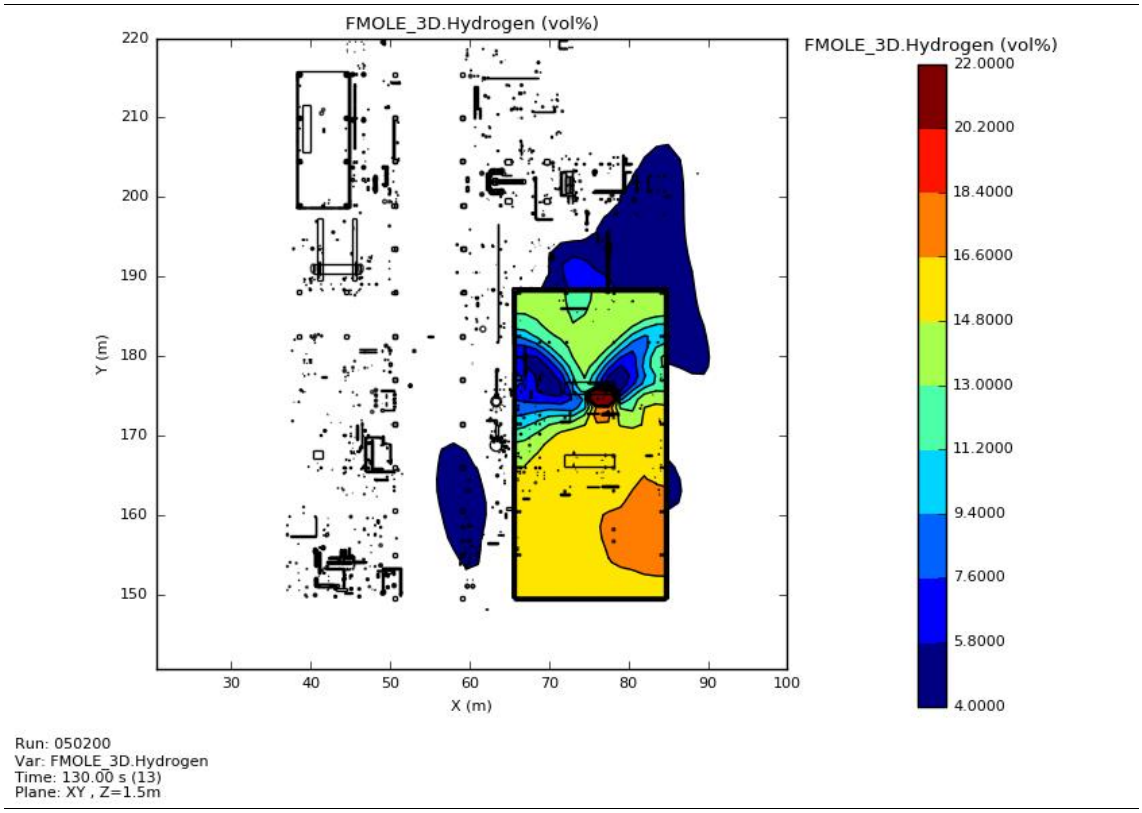

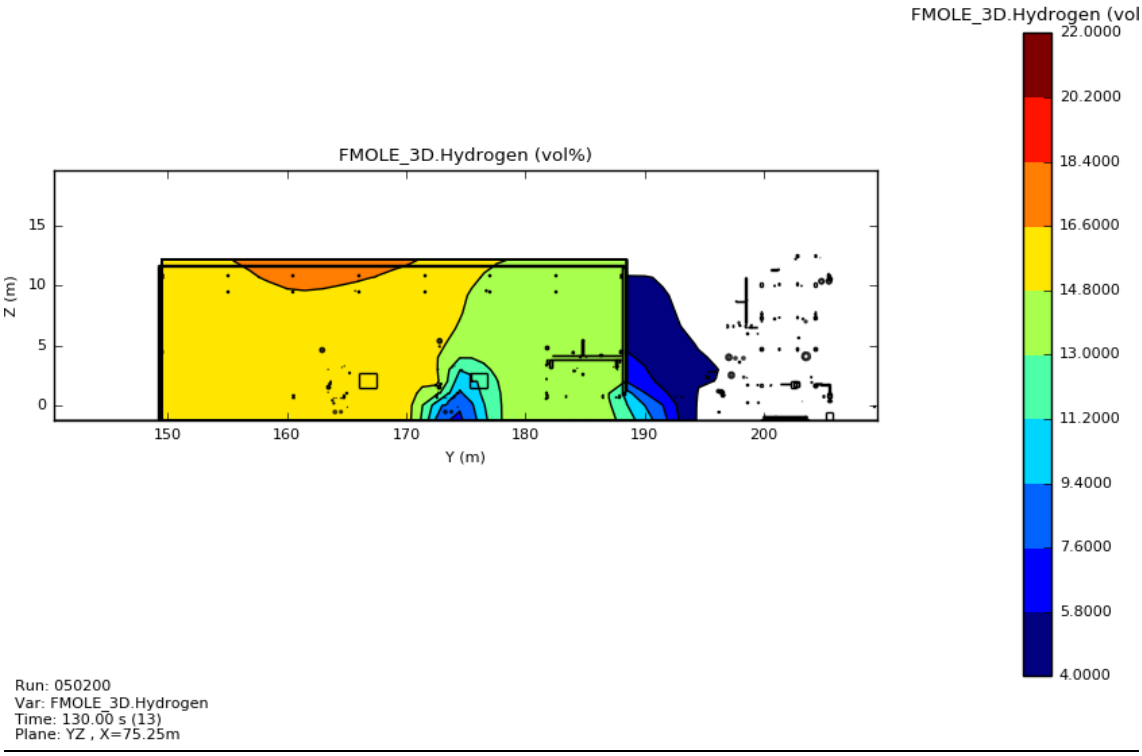

Figure 29. Hydrogen volume fraction (4-22 vol%) in compressor shelter at 100 seconds with 5D weather condition and south-westerly wind direction.

As can be seen in Figure 29 the amount of hydrogen volume fraction is smaller than in Model1. This can be assumed to be due to a flammable vapour cloud mass of less than 20 kg and a stoichiometric vapour cloud volume of less than 700 kg in Model2. The cloud also spreads more to the process area due to of faster wind velocity and direction.

6.1.3 Model3 – Complete modelling area

The dispersion simulation of Model3 was performed in an area where the volume blockage ratio was formed by objects within a radius of 100 metres from the compressor shelter. Figure 30 shows the volume blockage area of Model3 at height of 1.5 metres.

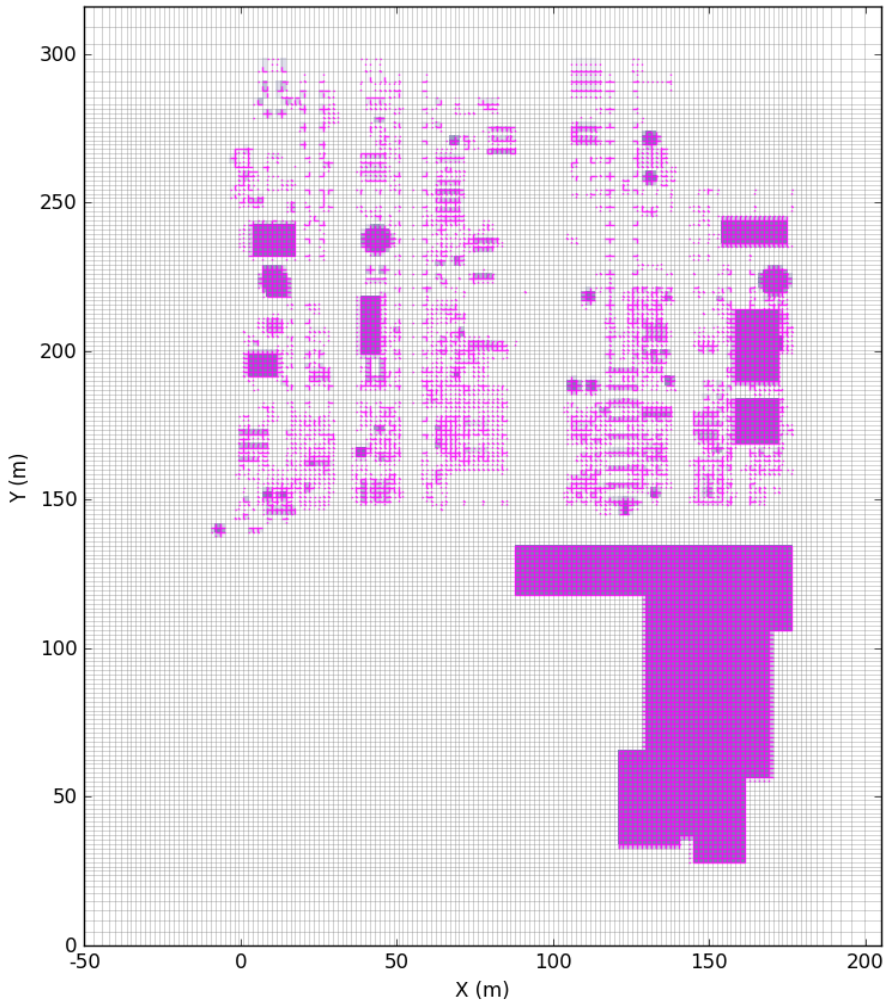

Figure 30. Volume blockage ratio (lilac) in Model2 at height of 1.5 metres.

Due to a strict schedule, dispersion simulations were done for Model3 only for two different scenarios where the weather types varied (5D and 2F) and the wind was chosen to be a south-westerly wind. Simulations were stopped as soon as they reached their maximum values as seen in Figure 31.

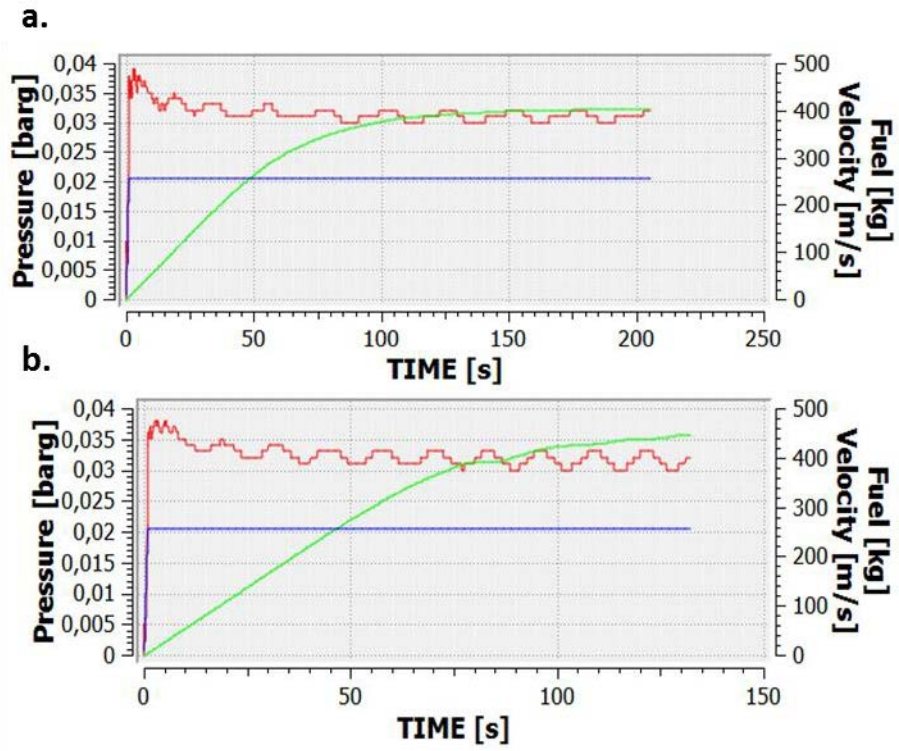

Figure 31. Dispersion simulation results in general simulation log files in different scenarios: a. 5D south-westerly wind direction, b. 2F south-westerly wind direction.

Based on these two scenarios worst case scenario for Model3 was chosen. Figure 32 shows the stoichiometric vapour cloud volume and mass of a flammable vapour cloud for both scenarios.

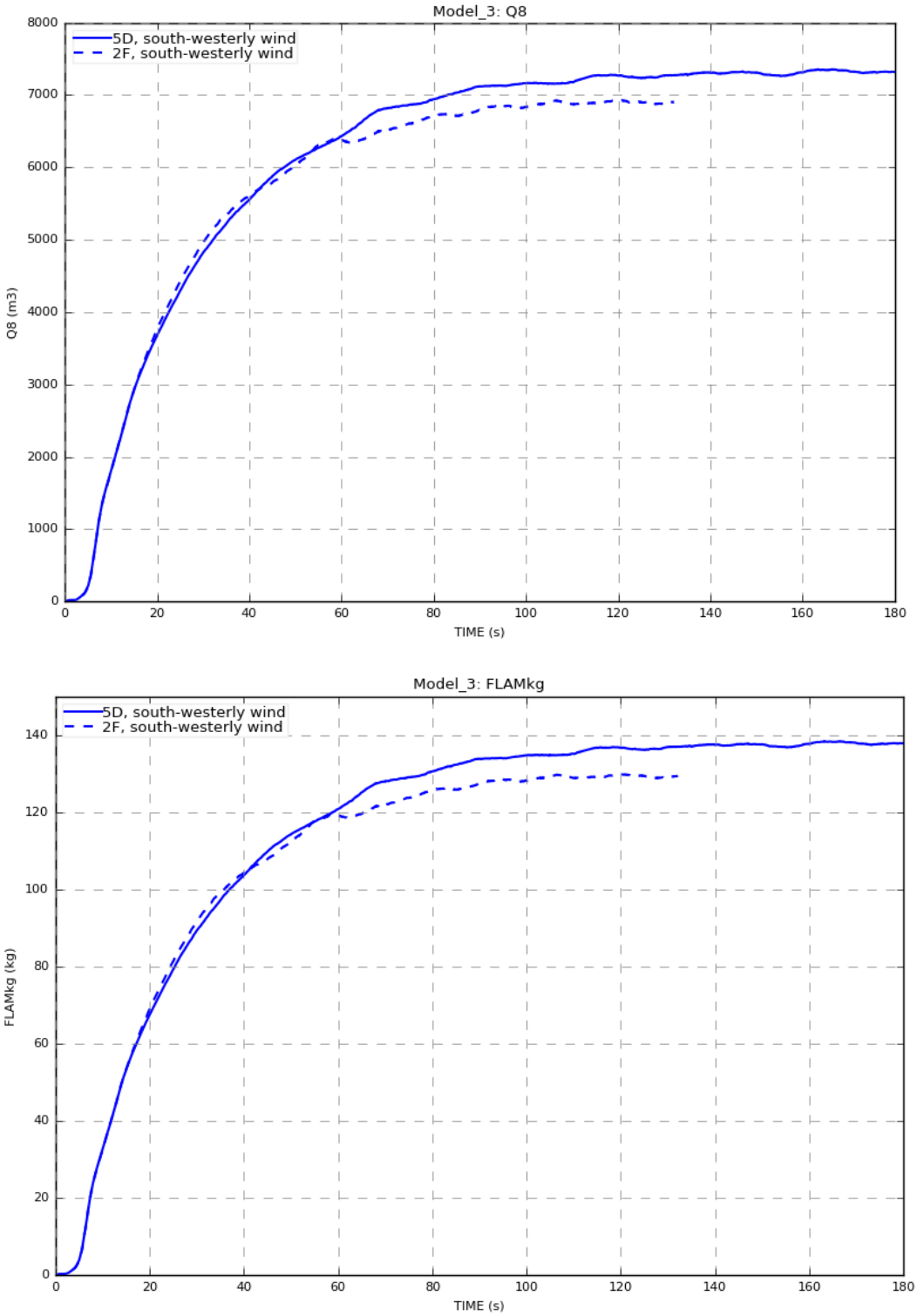

Figure 32. Volume-time plot of an equivalent stoichiometric vapour cloud (1.) and mass of a flammable vapour cloud (2.) in different scenarios.

As seen in Figure 32 the 5D scenario is better suited for a worst case scenario. The stoichiometric vapour cloud volume of 7400 m^3 (about 18.5 m x 47.5 m x 8.5 m) and mass of a flammable vapour cloud of 138 kg are reached approximately in 160 seconds. The flammable concentration of hydrogen in a vapour cloud and the dispersion of the gas are seen in Figure 33.

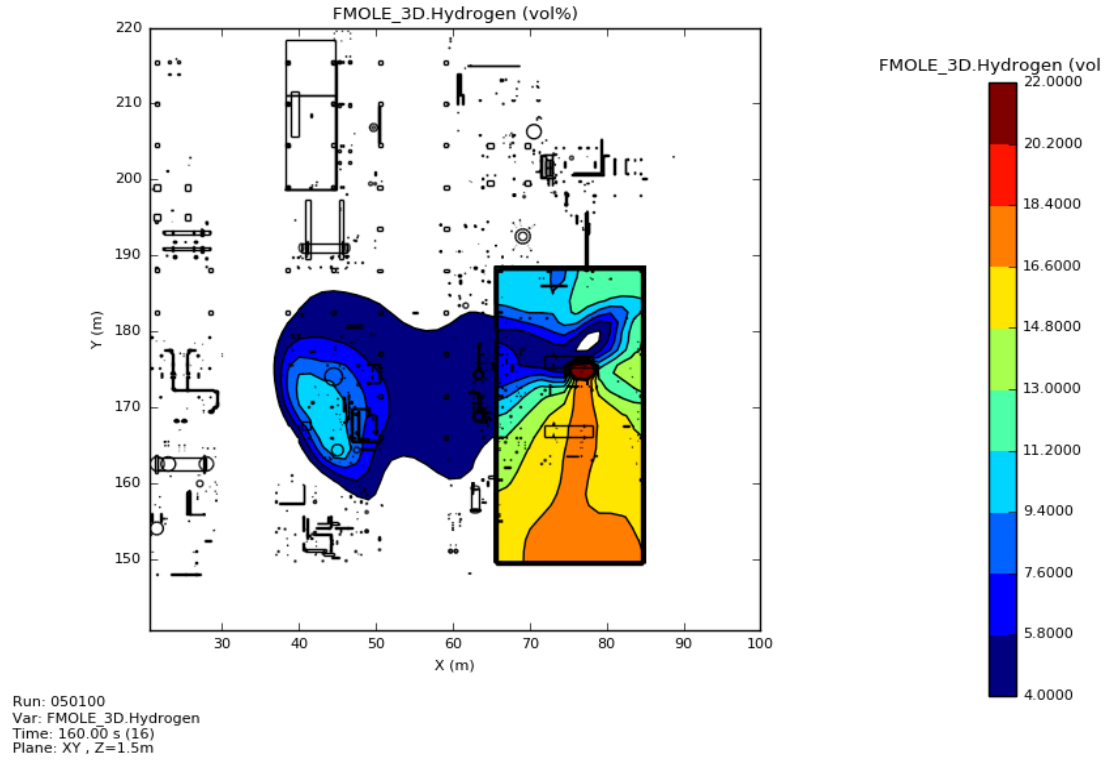

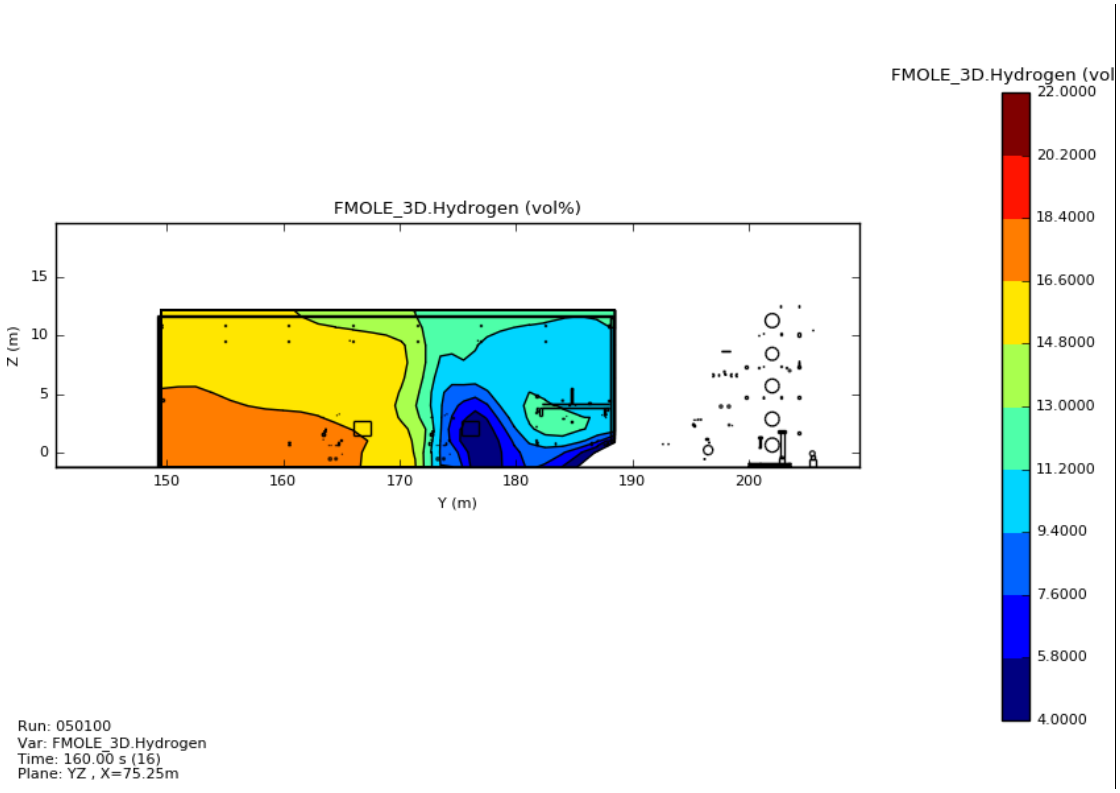

Figure 33. Hydrogen volume fraction (4-22 vol%) in compressor shelter at 160 seconds with 5D weather condition and south-westerly wind direction.

The concentration of hydrogen in Model3 is more like Model2 than Model1. Model2 and Model3 are similar; the results from these two models differed from each other due to the volume blockage ratio (larger in Model3). This resulted that Model2 had a bigger stoichiometric vapour cloud volume and mass of flammable gas.

6.2 Vapour cloud explosion simulations

Three VCE simulations with different ignition points were run for each model. In Appendix 4, the effects of different ignition points in terms of overpressure are shown. The scenarios were set according to Table 13. The aim was to investigate the effect of the volume blockage ratio on the formation of overpressures in the modelling area. Comparison of the results was not straightforward since the vapour clouds were of different sizes and the initial fuel amount was different in each model. The initial fuel is a mass amount of fuel which FLACS calculates at the beginning of a simulation; it has a lot of impacts on the formation of overpressure and flame acceleration. It is basically the density multiplied with the available volume (total fuel region volume reduced by blockage volume). Table 13 lists the total volume of a calculated domain blocked volume (i.e. volume blockage ratio) of a calculated domain and initial fuel amounts in different models. The results were compared with set monitor points for the models' worst case scenarios.

Table 13. Volume of a computational domain and initial fuel amount in different models.

Parameter	Model1	Model2	Model3
Total volume of a calculation domain [m^3]	8,219,160	8,219,160	8,219,160
Blocked volume of a calculation domain [m^3]	2,003	66,204	113,067
Initial fuel [kg]	202	186	179

6.2.1 Compressor shelter

Overpressures and pressure impulses were measured using four different monitor points in the compressor shelter. The locations of these monitor points are shown in Figure 34.

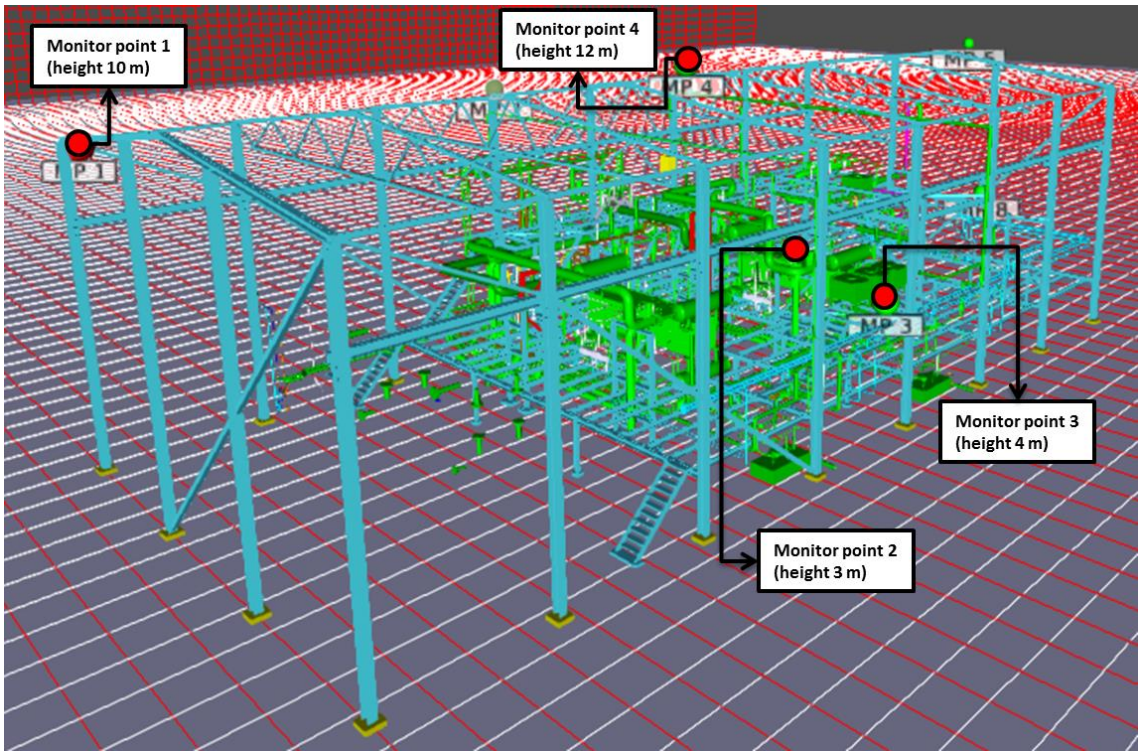

Figure 34. Monitor points inside the compressor shelter.

Figure 35 shows the overpressure peaks in four different monitor points in different models.

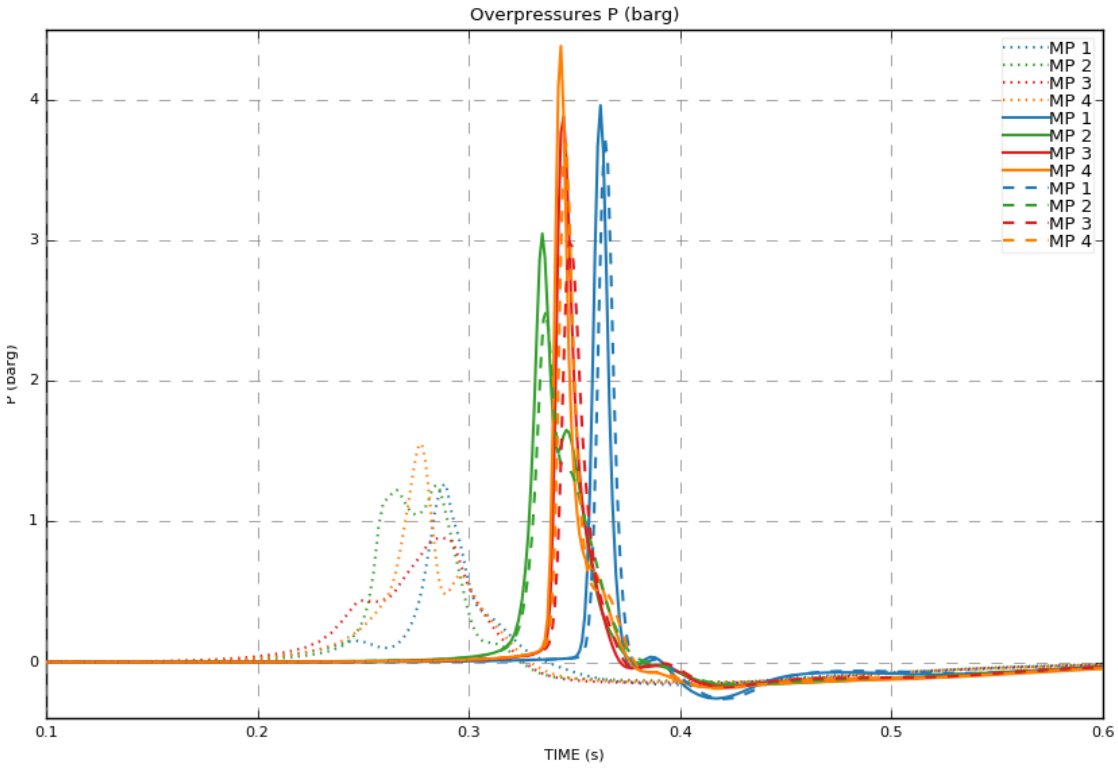

Figure 35. Overpressures measured inside the monitor points. Dotted lines represent the Model1, solid lines the Model2, and dash lines the Model3.

The highest overpressure peak was measured in the Model2 at monitor point 4 equalling 4.4 bar(g) (orange solid line line). In other monitor points the overpressures were between 3 bar(g) and 4 bar(g) in Model2. The values similar to Model2 were achieved also in Model3. In Model3 the maximum value 3.7 bar(g) was achieved also at monitor point 4. In other monitor points the values were between 3 bar(g) and 4 bar(g) except at monitor point 2 where the overpressure was approximately 2.5 bar(g). In Model1, the lowest overpressure peaks were measured. The difference between Model1 with two other models is significant as the maximum overpressure for Model1 was 1.3 bar(g) achieved also at monitor point 4.

The measured overpressures in Model2 and Model3 indicate a drastic discharge of energy and a shock wave (VCE detonates). It is essential to take into account that the location of the ignition point is exactly the same in both Models but the fuel region of Model2 is slightly bigger than in Model3. The volumes of the vapour clouds play a significant role between these two models as the volume blockage ratio is relatively the

same inside and immediately outside the compressor shelter. Figure 35 proves that objects have a very large effect on the flame acceleration and thus the formed blast wave. Model1 overpressures are significantly lower and the blast curves are the deflagration curve shaped. This is due the location of the ignition point which is not as in congested area as in Model2 and Model3. The flame acceleration is not high enough in Model1.

The effect of overpressure on structures is evaluated (in addition to overpressure) by the pressure impulse, which takes into account the pressure pulse in relation to time. The pressure impulse reaches its maximum after the peak pressure. Figure 36 shows the pressure impulses for the compressor shelter.

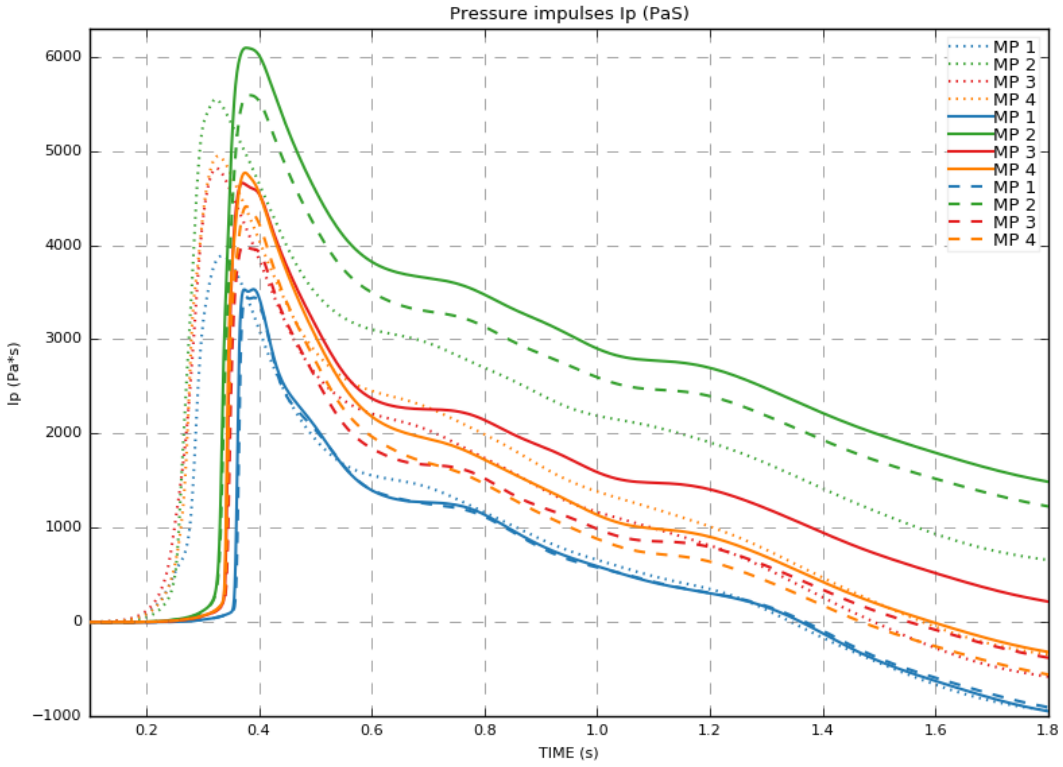

Figure 36. Pressure impulses inside the compressor shelter. Dotted line = Model1, solid line = Model2, and dashed line = Model3.

Potential damages caused by the pressure impulses are listed in Table 14. The effects of pressure impulses are determined by the maximum pressure impulse and its *overpressure effect* and compared with Table 3 (see section 2.4.1).

Table 14. Effects of pressure impulses inside the compressor shelter in different monitor points (see Figure 34) and Models.

Monitor point	Parameter	Model1	Model2	Model3
1	Overpressure [bar(g)]	1.3	4	3.7
	Pressure impulse [Pas]	3900	3530	3445
	Effects	Collapse of industrial steel frame structure, breakage of piping, collapse of pipe racks, heavy machinery damaged		
2	Overpressure [bar(g)]	1.3	3.1	2.5
	Pressure impulse [Pas]	5540	6080	5590
	Effects	Collapse of industrial steel frame structure, breakage of piping, collapse of pipe racks, heavy machinery damaged		
3	Overpressure [bar(g)]	0.8	3.38	3
	Pressure impulse [Pas]	4800	4650	4000
	Effects	Collapse of industrial steel frame structure, breakage of piping, collapse of pipe racks, heavy machinery damaged		
4	Overpressure [bar(g)]	1.5	4.4	3.7
	Pressure impulse [Pas]	4900	4770	4400
	Effects	Collapse of industrial steel frame structure, breakage of piping, collapse of pipe racks, heavy machinery damaged		

6.2.2 Control building

The location of the monitor point measuring overpressure effects on the control building is shown in Figure 37.

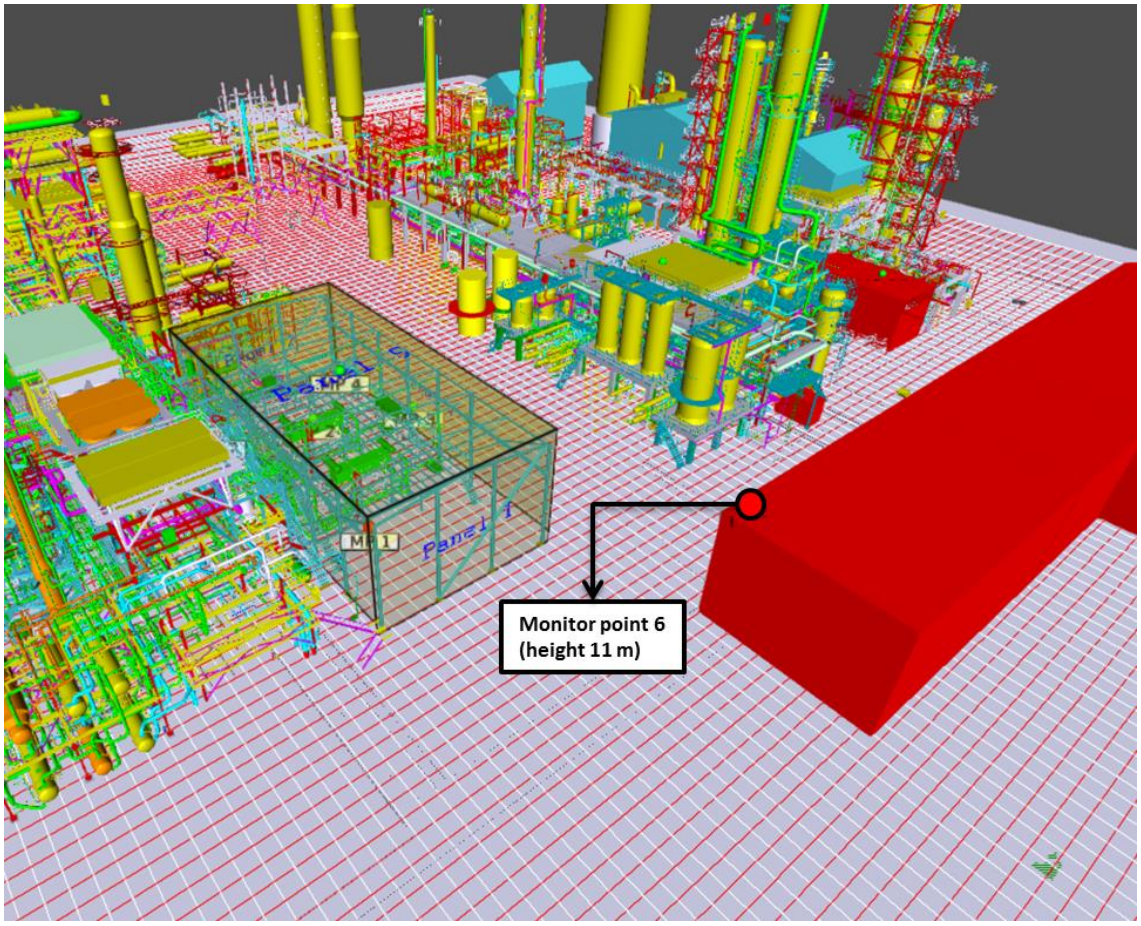

Figure 37. Monitor point of the control building.

The predicted overpressure to the control building was maximum 0.52 bar(g) (see Figure 38).

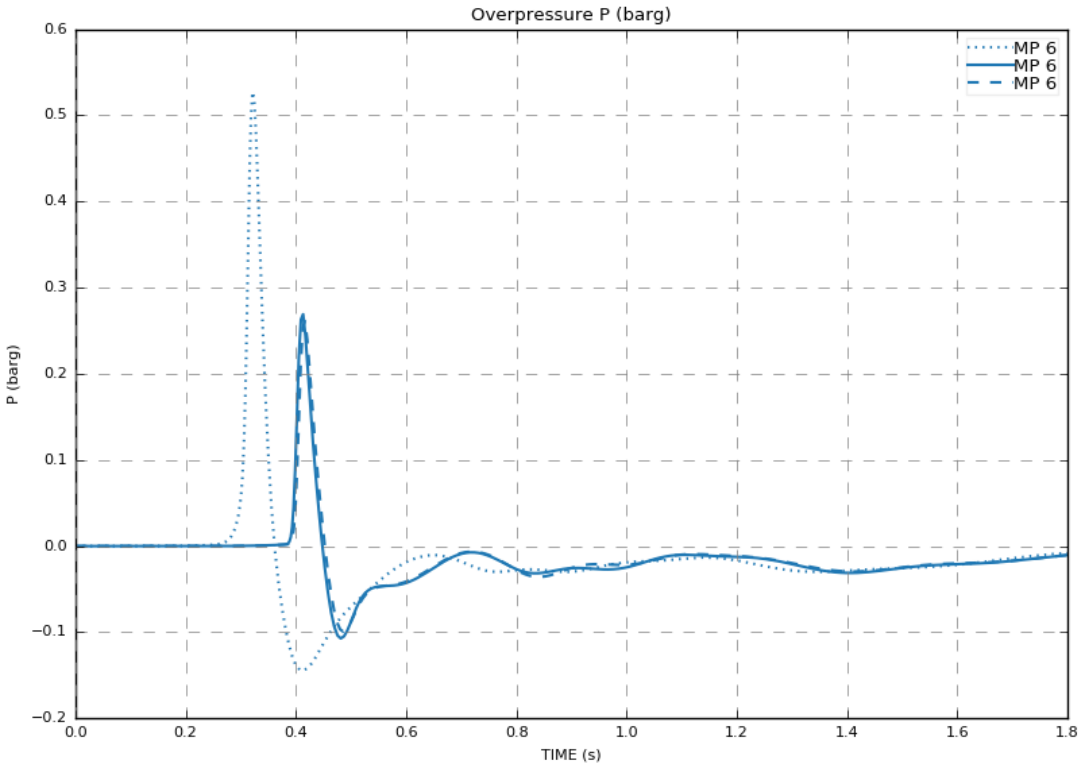

Figure 38. Overpressures measured in the monitor points. Dotted lines = Model1, solid lines = Model2, and dashed lines = Model3.

The highest overpressure peak was measured in Model1 (about 0.52 bar(g)) when in Model2 and Model3 the overpressure peaks were lower (about 0.27 bar(g)). The overpressures measured in a control building were significantly lower than those measured in a compressor shelter. This can be assumed to be due to the volume blockage ratio which is small between the ignition points and the control building (monitor point) in each model. This leads that there is relatively open space between compressor shelter and control building and the turbulence is not formed as much as it is in process area. Also, this can be explained by the fact that in Model1 the vapour cloud is much closer to the control building than in Model2 and Model3. The control building is very critical area as it is constantly occupied.

When the results between compressor shelter and control room are compared, it is noteworthy to see how quickly the overpressures dropped. Structural damages were measured by a pressure impulse as shown in Figure 39.

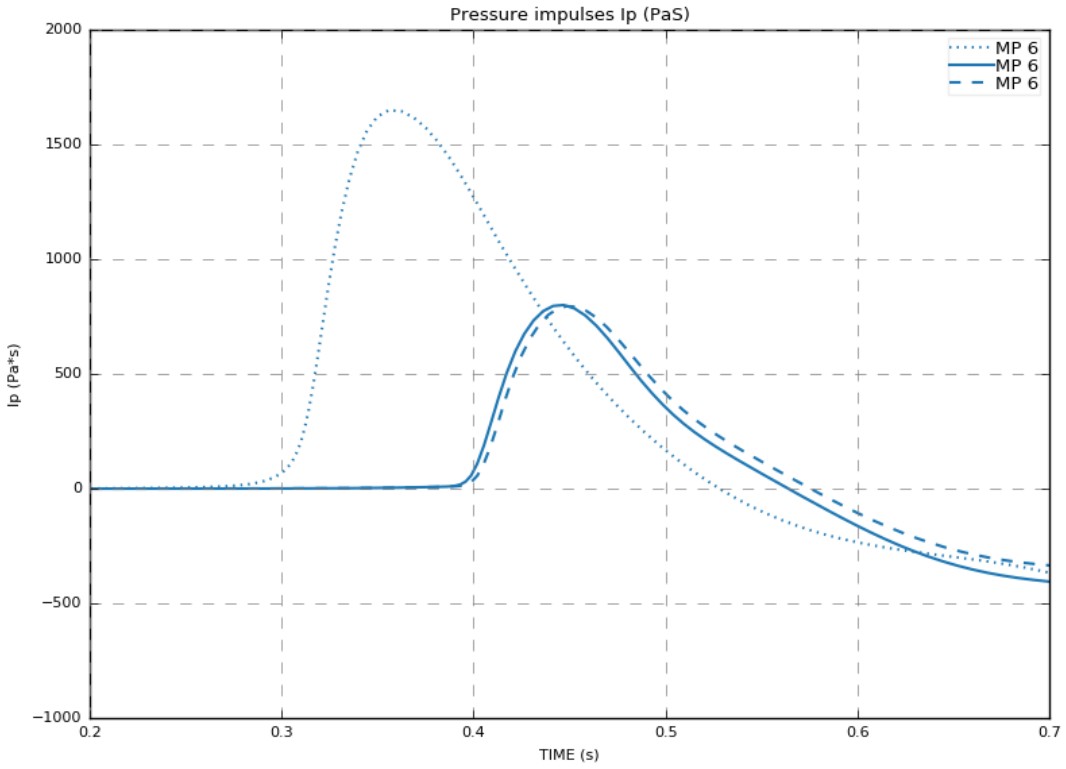

Figure 39. Pressure impulses in a control building. Dotted line = Model1, solid line = Model2, and dashed line = Model3.

The effects of the maximum pressure impulses are compared between models in Table 15. The pressure impulses and overpressure peaks were compared according to Figure 3 (see section 2.4.2). The pressure impulse curves are alike to overpressure peak curves as the maximum values were reached at Model1. According to Table 15, major structural damages to the control building are expected of all three models.

Table 15. Effects of pressure impulses in a control building in different monitor points and Models.

Monitor point	Parameter	Model1	Model2	Model3
6	Overpressure [bar(g)]	0.52	0.27	0.27
	Pressure impulse [Pas]	1650	800	795
	Effects	Major structural damage		

6.2.3 Diesel producing unit

Three monitor points were placed outside the compressor shelter in the process area of a diesel producing unit (see Figure 40). Overpressures were measured at the pipe rack (MP5), in the process area outside the compressor shelter (MP7) and at the distillation column (MP8).

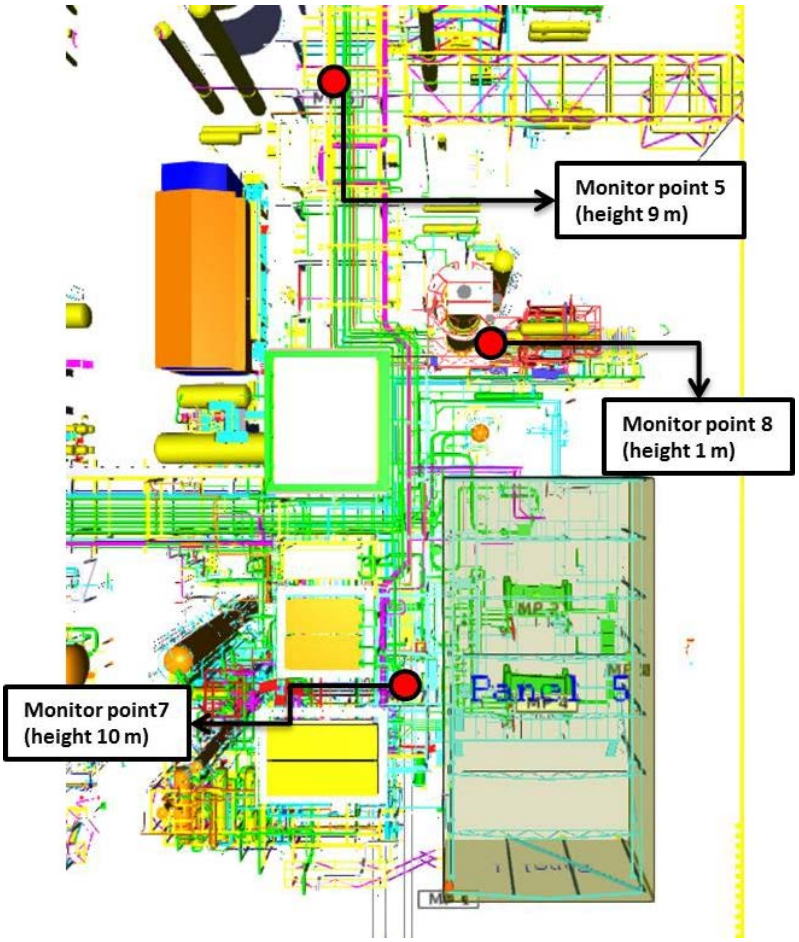

Figure 40. Locations of the monitor points in a process area of a diesel producing units.

The overpressures measured in those monitor points are shown in Figure 41.

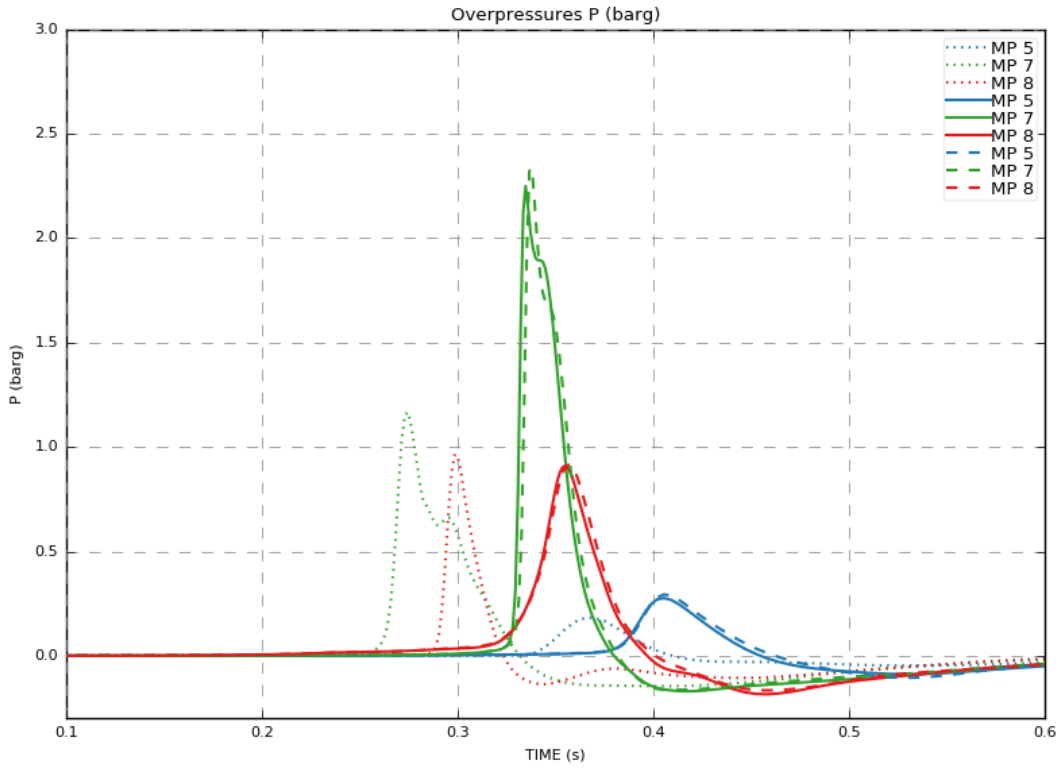

Figure 41. Overpressures measured in diesel producing unit. Dotted lines represent the Model1, solid lines the Model2, and dashed lines the Model3.

As seen from Figure 41, for Model2 and Model3 overpressure peaks rise very quickly to high values; a shock wave is possible. In MP7, for Model2 the maximum overpressure was 2.25 bar(g) and for Model3 2.3 bar(g). The pressure increase time for both models is less than 30 milliseconds. Also in Model1 the highest overpressure peak was 1.2 bar(g) has a very fast pressure increase time, about 10 milliseconds. The measured overpressure peaks are sufficient for destroying pipes and cable racks. There are many pipelines in the adjacent process area containing hydrocarbons and other hazardous chemicals.

Overpressures measured near the column (MP8) increased very fast to significant readings (about 0.9 bar(g)) in Model1. In Model2 and Model3 the overpressure peaks are more alike to an ideal deflagration curve and their values are about 0.8 bar(g). The significantly lower value (compared with MP7) for Model2 and Model3 can be explained by the fact that in both models the ignition point is very near to the monitor

point (MP8) and therefore the flame acceleration is much smaller than what it is in the pipeline area and there is more open space between MP8 and compressor shelter.

The highest measured overpressure peaks in monitor point 5 for Model1 was 0.2 bar(g) and for Model2 and Model3 about 0.3 bar(g). The measured highest overpressure peaks are not able to cause a collapse of the pipe racks but the displacement of a pipe rack and breakage of piping is however possible and likely to occur. Some vessels are located near pipe racks which may be damaged.

Structural damages in process area were evaluated (in addition to overpressures) with pressure impulses shown in Figure 42.

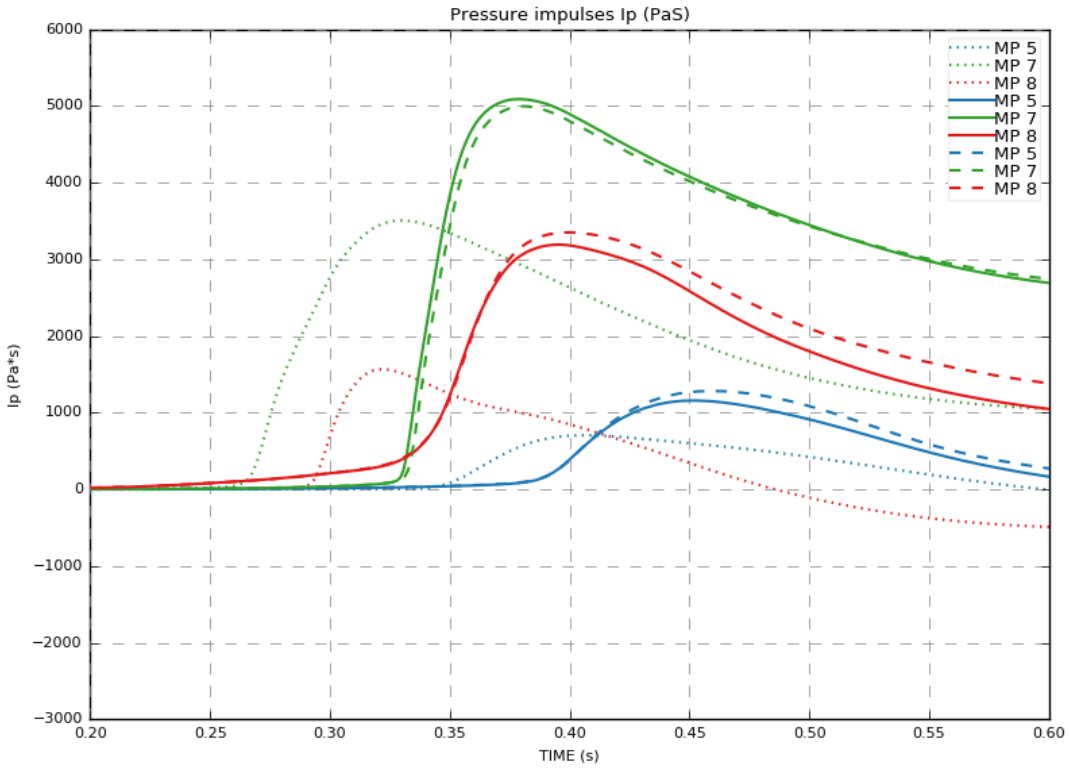

Figure 42. Pressure impulses in a control building. Dotted line = Model1, solid line = Model2, and dashed line = Model3.

As seen from Figure 42, the pressure impulses are like the overpressure peak curves. The effects of the maximum values of pressure impulses are shown in Table 16.

Table 16. Effects of pressure impulses in the process area of a diesel producing units at different monitor points and in different Models.

Monitor point	Parameter	Model1	Model2	Model3
5	Overpressure [bar(g)]	0.2	0.3	0.3
	Pressure impulse [Pas]	705	1160	1280
	Effects	Displacement of pipe racks, breakage of piping		
7	Overpressure [bar(g)]	1.2	2.25	2.3
	Pressure impulse [Pas]	3500	5090	5000
	Effects	Collapse of pipe racks, failure of pipes, heavy machinery damaged		
8	Overpressure [bar(g)]	0.9	0.8	0.8
	Pressure impulse [Pas]	1560	3200	3350
	Effects	Displacement of pipe rack, damage to column structures		

As seen from Table 16 the measured pressure impulses at a pipe rack (MP5) will cause major damage to structures. Pressure impulses in the pipeline area and at the column (MP8) can cause partial demolition of structures.

When comparing the results with those measured inside the compressor shelter (MP1-4), the resulting overpressure differences are relatively notable. Both areas have the features of a detonation explosion, depending on the model, and it is interesting to see how the ignition point affects to the formed overpressure curves. The ignition point of Model2 and Model3 are close to monitor point 8, when the overpressure peaks remain significantly lower compared with Model1.

6.2.4 Units producing light petrol product and lubricating oil

The modelled area also includes two units: Unit A, which produces a light petroleum product and Unit B, which produces lubrication oil. Both units contain flammable substances such as light petroleum and hydrogen gas. Both units had one measuring point; MP9 for unit A and MP10 for unit B (see Figure 43). The distance between the compressor shelter and Unit A is about 5 metres. In Unit B it is essential to take into account that the unit has an own smaller scaled compressor shelter. It contains one piston compressor, which compress hydrogen gas.

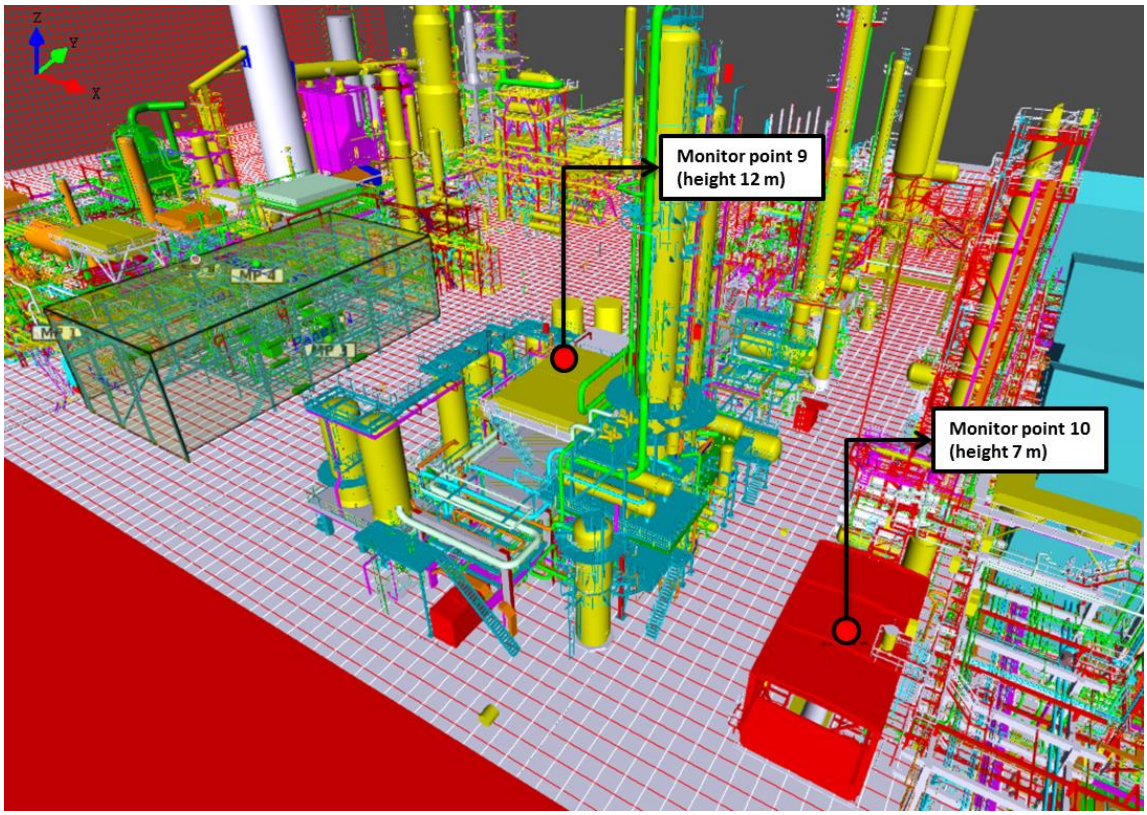

Figure 43. Location of the monitor points in a unit A and unit B. Monitor point 9 is located in the unit A producing light petrol and Monitor point 10 located unit B producing lubricating oil.

The peak overpressures are shown in Figure 44.

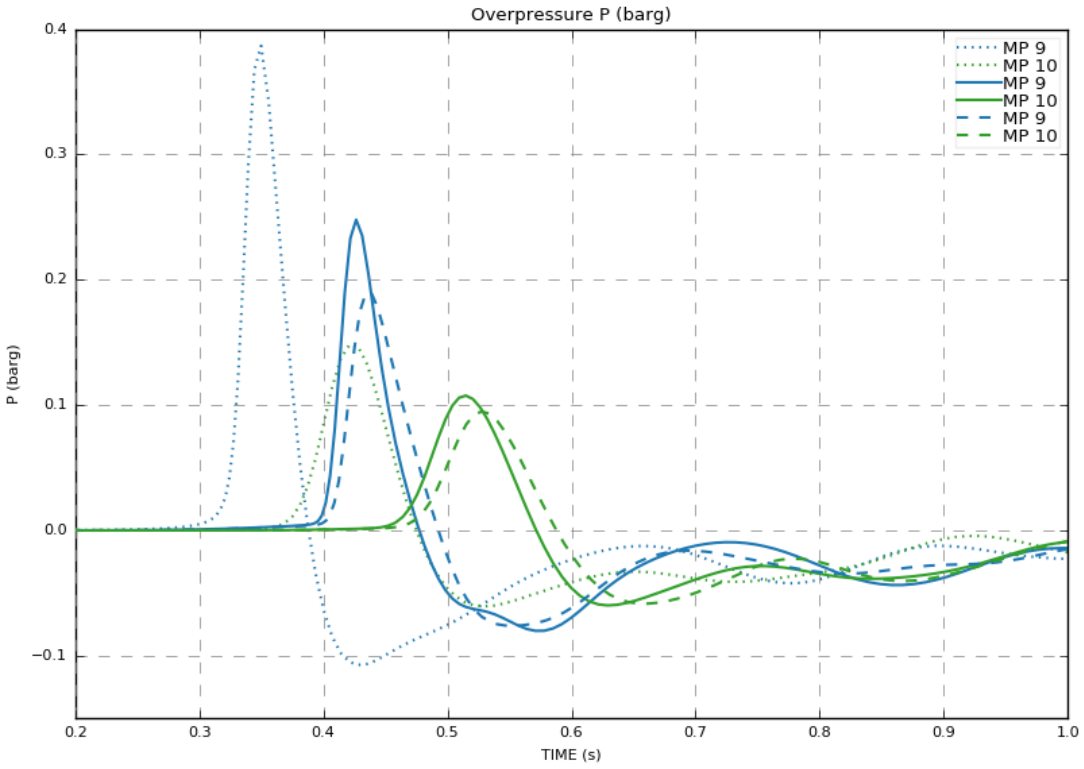

Figure 44. Overpressures measured in unit A (MP9) and unit B (MP10). Dotted lines represent the Model1, solid lines the Model2, and dashed lines the Model3.

The measured overpressures in Unit A and B remind a bit of the overpressures measured in a control building. In Unit A, the highest overpressure peaks were measured in Model1 (0.39 bar(g)). In Model2 and Model3 the pressure did not increase as high as in Model1 (Model2 0.25 bar(g) and in Model3 0.19 bar(g)). This is because of the long distance between the ignition points and the units (MPs) as well as the low volume blockage ration. The pressure impulses measured in the units are shown in Figure 45.

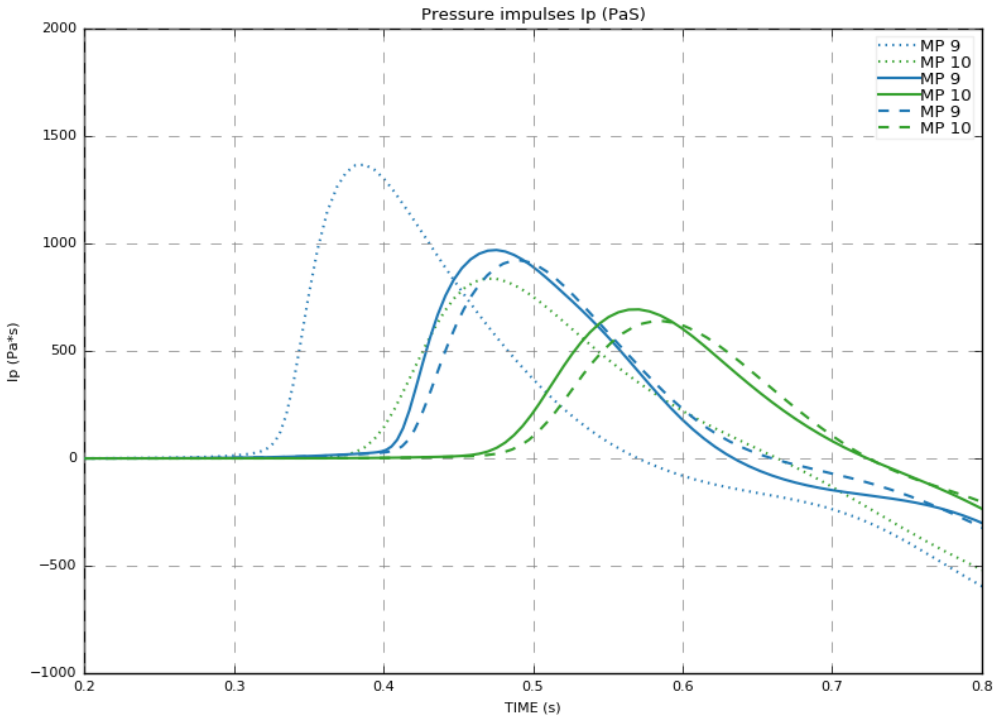

Figure 45. Pressure impulses measured in unit A (MP9) and unit B (MP10). Dotted line = Model1, solid line = Model2, and dashed line = Model3.

Table 17 lists the effects of pressure impulses to the structures in Unit A and Unit B.

Table 17. Effects of pressure impulses in the Unit A and Unit B at different monitor points and in different Models.

Monitor point	Parameter	Model1	Model2	Model3
9	Overpressure [bar(g)]	0.39	0.25	0.19
	Pressure impulse [Pas]	1360	965	920
	Effects	Displacement of pipe rack, damage to structures		
10	Overpressure [bar(g)]	0.15	0.11	0.09
	Pressure impulse [Pas]	835	690	640
	Effects	Damages to steel structures and to concrete structures		

Major structural damages are expected of pressure impulses in Model1 and Model2 for unit A. In unit B for all models and also in unit A for Model3 the minor structural damages are more likely to occur.

6.3 Discussion of the results

When comparing all three models during the dispersion simulations, it was seen that the timing of overpressure peaks formation differed at each model. Table 18 lists worst case scenarios in dispersion simulations for the models.

Table 18. Worst case scenarios for different models.

Parameter	Model1	Model2	Model3
Scenario	2F easterly wind	5D south-westerly wind	5D south-westerly wind
Volume of a stoichiometric vapour cloud [m^3]	8200	7500	7400
Mass of a flammable vapour cloud [kg]	160	140	138
Time [s]	100	130	160

As seen from Table 18 the biggest vapour cloud was in Model1 with the highest mass of a flammable vapour cloud. The vapour clouds in Model2 and Model3 were very similar and they differed from the vapour cloud of Model1 significantly. This can be explained by the fact that in Model2 and Model3 the volume blockage ratio (close by compressor shelter) is significantly higher than in Model1.

Before dispersion simulations were performed, it was considered that the weather type 2F is more dangerous than the weather type 5D. It was assumed that a lower wind velocity will result in a bigger vapour cloud since the cloud could remain in the process area. However, this assumption applied only to Model1 that has the least confined area of the three models. As seen from the dispersion simulation results in partly confined

modelling areas the weather type 5D will result in a bigger vapour cloud (the mass and volume of the cloud). It can be assumed that a higher wind velocity spreads the cloud in the congested pipeline area where it is trapped inside narrow spaces.

It is essential to take into account that in Model2 the worst case scenario for dispersion occurs at the dominant weather type (5D south-westerly wind) unlike in Model1. In Model3 there is a small uncertainty about the worst case scenario since the modelling was performed only for two scenarios with the dominant weather type. Reviewing the VCEs results for the three modelling areas it can be concluded that the overpressures measured at each monitor point (regardless of the models) have significant consequences. Domino effects are likely due to the congested process area. Table 19 summarizes the peak overpressures and pressure impulses in each model.

Table 19. Worst overpressure and pressure impulse levels in different areas for Model1, Model2 and Model3 (LaChance *et al*. 2011; Casal 2008).

		Model1	**Model2**	**Model3**
Compressor shelter	Monitor point	MP4	MP4	MP4
	Overpressure Pressure impulses	1.5 bar(g) 4900 Pas	4.4 bar(g) 4770 Pas	3.7 bar(g) 4400 Pas
	Effects on people	50% probability of fatality from lung haemorrhage		
	Effects on structures	Collapse of industrial steel frame structure, breakage of piping, collapse of pipe racks, heavy machinery damaged		
Control building	Monitor point	MP6	MP6	MP6
	Overpressure Pressure impulses	0.5 bar(g) 1650 Pas	0.25 bar(g) 800 Pas	0.25 bar(g) 795 Pas
	Effects on people	50% probability of eardrum rupture		
	Effects on structures	Major structural damage		
Diesel producing unit	Monitor point	MP7	MP7	MP7
	Overpressure Pressure impulses	1.2 bar(g) 3500 Pas	2.25 bar(g) 5090 Pas	2.3 bar(g) 5000 Pas
	Effects on people	90% probability of fatality from lung haemorrhage		
	Effects on structures	Collapse of pipe racks, failure of pipes, heavy machinery damaged		
Units A and B	Monitor point	MP9	MP9	MP9
	Overpressure Pressure impulses	0.39 bar(g) 1360 Pas	0.25 bar(g) 965 Pas	0.19 bar(g) 920 Pas
	Effects on people	50% probability of eardrum rupture		
	Effects on structures	Displacement of pipe rack, damage to structures		

The Table 19 summaries the worst case effects of overpressure peaks and pressure impulses on structures and direct effects from blast to personnel. The effects are based on Figure 2 and Table 3 (in chapter 2). As seen in Table 19 inside the compressor shelter and in the diesel producing unit the formed overpressures are very high. In each model it can be concluded that hydrogen VCE detonated in those areas. In overall the overpressure peaks, with drastic increase and high values, show that hydrogen VCE can occur as DDT in each model. The highest overpressure peaks were achieved in Model2 and Model3.

For all three models, almost a complete destruction of the compressor shelter is likely. Outside the compressor shelter in the process area a total destruction of buildings is possible. The critical building in the process area is the control building as it is constantly occupied. The overpressure peaks for all models can damage the control building significantly causing a high risk of fatalities. Process equipment and their structures as well as pipe racks will also be damaged because of the high overpressures. Additionally, fatalities are likely since the overpressure is higher than 0.7 bar(g).

Domino effects are likely to occur due to damage of process equipment and pipelines. The diesel producing unit and other units contain various flammable hydrocarbons and chemicals that are toxic and hazardous to the environment. Fatalities are also likely due to flying objects such as fragments and equipment parts.

A similar hydrogen VCE in a compressor shelter has previously been simulated with the PHAST (7.2) software. In PHAST, the geometry cannot be set at the same accurate level as in FLACS. Therefore PHAST cannot reliably simulate higher volume blockage ratios. It was separately calculated that the compressor shelter was filled up in less than five minutes and that the mass of the flammable vapour cloud was approximately 600 kg. Conservative assumptions were used. As a result, PHAST calculated an overpressure of 1 bar(g) in the compressor shelter and its vicinity.

When these are compared with the results of FLACS, it can be seen that the vapour cloud is formed faster, in about 2.5 minutes (Model3), with a flammable vapour cloud mass of 138 kg that is 4.3 times smaller amount than a separately calculated amount for a PHAST simulation. In FLACS, the maximum overpressure in the compressor shelter was 4.4 bar(g) and in its vicinity 2.3 bar(g) giving a remarkable difference compared with PHAST.

7 CONCLUSION

In the chemical and petrochemical industries flammable liquids and gases are constantly processed and thus a risk of an explosion exists. Consequences of explosions caused by VCEs are generally destructive to industrial areas. The most hazardous vapour cloud explosions occur in partly confined areas and in congested areas where the overpressures can rise to very high measures only in a few milliseconds. Modelling of partly confined areas, in particular, has been challenging as the objects in the area cause turbulence. Programmes suitable for modelling those areas are generally very expensive and require a lot of computing power.

The main objective of this study was to simulate the partly confined hydrogen vapour cloud explosions in three different models with varying volume blockage ratios. The modelling was done with FLACS v10.8 software. Simulations were done for dispersions and consequently for VCEs. With dispersion simulations, the objectives were to estimate formed flammable vapour clouds of the flange leakage and the mass of a flammable vapour clouds. Consequently with the VCE simulations the aim was to estimate overpressure and pressure impulse peaks. Also the usability of the FLACS software was tested.

7.1 Dispersion simulations

The criteria for the worst case hydrogen vapour cloud in this study were the largest mass of a flammable vapour cloud and the largest flammable vapour cloud volume. For each scenario different weather conditions (5D and 2F) were run. FLACS evaluates the flammable vapour cloud according to a special equivalent stoichiometric gas cloud. The Q8 vapour cloud type was used as a stoichiometric gas cloud since the hydrogen vapour at its flammability limits fills the compressor shelter. In addition, hydrogen is also a reactive fuel with a fast laminar velocity which makes it possible to form a DDT.

The simulations for all scenarios were ended when they had reached their maximum values for pressure, flammable material (fuel), and leakage velocity. The worst case

results for the dispersion simulations for Model1 with weather condition 2F easterly wind resulted in a vapour cloud volume of 8200 m^3 and mass of a flammable vapour cloud of 160 kg. For Model2, worst case scenario occurred in weather condition 5D south-westerly wind with a vapour cloud volume of 7500 m^3 and a mass of a flammable vapour cloud of 140 kg. For Model3, worst case scenario was in weather condition 5D south-westerly wind resulting in a vapour cloud volume of 1400 m^3 and a mass of a flammable vapour cloud of 138 kg.

Before dispersion simulations were performed, it was considered that 2F weather type is more hazardous than 5D weather type. This was based on the assumption that with lower wind speed the hydrogen vapour cloud would much easily got trapped in process area than at higher wind speed. In general, 2F as more dangerous weather condition applies in leakage scenarios in which the leakage material (for example hydrocarbons such as gasoline) is heavier than air. In such cases, the flammable vapour cloud is formed near to a ground level.

In this study, the assumption applied only to Model1, which has the most open area of three models. However, as seen from the dispersion simulation results, in more congested partly confined modelling areas, 5D weather type is more dangerous. It is likely that with a higher wind velocity the hydrogen gas spreads more to the congested pipeline area and is trapped inside the narrow spaces.

It is essential to take into account that in Model2 worst case scenario for dispersion occurs at the dominant weather type, unlike in Model1. With Model3 a small uncertainty about worst case scenario occurs since the modelling was performed only for two scenarios. The vapour cloud explosions were simulated according to simulated worst case dispersion simulation scenarios; the results of VCEs are explained in the next section (7.2).

7.2 Vapour cloud explosion simulations

Three VCE simulations with different ignition points were modelled for each model. The aim was to investigate the effect of volume blockage ratio on the formation of

overpressures in the modelling area. Comparison of the results was not straightforward since the vapour clouds were of different sizes and the initial fuel amount was different in each model. The mass of a flammable vapour cloud had the most significant impact on the overpressure results. It can be said that the overpressure measured at each monitor point (regardless of the model) has significant consequences that can lead to the domino effects. The highest overpressures were measured in Model2 and Model3 inside the compressor shelter (monitor point MP4): Model2 4.4 bar(g) and Model3 3.7 bar(g). The overpressure peaks increased to significant values outside the compressor shelter (diesel producing unit) where the overpressure for Model2 was 2.25 bar(g) and for Model3 2.3 bar(g) (in monitor point MP7). For other monitor points the values were significantly lower. All three models showed that almost a complete destruction of the compressor shelter is likely. Additionally, for the control building overpressure peaks can damage the building significantly causing a high risk of fatalities. Cable racks are damaged.

Domino effects are also likely to occur due to damage of the process equipment. The process area has pipe racks which may move and partially collapse due to explosion overpressures causing new leakages and possible damages to the nearest vessels. Unit A (located close to the compressor shelter) produces a light petrol product which is classified as a highly flammable and environmentally hazardous substance that is dangerous to personnel. Fatalities are likely due to explosion overpressures (over 0.7 bar(g)), flying objects such as fragments and equipment parts, and domino effects (such as fires, toxic leakages and possible explosions).

7.3 Simulation with FLACS

FLACS software is user friendly software where the scenario build-up is relatively easy and clear. Also, the mandatory FLACS course, proper instructions provided by Gexcon and expeditious FLACS support made the use of the FLACS easier. FLACS require a lot of computing power which was resulted especially in a long dispersion simulation times. The dispersion simulations took several days and they were interrupted. With VCE simulations, the simulation times were significantly shorter from an hour to a maximum of four hours. It is important to take into account that the capacity of the

computer has a significant impact on the timing. To speed up the simulation time it is possible to run simulation with several computer cores. This function also makes it possible to run several simulations at the same time. In this study, the computer had four cores (quad-core) and dispersion simulations were singly run and were distributed to four cores.

The simulation results are highly dependent on the selected cell size of computational mesh which is shown in appendix 1. As this study showed the smaller cell sizes the formed overpressures from VCEs are higher. For gas explosion scenarios, the selection of right equivalent stoichiometric vapour cloud is essential. The result differences between Q8 and Q9 vapour cloud are significant as seen from appendix 2 which includes the results of the Q9 vapour cloud simulation.

LIST OF REFERENCES

Aarnivuo U., Vauhkonen I. (2004) Onnettomuustutkintaraportti. Vetyräjähdys ksyloosin hydrauslaitoksella 13.1.2004. Dnro 1062/36/2004.

Atanga G., Lakshmipathy S., Skjold T., Hisken H., Hanssen A. G. (2018) Structural response for vented hydrogen deflagrations: Coupling CFD and FE tools. International Journal of Hydrogen Energy: 1-11.

Bauwens C. R., Dorofeev S. B. (2014) CFD modelling and consequence analysis of an accidental hydrogen release in a large scale facility. International Journal of Hydrogen Energy, vol. 39: 20447-20454.

Bjerketvedt D., Mjaavatten A. (2015) A Hydrogen-Air Explosion in a Process Plant: A Case History. Faculty of Technology, Telemark University College. ResearchGate.

Bjerketvedt D., Bakke J. R., Wingerden K. (1997) Vapour cloud explosion Handbook. GexCon

Boch van den C. J. H., Weterings R. A. P. M. (2005) Methods for the calculation of physical effects. Yellow Book. CPR 14E. 3rd edition 2nd revised print 2005. Ministerie van Verkeer en Waterstaat.

Caliri G. V. (2000) Introduction to Analytical Modeling. BMC Software, Inc. Waltham MA USA.

Casal J. (2008) Evaluation of the Effects and Consequences of Major Accidents in Industrial Plants. Industrial Safety Series, 8. Centre for Studies on Technological Risk Department of Chemical Engineering Universitat Politècnica de Catalunya Barcelona, Spain. First edition 2008, Elsevier. ISBN: 978-0-444-53081-3: 119-145.

Denton S. (2015) Buncefield Anniversary: A look at the explosion and the fallout from it 10 years on. [online] Available at: https://www.postonline.co.uk/claims/2438927/buncefield-anniversary-a-look-at-the-explosion-and-the-fallout-from-it-10-years-on [cited: 15.11.2019].

DNV GL (2019a) About us. [online] Available at: https://www.dnvgl.com/about/index.html [cited: 17.7.2019].

DNV GL (2019b) Explosion modelling software - Vapour cloud explosion tool - Phast 3D Explosions. [online] Available at: https://www.dnvgl.com/services/explosion-modelling-software-vapour-cloud-explosion-tool-phast-3d-explosions-1698 [cited: 5.8.2019].

Clarke Energy (2019) Laminar Flame Speed. [online] A Kohler Company. Available at: https://www.clarke-energy.com/laminar-flame-speed/ [cited: 20.5.2019].

Crowl D. A. (2003) Understanding Explosions. Department of Chemical Engineering Michigan Technological University. American Institute of Chemical Enginers. ISBN: 0-8169-0779-X: 1-112.

Davis S. G., Hinze P., Hansen O. R., Wingerden van K. (2010) 2005 Buncefield Vapor Cloud Explosion: Unraveling the Mystery of the Blast. ResearchGate.

Eckhoff R. K. (2016) Explosion Hazards in the Process Industries. University of Bergen. Second edition. ISBN: 978-0-12-803273-2: 11-148.

explosionsolutions (2019) Minimum Ignition Energy (MIE) [online] Available at: http://explosionsolutions.co.uk/110411020.pdf [cited: 1.11.2019].

Exponent Failure Analysis Associates (2013) Silver Eagle Refinery Explosion Investigation: Metallurgical Analysis. U.S. Chemical Safety Board (CSB).

FM Global (2019) Open Source Fire Modelling [online] Available at: https://www.fmglobal.com/research-and-resources/research-and-testing/theoretical-

computational-and-experimental-research/open-source-fire-modeling [cited: 13.3.20199].

Gant S., Hoyes J. (2010) Review of FLACS version 9.0 – Dispersion modelling capabilities. Health and Safety Laboratory. Research Report RR779: 1-2.

Gexcon (2018) FLACS Software [online] Available at: https://www.gexcon.com/products-services/FLACS-Software/22/en [cited: 21.2.2019].

Gexcon AS (2018) FLACS v10.8 User's Manual. Updated: October 08 2018.

Hansen O. R., Gavelli F., Davis S. G., Middha P. (2013) Equivalent cloud methods used for explosion risk and consequence studies. Journal of Loss Prevention in the Process Industries, vol. 26: 511-527.

Helmenstine A. M. (2017) Combustion Definition (Chemistry). ThoughtCo. [online] Available at: https://www.thoughtco.com/definition-of-combustion-605841 [cited: 28.1.2019].

HySafe (2019) Chapter 1: Hydrogen Fundamentals. Biennial Report on Hydrogen Safety (Version 1.2). [online] Available at: http://www.hysafe.org/download/1196/BRHS_Chap1_V1p2.pdf [cited: 17.6.2019].

Inanloo B., Tansel B. (2015) Explosion impacts during transport of hazardous cargo: GIS-based characterization of overpressure impacts and delineation of flammable zones for ammonia. Journal of Environmental Management, vol. 156: 1-9.

Javidi M., Abdolhamidzadeh B., Reniers G., Rashtchian D. (2015) A multivariable model for estimation of vapor cloud explosion occurrence possibility based on a Fuzzy logic approach for flammable fuels. Journal of Loss Prevention in the Process Industries, vol. 33: 140-150.

Jaakkola P. (2014) LTP++ Virtausopin perusteet. Tampere University of Technology.

Johnson D. M., Tomlin G. B., Walker D. G. (2015) Detonations and vapor cloud explosions: Why it matters. Journal of Loss Prevention in the Process Industries, vol. 36: 358-364.

Kimura K. (2016) Chapter 3: Wind loads. Book: Pipinato A. (2016) Innovative Bridge Design Handbook. Construction, Rehabilitation and Maintenance. Pages 37-48. ISBN: 978-0-12-800058-8.

LaChance J., Tchouvelev A., Engebo A. (2011) Development of uniform harm criteria for use in quantitative risk analysis of the hydrogen infrastructure. International Journal of Hydrogen Energy, vol. 36: 2381-2388.

Lautkaski R. (1997) Understanding vented vapour cloud explosions. VTT Research notes 1812. ISBN 951-38-5087-0.

Mannan S., Lees F. P. (2012) Lees' Loss Prevention in the Process Industries : Hazard Identification, Assessment and Control. Vol. 1. (4th edition). ISBN: 978-0-12-397189-0: 1375-1678.

McGrattan K., Hostikka S., Floyd J., Baum H., Rehm R. (2007) Fire Dynamics Simulator (Version 5) Technical Reference Guide. NIST Special Publication 1018-5. In cooperation with: VTT Technical Research Centre of Finland: p. 10.

NIST (2016) FDS and Smokeview [online] Available at: https://www.nist.gov/services-resources/software/fds-and-smokeview [cited: 6.3.2019].

Nolan D. P. (2011) Handbook of Fire and Explosion Protection Engineering Principles: for Oil, Gas, Chemical and Related Facilities. Second edition. ISBN: 978-1-4377-7857-1: 1-11.

Pandya N., Marsden E., Floquet P., Gabas N. (2008) Toxic Release Dispersion Modelling with PHAST: Parametric Sensitivity Analysis. CISAP - 3rd International Conference on Safety & Environment in Process Industry, 11-14.

Panchal D. R. (2014) Study of Various Parameters on Design of Compressor Shelter. International Journal of Engineering Research & Technology (IJERT). Vol. 3 Issue 6. ISSN: 2278-0181.

Pekalski A. A., Zevenbergen J. F., Lemkowitz S. M., Pasman H. J. (2005) A Review Of Explosion Prevention And Protection Systems Suitable As Ultimate Layer Of Protection In Chemical Process Installations. 2005 Institution of Chemical Engineers. Process Safety and Environmental Protection, vol. 83(B1): 1–17.

Piping Engineering (2018) Compressor Shelters: Introduction, Layout, Types, Sizing. [online] Available at: http://www.piping-engineering.com/compressor-shelters-introduction-layout-types-sizing.html [cited: 8.4.2019].

Ponchaut N. F., Colella F., Marr K. C. (2016) Vapor Clouds. Book: Hurley M. J. (2016) SFPE Handbook of Fire Protection Engineering. Society of Fire Protection Engineers 2016, Springer, Fifth edition, vol. 3, ISBN: 978-1-4939-2564-3: 2664-2704.

Pöyry (2018) Seurausanalyysit. [online] Available at: https://www.poyry.fi/sites/www.poyry.fi/files/media/related_material/seurausanalyysit_esite.pdf [cited: 16.7.2019].

Raiko R., Kurki-Suonio I., Saastamoinen J., Hupa M. (1995) Poltto ja palaminen. International Flame Research Foundation (IFRF) – Suomen kansallinen osasto. Teknillisten Tieteiden Akatemia (TTA): 27-35.

Rembe (2019) Conventional Explosion Venting With Explosion Vents [online] Available at: https://www.rembe.com/products/explosion-safety/explosion-vents/ [cited: 26.2.2019].

Salomäki S., Liimatainen J., Kononen H. (2005) Onnettomuustutkintaraportti. Kuivaimen räjähdys Finnish Chemicals Oy:n pulveritehtaalla. Dnro 4381/06/2005

Salvado F. C., Tavares A. J., Teixeira-Dias F., Cardoso J. B. (2017) Confined explosions: The effect of compartment geometry. Journal of Loss Prevention in the Process Industries, vol. 48: 126-144.

Saxholm S., Rantanen M. (2011) Paineen mittaus. Mikes Metrologia. Mittatekniikan keskus: 41.

Schiavetti M., Pini T., Carcassi M. (2018) The effect of venting process on the progress of a vented deflagration. International Journal of Hydrogen Energy: 1-9.

Sharma R. K., Gurjar B. R., Wate S. R., Ghuge S. P., Agrawal R. (2013) Assessment of an accidental vapour cloud explosion: Lessons from the Indian Oil Corporation Ltd. accident at Jaipur, India. Journal of Loss Prevention in the Process Industries, vol. 26: 82-90.

Skjold T., Souprayen C., Dorofeev S. (2018) Fires and explosions. Progress in Energy and Combustion Science, vol. 64: 2-3.

Suits B. H. (2019) Physics of Music – Notes. [online] Physics Department, Michigan Technology University (1998-2019). Available at: https://pages.mtu.edu/~suits/SpeedofSoundOther.html [cited: 6.6.2019].

Tauseef S. M., Rashtchian D., Abbasi T., Abbasi S. A. (2011) A method for simulation of vapour cloud explosions based on computational fluid dynamics (CFD). Journal of Loss Prevention in the Process Industries, vol. 24: 638-647.

Tobashi R., Kawamura S., Kuwana K., Nakayama Y. (2011) Consequence analysis of blast wave from accidental vapour cloud explosions. Proceeding of the Combustion Institute, vol. 22: 2295-2301.

Tu J., Yeoh G., Liu C. (2013) Computational Fluid Dynamics: A Practical Approach (2nd edition). ISBN: 978-0-08-098243-4: 1-29.

Työterveyslaitos (2017) OVA-ohje: Vety. ttl. [online] Available at: http://www.ttl.fi/ova/vety.html [cited: 28.1.2019].

Witlox H. W. M. (2010) Overview of Consequence Modelling In the Hazard Assessment Package PHAST. DNV Software, London, UK. ResearchGate.

Zalosh R. (2016) Flammable vapour cloud and Vapor Explosions. Book: Hurley M. J. (2016) SFPE Handbook of Fire Protection Engineering. Society of Fire Protection Engineers 2016, Springer, Fifth edition, vol. 3, ISBN: 978-1-4939-2564-3: 2664-2704.

Zhang Y., Cao Y., Ren L., Liu X. (2018) A new equivalent method to obtain the stoichiometric fuel-air cloud from the inhomogeneous cloud based on FLACS-dispersion. Theoretical & Applied Mechanics Letters, vol. 8: 109-114.

Zhu C., Zhu J., Wang L., Mannan M. S. (2017) Lessons learned from analyzing a VCE accident at a chemical plant. Journal of Loss Prevention in the Process Industries, vol. 50: 397-402.

APPENDIX 1: TESTING OF A DIFFERENT CELL SIZES IN COMPUTATIONAL MESH

During this study the affection of a computational mesh cell size to the hydrogen VCE results were tested with three different cell sizes. This modelling test was performed to a Model1 in which the blockage ratio was formed from compressor shelter and the equipment inside (see section 6.1.1). According to Gexcon AS (2018) guidance, a finer computational mesh for reactive gas (such as hydrogen) is recommended. However, the capacity of the computer has to be taken into account, as a computing network with more than one to two million cells can have a very long simulation time. A total of three hydrogen gas explosion test simulations were performed, with a cell size of 1.0 metres for the scenario1, 1.5 metres for the scenario2 and 2.0 metres for the scenario3 computing network.

The test was performed to Model1 in which the vapour cloud filled the whole compressor shelter (volume of cloud was 8200 m^3). The ignition point location was the same for all three scenarios and it can be seen from Figure 1 together with vapour cloud. The total volume of computational domain in scenarios was the same as in Model1 (8,219,160 m^3).

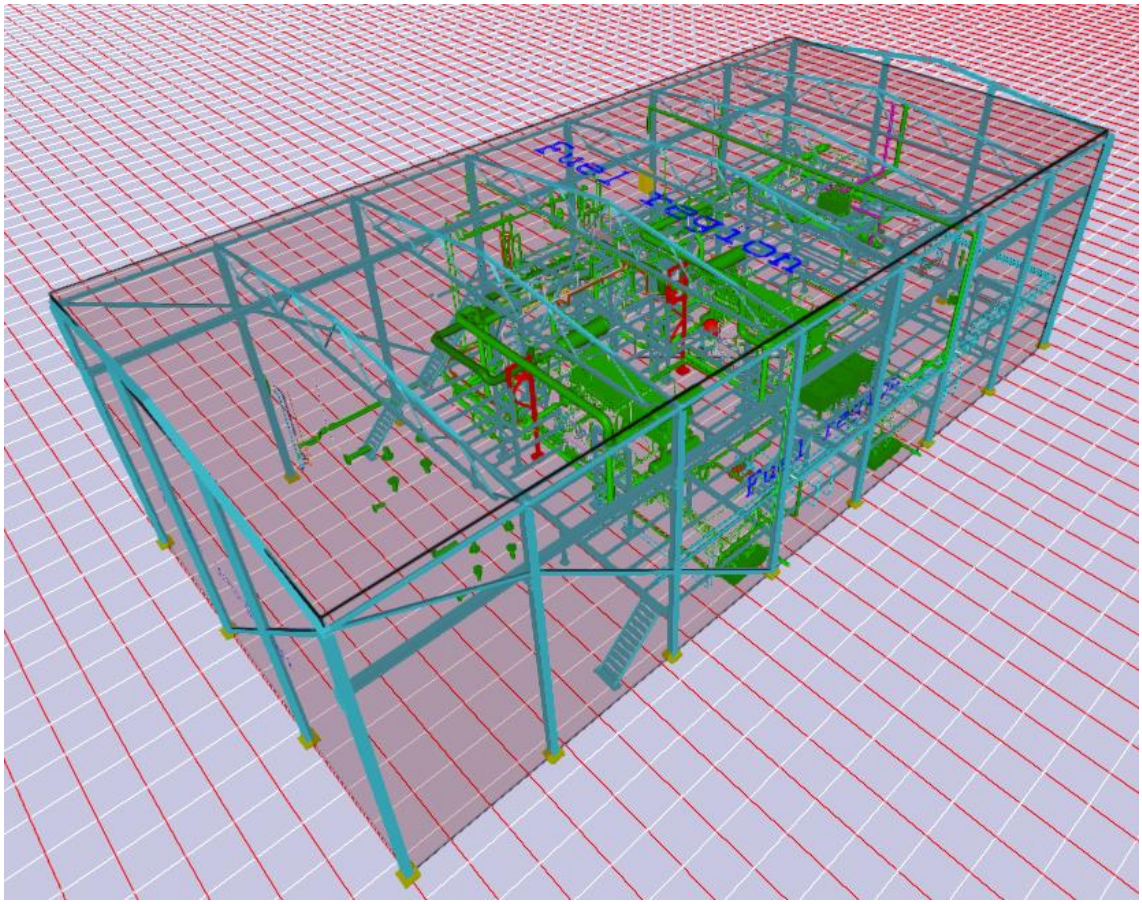

Figure 1. Testing modelling area (Scenario2 in which mesh size is 1.5 metres).

The overpressures and pressure impulses were examined through four monitor points located in the compressor shelter (same points as in section 6.2.1.). The cell sizes between the different scenarios were selected according to the recommended cell size for this study being 1.5 metres. According to that cell size 0.5 metres smaller and bigger cell sizes were chosen. A cell size of 1 metre (Scenario1) is recommended value for modelling gas explosion containing reactive gases with fast flame speed such as hydrogen as "*the fast flames may generate pressure gradients in the flame front which also should be resolved"* (Gexcon AS 2018). However, in this study, with a 1 metre cell size the computational mesh would contain over 3 million cells, which is resulting in a very heavy modelling file. For Model1, the simulation time can be relatively fast because the volume

blockage ratio is relatively low, but for example for Model2 the simulation time can be already very long. A cell size of 1.5 metres is therefore a better alternative than 1 metre. The number of mesh cells decreased significantly (1-2 million) and the simulation time was significantly reduced. A cell size of 2 metres was selected for comparison of the results. A cell size of 2 metres is not recommended because it is no longer able to take into account at the same accuracy as with the smaller cell sizes the flame velocity and thus the overpressure that is generated are more indicative value. A Table 1 lists for three scenarios a total volume of a computational domain, blocked volume of a calculation domain and initial fuel, which FLACS calculates at the very beginning of the simulations and which determine the severity of the explosion.

Table 1. Properties calculated in FLACS in different scenarios which affects to the explosion results.

Parameter	Scenario1	Scenario2	Scenario3
Total volume of a calculation domain [m^3]	8,219,160	8,219,160	8,219,160
Blocked volume of a calculation domain [m^3]	314	424	530
Initial fuel [kg]	205	202	204

As seen from Table 1 the blocked volume of a calculated domain is different for each scenario. With a larger cell size the blocked volume is increasing. With an initial fuel it is not that straightforward. The initial fuel was not seemed to differ that much even though the blocked volume increased significantly. In Figure 2 the comparison of overpressure peaks of the three different scenarios are shown.

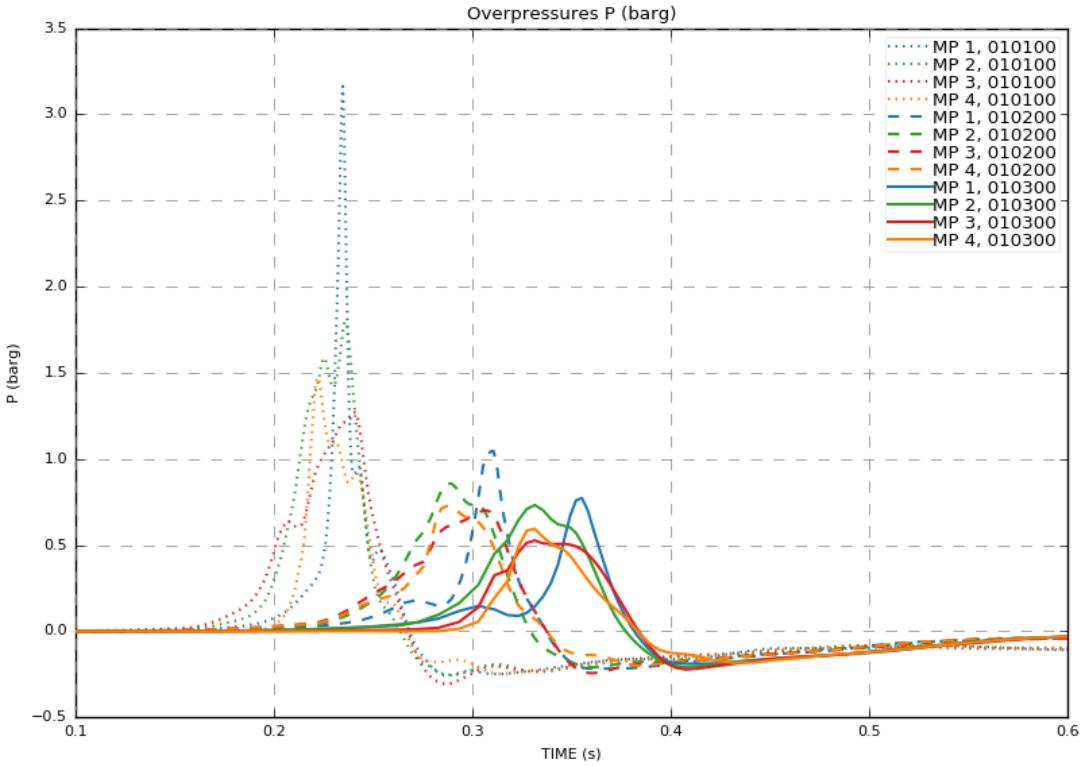

Figure 2. Overpressures in different Scenarios. Dotted lines (010100) = Scenrio1, Dashed lines (010200) = Scenario2, and Solid lines (010300) = Scenario3.

As seen from Figure 2, the cell size of computational mesh affects significantly to the occurring time of explosion as well as to formed values of overpressure peaks. It is essential to take into account that with a smaller cell sized mesh it is possible that the results can be over predicted (Gexcon AS 2018). When comparing the overpressure results in Figure 47 it is seemed that in MP1 the overpressure peak is over predicted. The MP1 peak in other two scenarios is also giving the highest peak values but the difference with other monitor points are less. If ignored the MP1 of Scenario1, it is seemed that the overpressure values are almost exponentially decreasing as the cell size of computational mesh increasing. The start time of an explosion also delays as the cell size increases. With the test results obtained, it can be said that the cell size of a computational mesh is affecting significantly to the simulation results and the differences between cell sizes are notable.

APPENDIX 2: COMPARISON OF AN EQUIVALENT STOICHIMETRIC GAS CLOUDS Q8 AND Q9

In Appendix 2 the comparison of equivalent stoichiometric vapour cloud was compared with each other. The comparison was performed to Model2. Figure 3 shows the differences between the volume sizes of a two different cloud type.

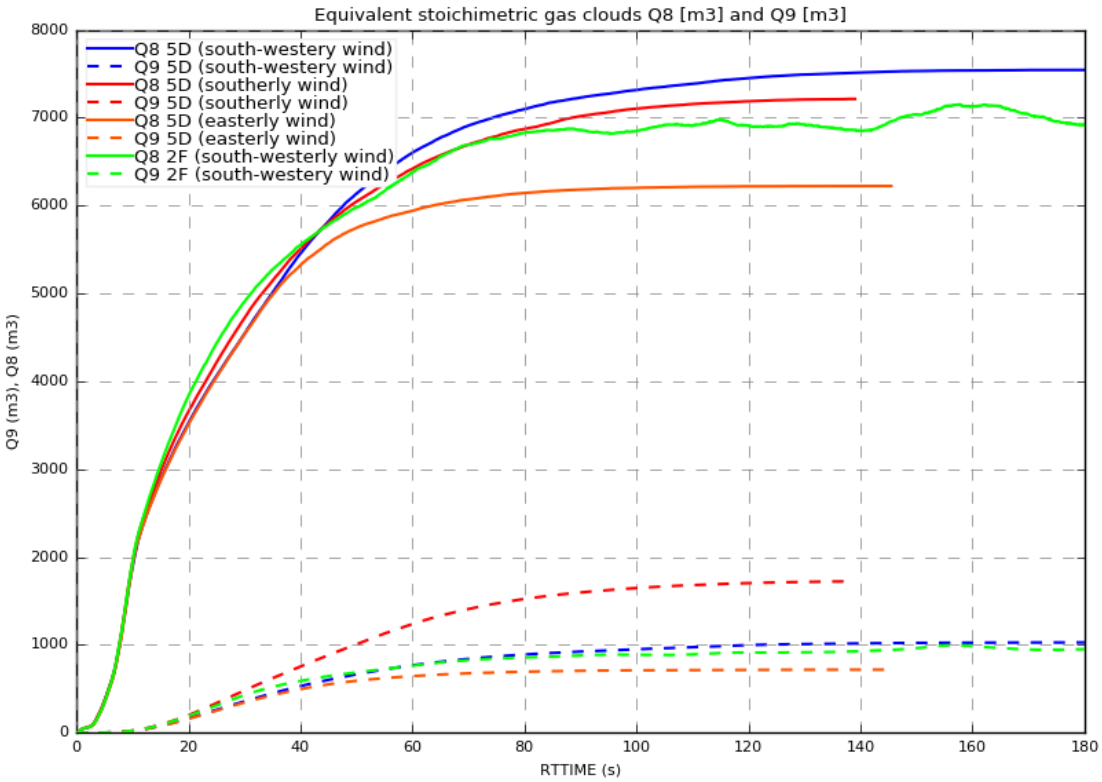

Figure 3. Volume-time plot of an equivalent stoichiometric vapour clouds. Solid lines represent the Q8 cloud type and dashed lines represents the Q9 cloud type.

As seen from Figure 3 the differences between the cloud volumes are very significant. In both cloud types the volume curves at different weather conditions stabilized approximately at the same time. However, the maximum cloud sizes for Q8 and Q9 clouds were obtained in different weather types. In Q8 the maximum value (7500 m^3) was obtained in 5D south-westerly wind direction and in Q9 the maximum value (1700 m^3) was obtained in 5D southerly wind direction. The major difference in these two cloud types is that in Q8 equivalent stoichiometric vapour cloud takes into account volume expansion of vapour cloud and in Q9 type also the laminar burning velocity is

taken into account. With the obtained maximum volumes, the following clouds were applied to modelling (see Figure 4).

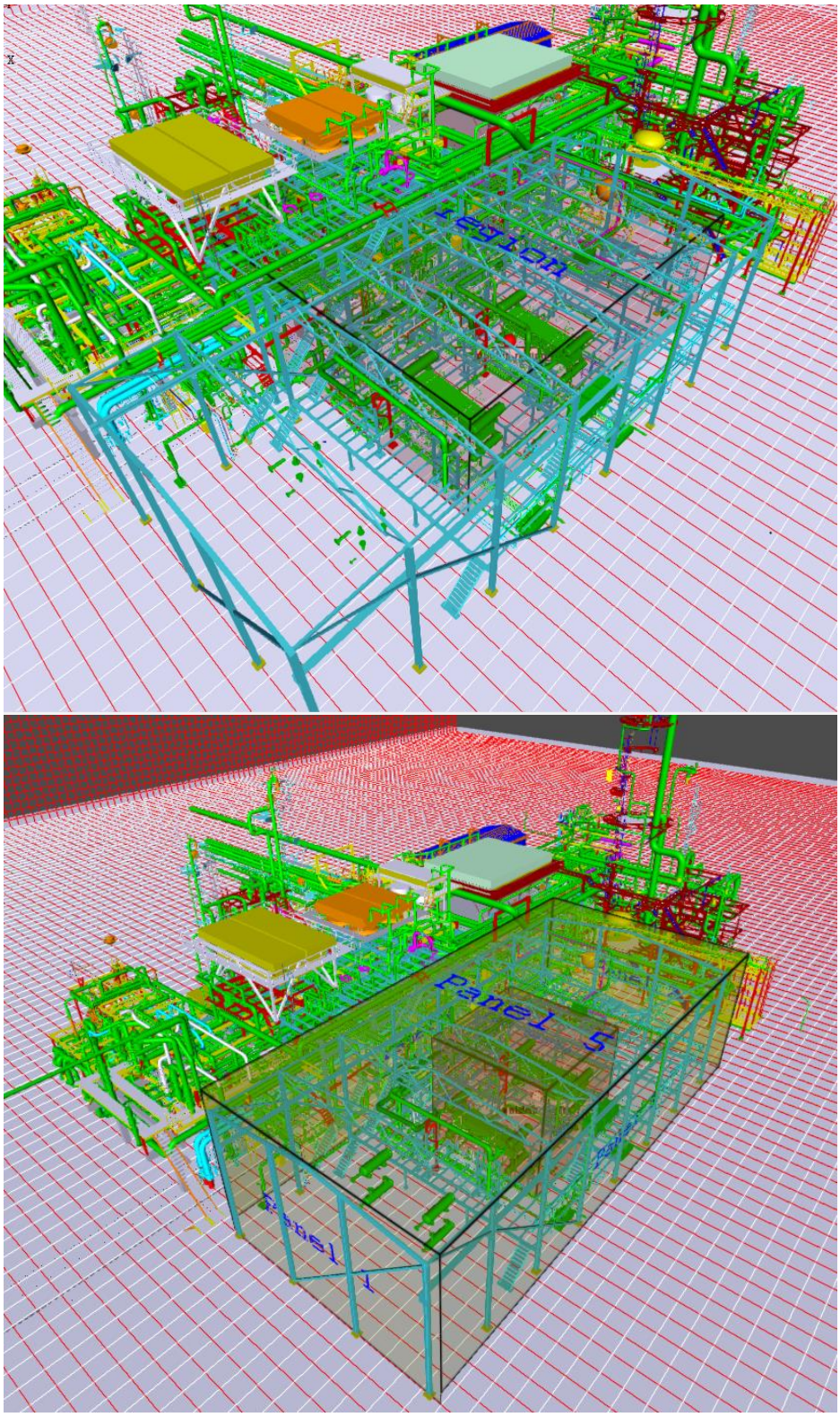

Figure 4. Q8 vapour cloud (a) and Q9 vapour cloud (b) for Model2.

The total volume of a calculation domain was for both scenarios the same (7,959,060 m^3) in which the blocked volume was 66,150 m^3. The major differences between these two models which affected majorly to the resulted overpressure peaks were the amount of the initial fuel. Since FLACS calculates the initial fuel by multiplying density with available volume the amount of flammable hydrogen is significantly lower in Q9 than it is in Q8. For Q8 the initial fuel amount was *186 kg* and in Q9 the amount was *only 24 kg*. This affection can be seen from the resulted overpressure peaks and pressure impulses shown in Figure 5.

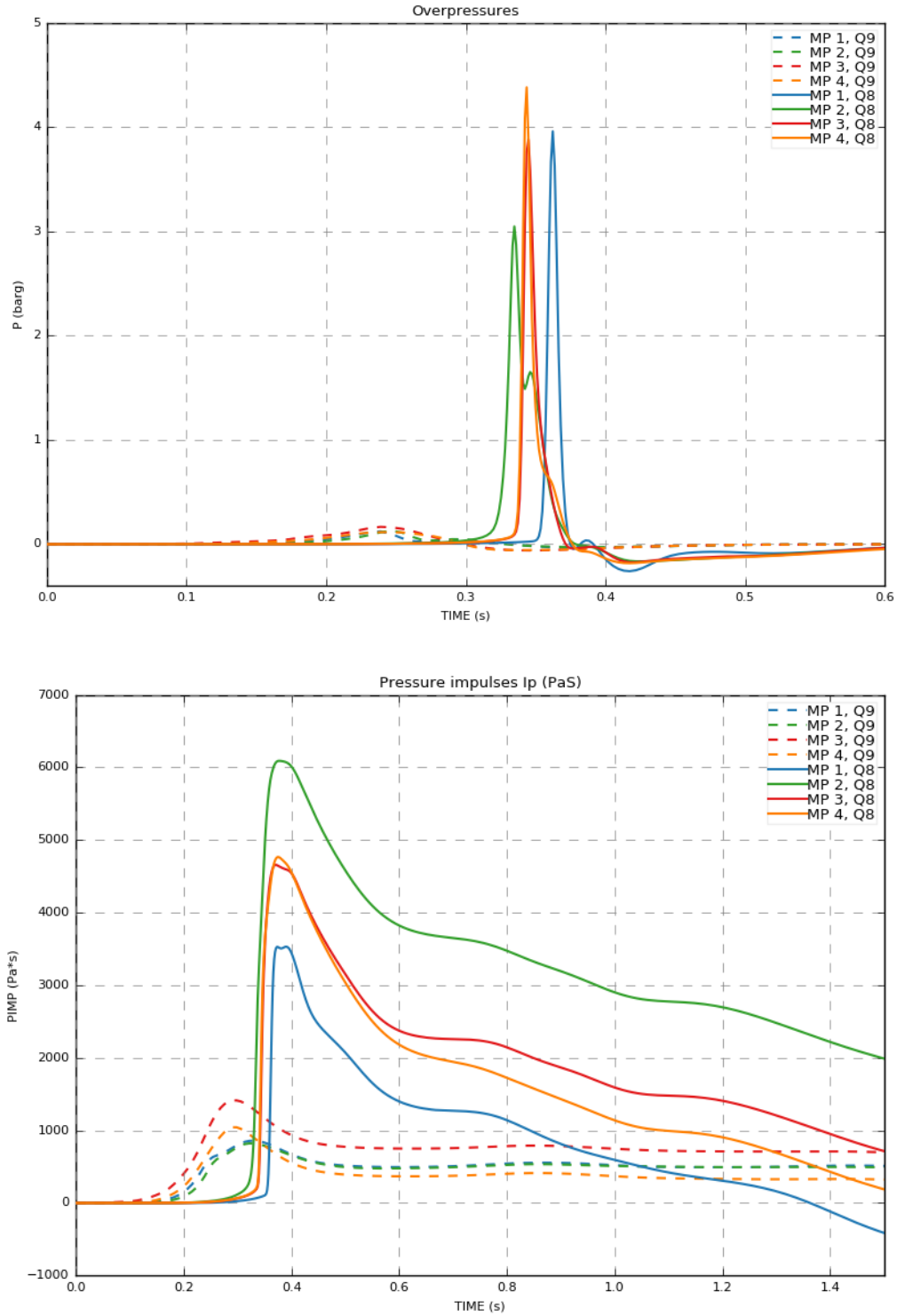

Figure 5. Comparison of Q8 and Q9 overpressures (1) and pressure impulses (2).

The overpressure peaks and pressure impulses were measured in monitor points located inside the compressor shelter (same as in section 6.2.1). The ignition points were the same for both scenarios.

It is seen from Figure 5 that the overpressure peaks in Q9 scenarios occurred a slightly earlier than in Q8 scenario. The overpressure peaks were very small (less than 0.5 bar(g)) and did not represent the values which were expected for the Model2 very congested area. The Q9 cloud was not enough conservatives for this study as Q8 cloud and after revision with Gexcon it was decided that more suitable vapour cloud type for this study was Q8 cloud.

APPENDIX 3: VOLUME FRACTIONS FOR MODEL1, MODEL2 AND MODEL3

Hydrogen vapour cloud dispersion in time for Model1 (volume fraction 4-22 vol-%) with 2F weather condition and easterly wind direction

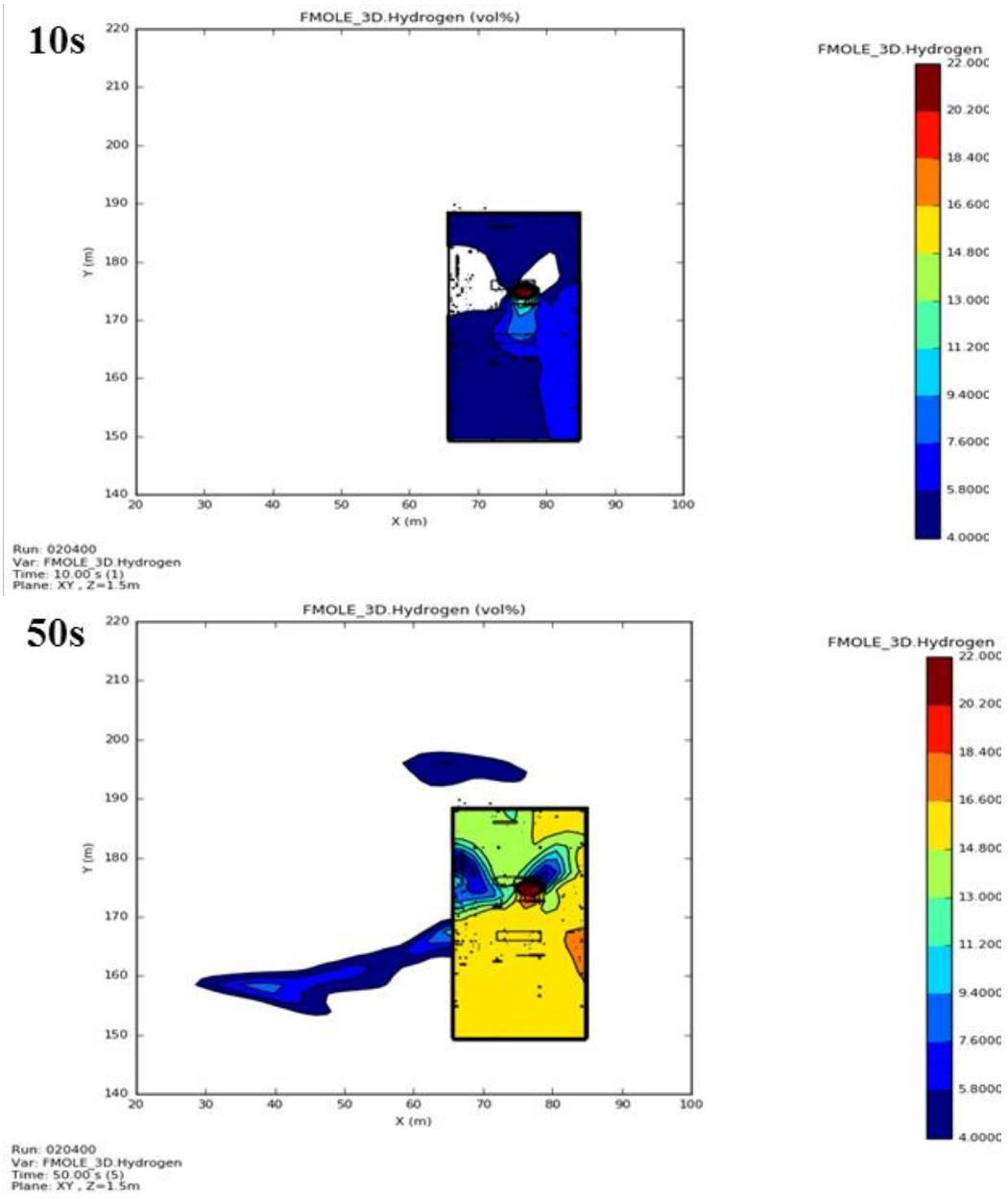

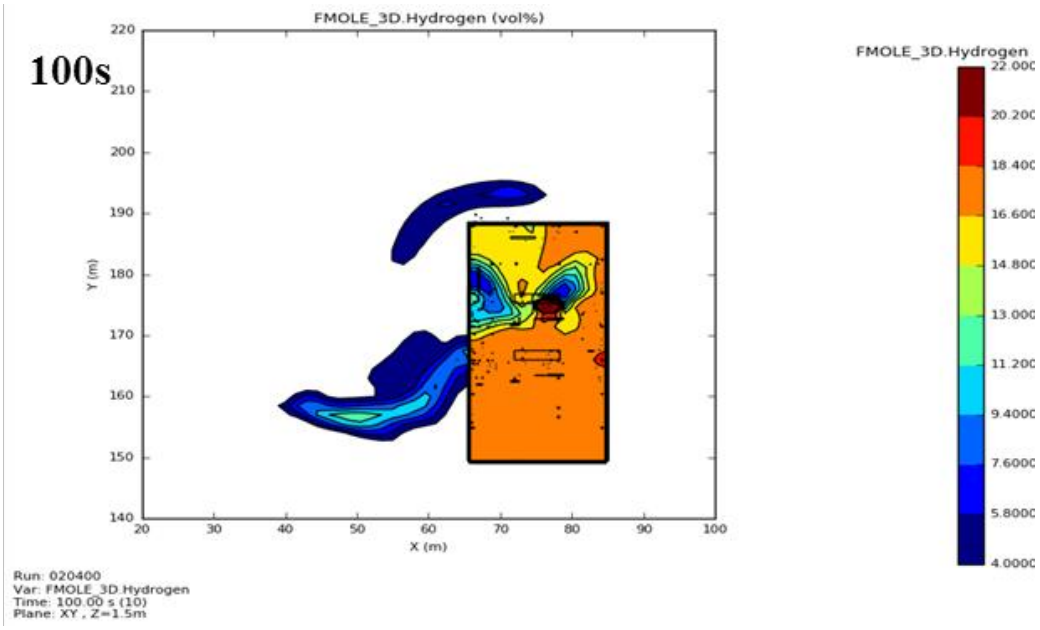
100s
FMOLE_3D.Hydrogen (vol%)
Y (m)
X (m)
FMOLE_3D.Hydrogen
Run: 020400
Var: FMOLE_3D.Hydrogen
Time: 100.00 s (10)
Plane: XY , Z=1.5m

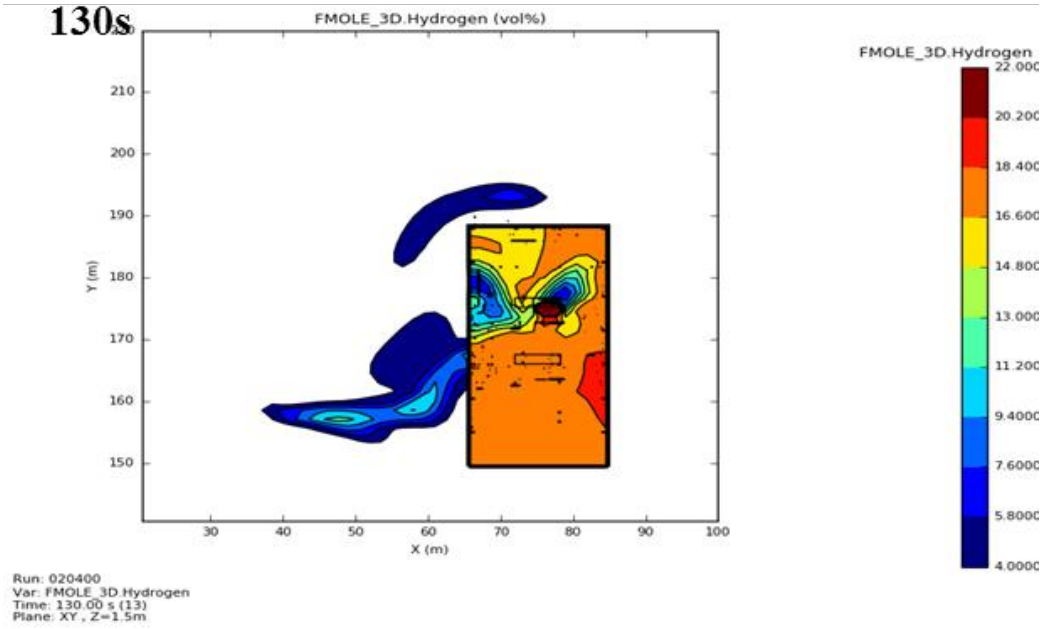
130s
FMOLE_3D.Hydrogen (vol%)
Y (m)
X (m)
FMOLE_3D.Hydrogen
Run: 020400
Var: FMOLE_3D.Hydrogen
Time: 130.00 s (13)
Plane: XY , Z=1.5m

160s

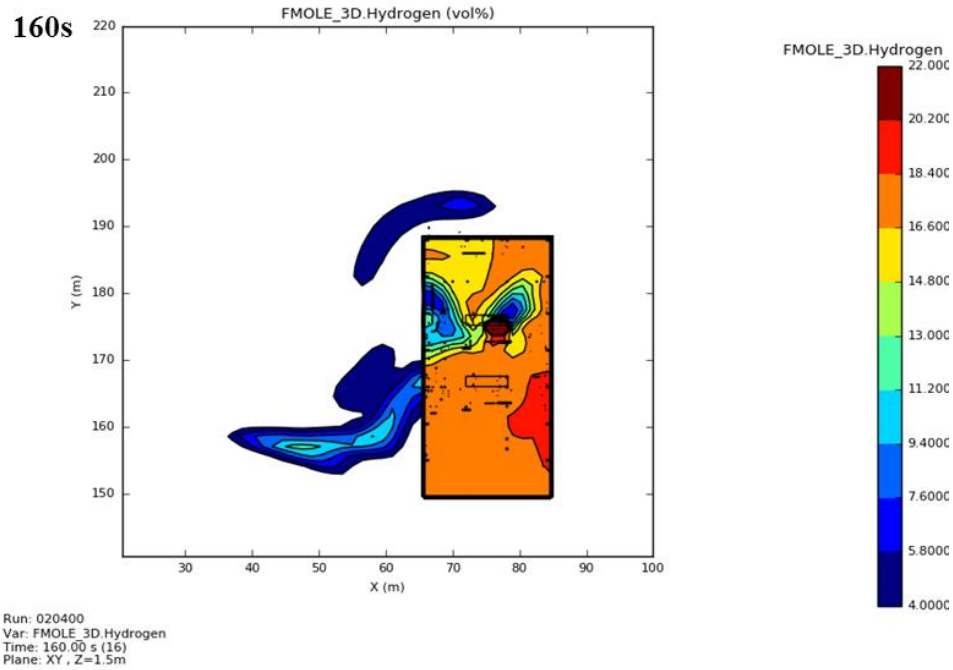

Run: 020400
Var: FMOLE_3D.Hydrogen
Time: 160.00 s (16)
Plane: XY , Z=1.5m

180s

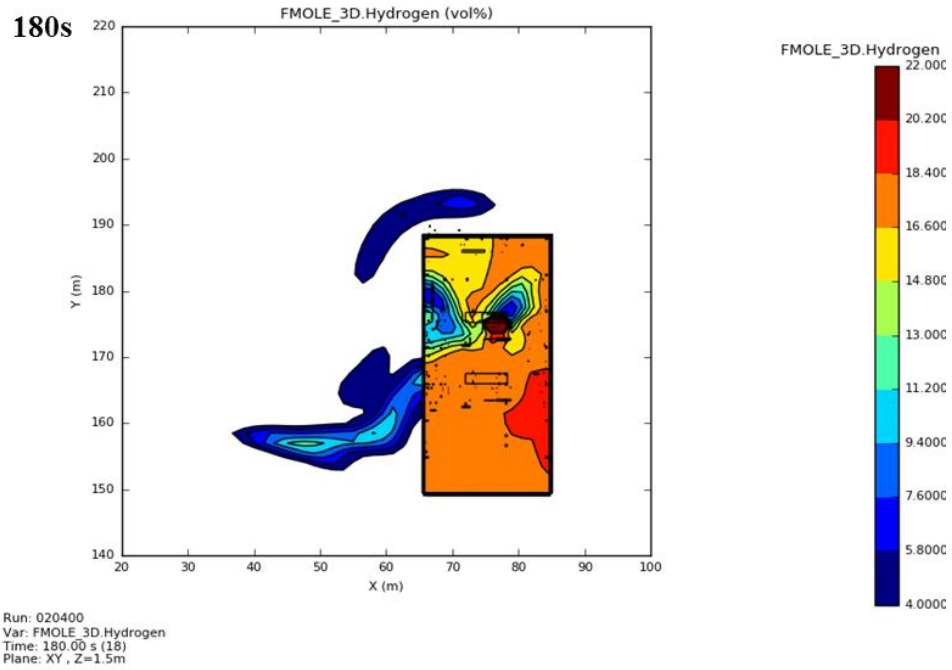

Run: 020400
Var: FMOLE_3D.Hydrogen
Time: 180.00 s (18)
Plane: XY , Z=1.5m

Hydrogen vapour cloud dispersion in time for Model2 (volume fraction 4-22 vol-%) with 5D weather condition and south-westerly wind direction

10s

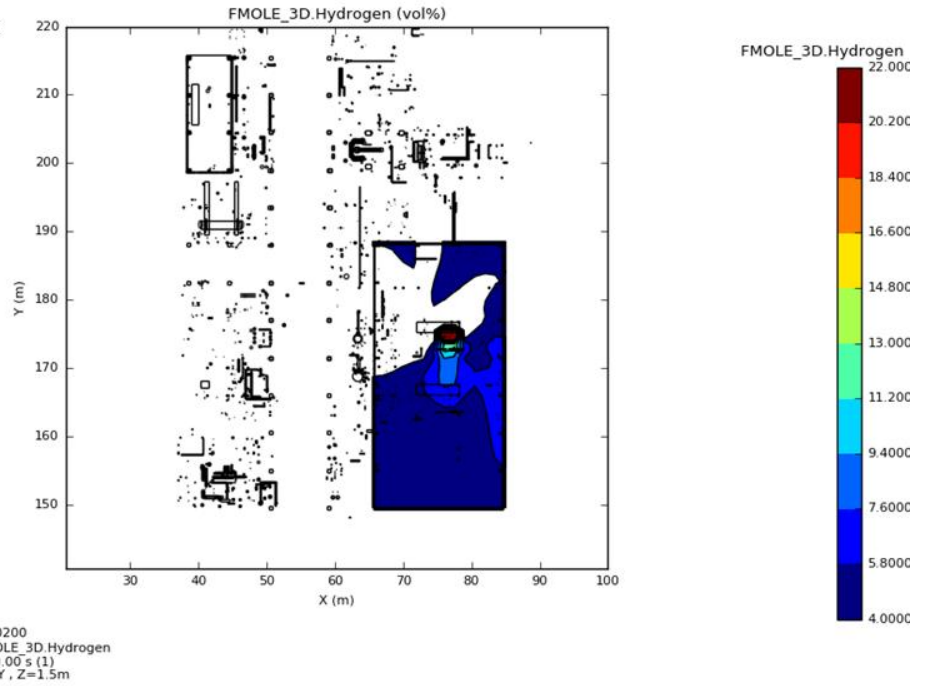

50s

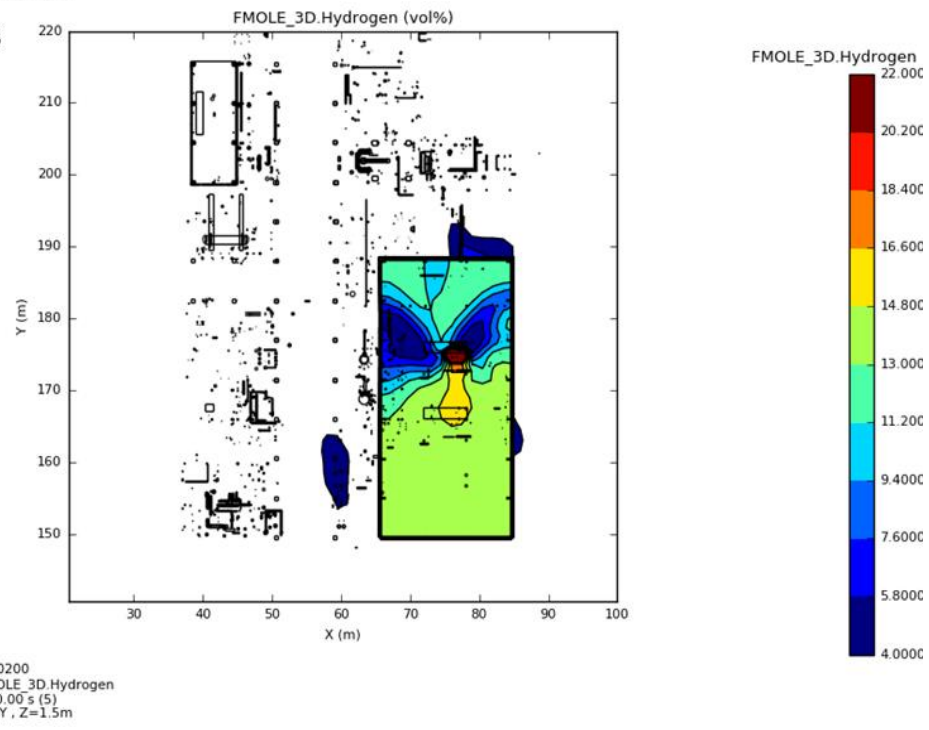

100s

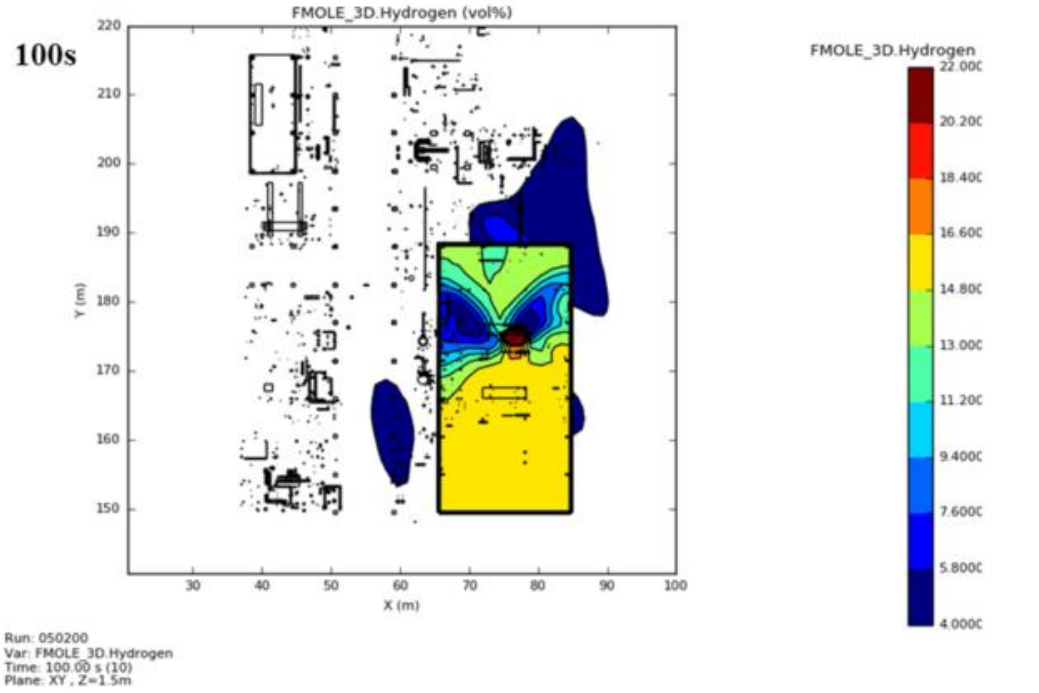
FMOLE_3D.Hydrogen (vol%)
Y (m)
X (m)
FMOLE_3D.Hydrogen
22.00
20.20
18.40
16.60
14.80
13.00
11.20
9.400
7.600
5.800
4.000
Run: 050200
Var: FMOLE_3D.Hydrogen
Time: 100.00 s (10)
Plane: XY , Z=1.5m

130s

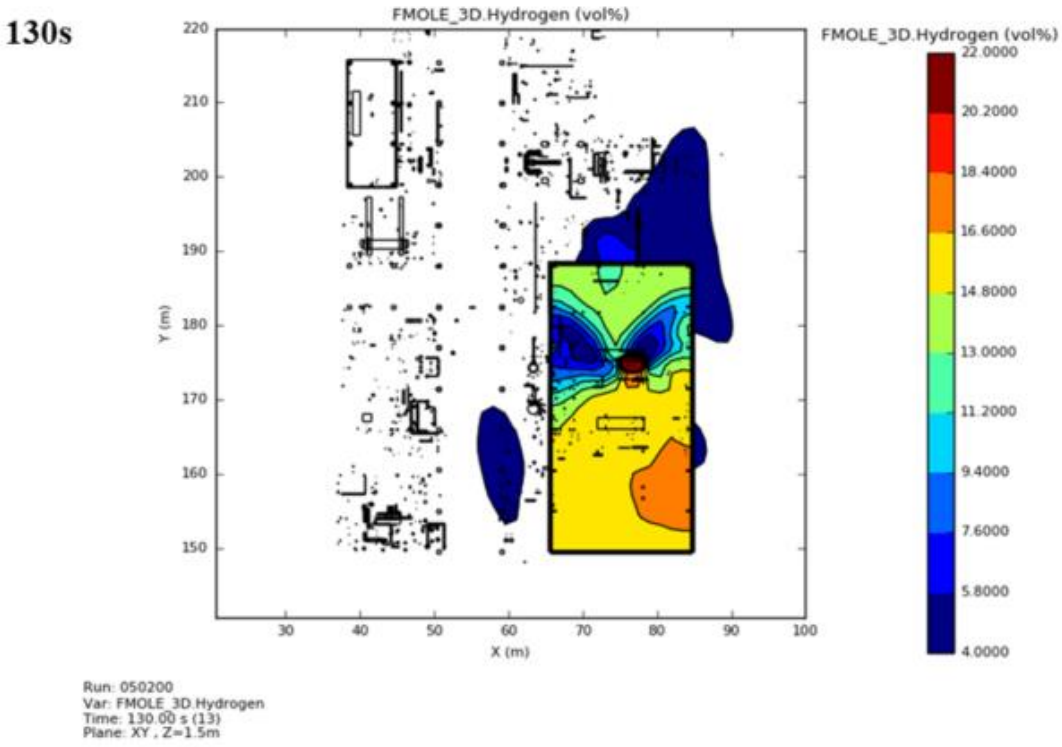
FMOLE_3D.Hydrogen (vol%)
Y (m)
X (m)
FMOLE_3D.Hydrogen (vol%)
22.0000
20.2000
18.4000
16.6000
14.8000
13.0000
11.2000
9.4000
7.6000
5.8000
4.0000
Run: 050200
Var: FMOLE_3D.Hydrogen
Time: 130.00 s (13)
Plane: XY , Z=1.5m

Hydrogen vapour cloud dispersion in time for Model3 (volume fraction 4-22 vol-%) with 5D weather condition and south-westerly wind direction

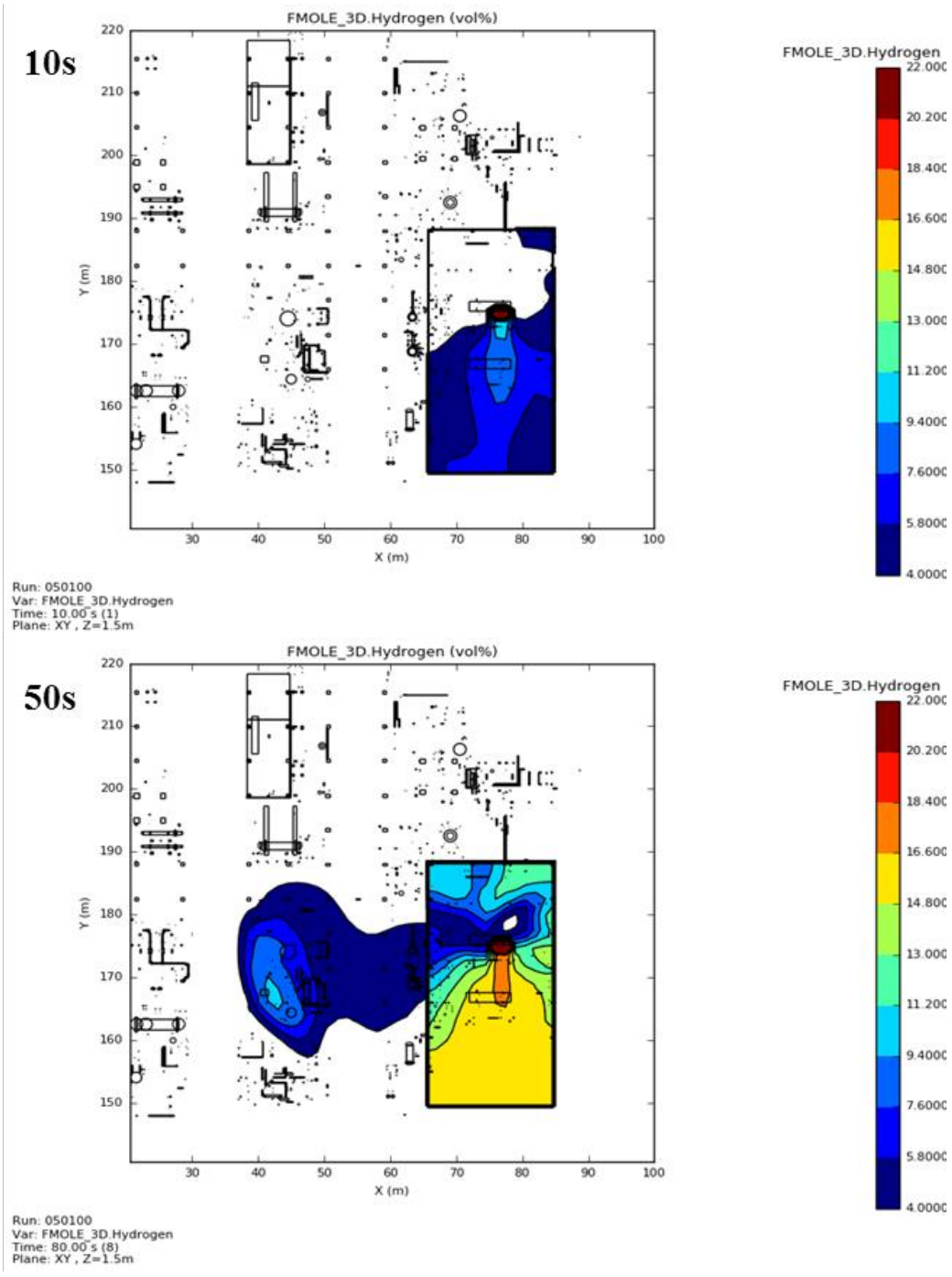

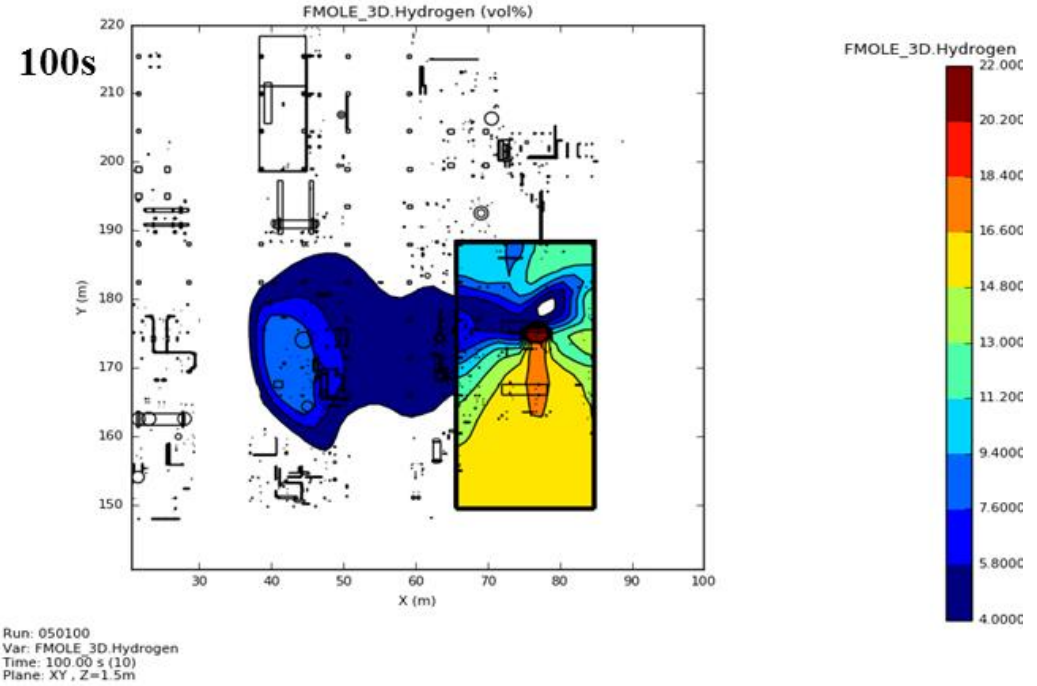
100s
FMOLE_3D.Hydrogen (vol%)
Y (m)
X (m)
FMOLE_3D.Hydrogen
Run: 050100
Var: FMOLE_3D.Hydrogen
Time: 100.00 s (10)
Plane: XY , Z=1.5m

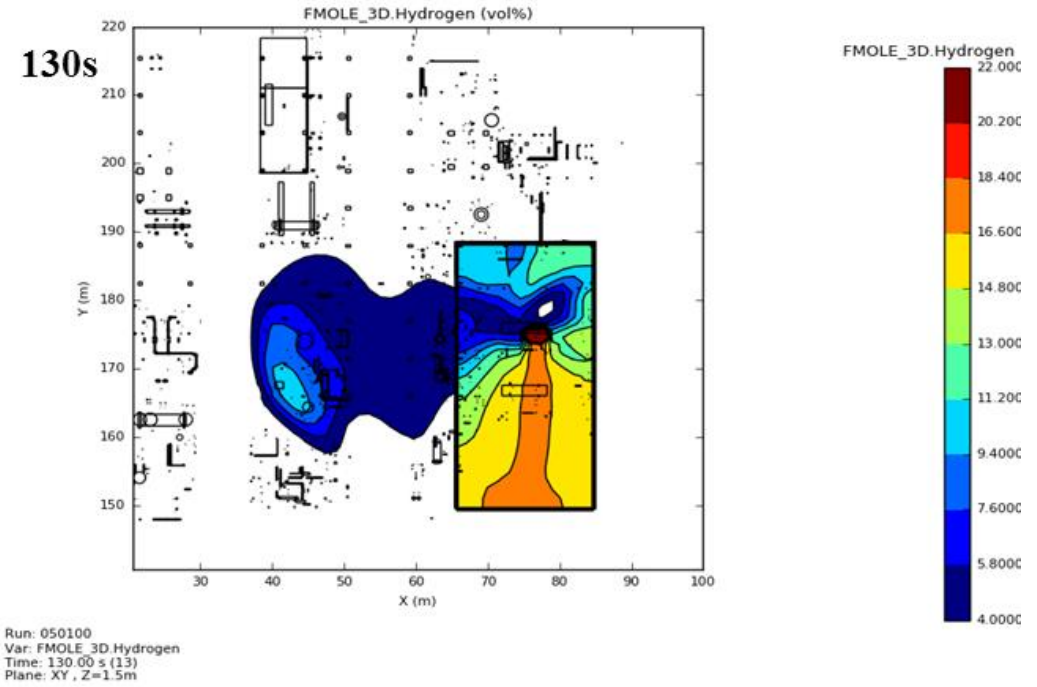
130s
FMOLE_3D.Hydrogen (vol%)
Y (m)
X (m)
FMOLE_3D.Hydrogen
Run: 050100
Var: FMOLE_3D.Hydrogen
Time: 130.00 s (13)
Plane: XY , Z=1.5m

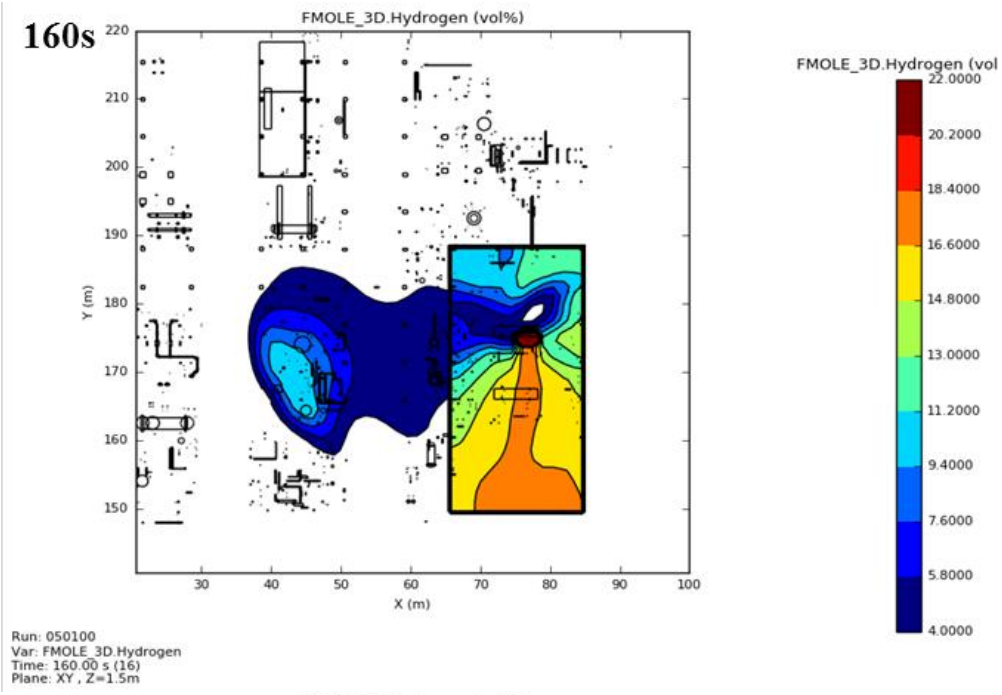
160s
FMOLE_3D.Hydrogen (vol%)
Y (m)
X (m)
FMOLE_3D.Hydrogen (vol
22.0000
20.2000
18.4000
16.6000
14.8000
13.0000
11.2000
9.4000
7.6000
5.8000
4.0000
Run: 050100
Var: FMOLE_3D.Hydrogen
Time: 160.00 s (16)
Plane: XY , Z=1.5m

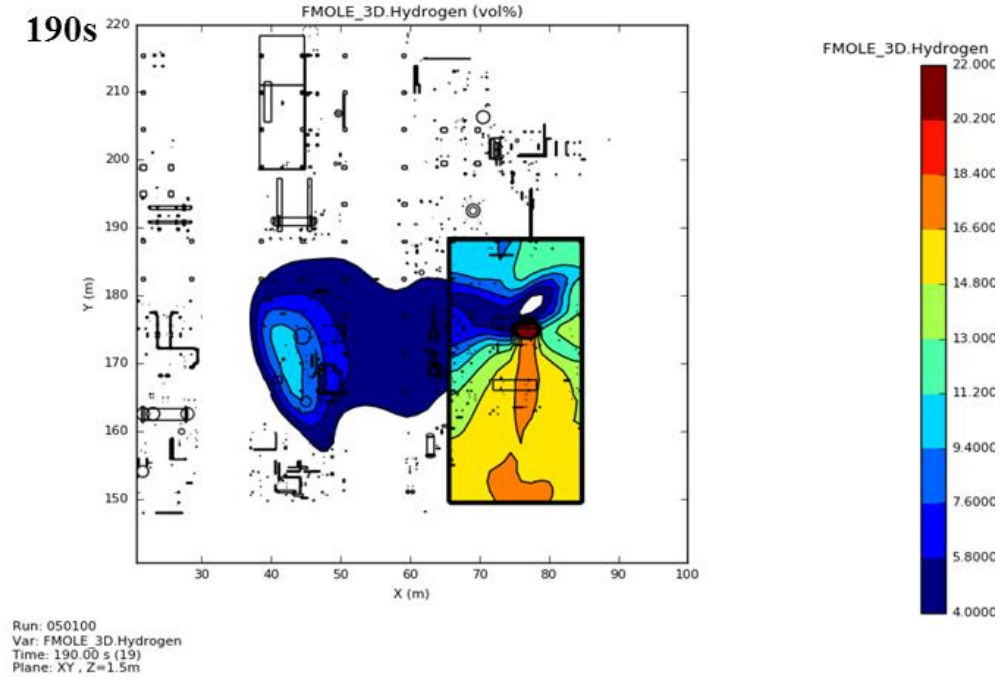
190s
FMOLE_3D.Hydrogen (vol%)
Y (m)
X (m)
FMOLE_3D.Hydrogen
Run: 050100
Var: FMOLE_3D.Hydrogen
Time: 190.00 s (19)
Plane: XY , Z=1.5m

APPENDIX 4: IGNITION POINT LOCATIONS IN DIFFERENT MODELS

In this study, a total of three different scenarios were performed for each explosion models with varying ignition points. The locations of the ignition points were used to determine how the location affects the flame acceleration and thus the pressures generated. The following sections consider the ignition points for the different models.

Model1 – Compressor shelter

For Model1, the locations of the ignition points were slightly different from Model2 and Model3 because the size and location vapour cloud of Model1 was different (located entirely in the compressor shelter). The Model1 was best suited for the studying of the effects of room shape. The locations of the Model1 ignition points are shown in Figure 6.

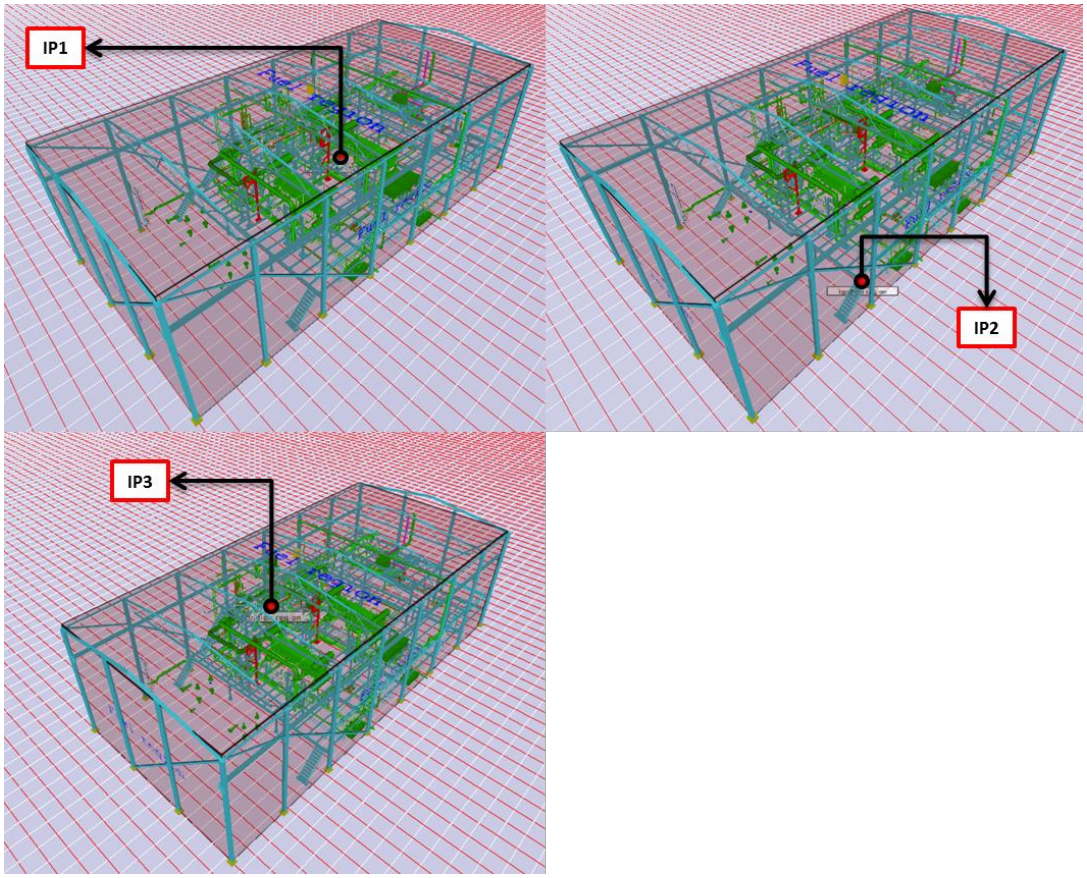

Figure 6. Location of ignition points (IP) in Model1.

The IP1 location was close to a leaking compressor (at about 1 metre height), the IP2 location was near the cloud edge and the IP3 location was quite in the centre of the compressor shelter, at approximately 4 metres height. The effect of the locations is seen in the measured overpressures as shown in Figure 7.

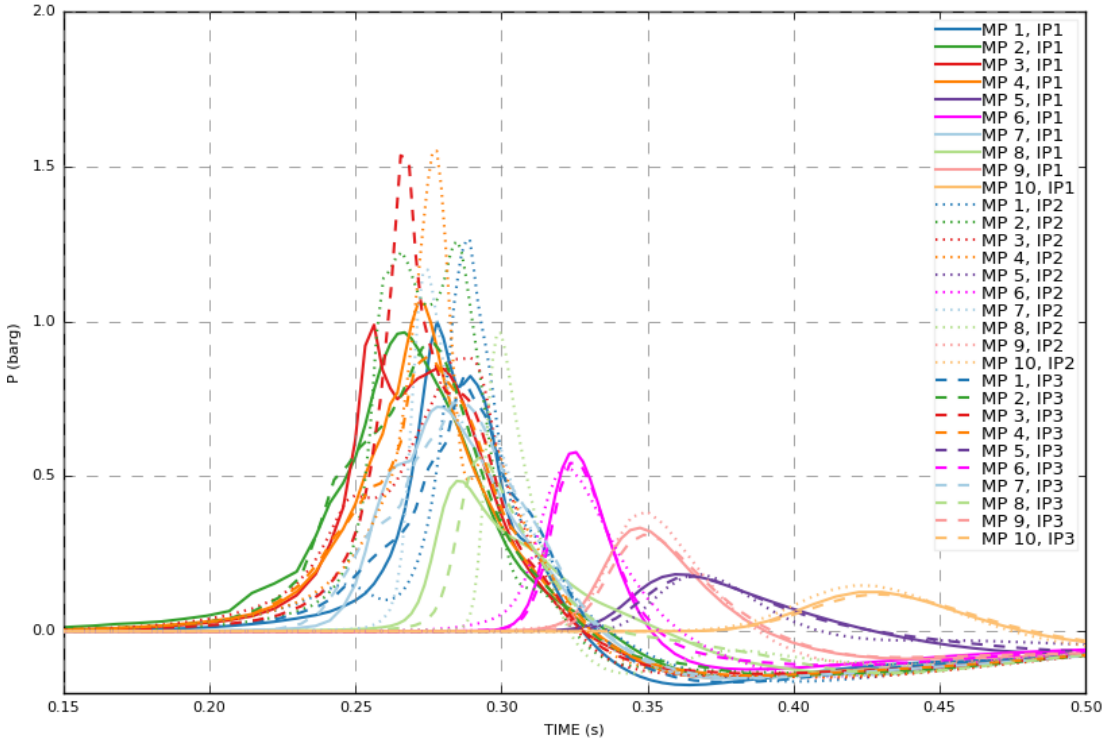

Figure 7. Overpressures for different monitor points in different IPs. IP1= solid line, IP2 = dotted line and IP3 = dashed line.

In Figure 7, the overpressures were viewed through 10 different monitor points. The results show that the highest values are achieved in IP2 in monitor point MP4 (1.5 bar(g)) . The overpressures measured in particular inside the compressor shelter varied greatly, simply because the flame accelerates differently depending on the location of the points. As mentioned in chapter 3.5 the flame must propagate as long as possible as a spherical form. The spherical form is more likely when the ignition point is in the centre of the vapour cloud as it forms in initial stage of the explosion when the flame front has not “wrinkled”. In addition, IP2 is located in a way that the flame front is significantly longer compared with the flame front from IP1 and IP3 resulting that the turbulence is stronger when the explosion starts from the IP2. Outside the compressor shelter, the curves of the different ignition points are more closely aligned. For Model1, IP2 was chosen as worst case scenario.

Model2 (diesel producing unit) and Model3 (total modelling area)

Model2 and Model3 are similar since the gas clouds are almost the same size and the immediate vicinity of the compressor shelter is similar in both models. For Model2 and Model3 the locations of the ignition points were the same. Figure 8 shows the ignition points for Model2.

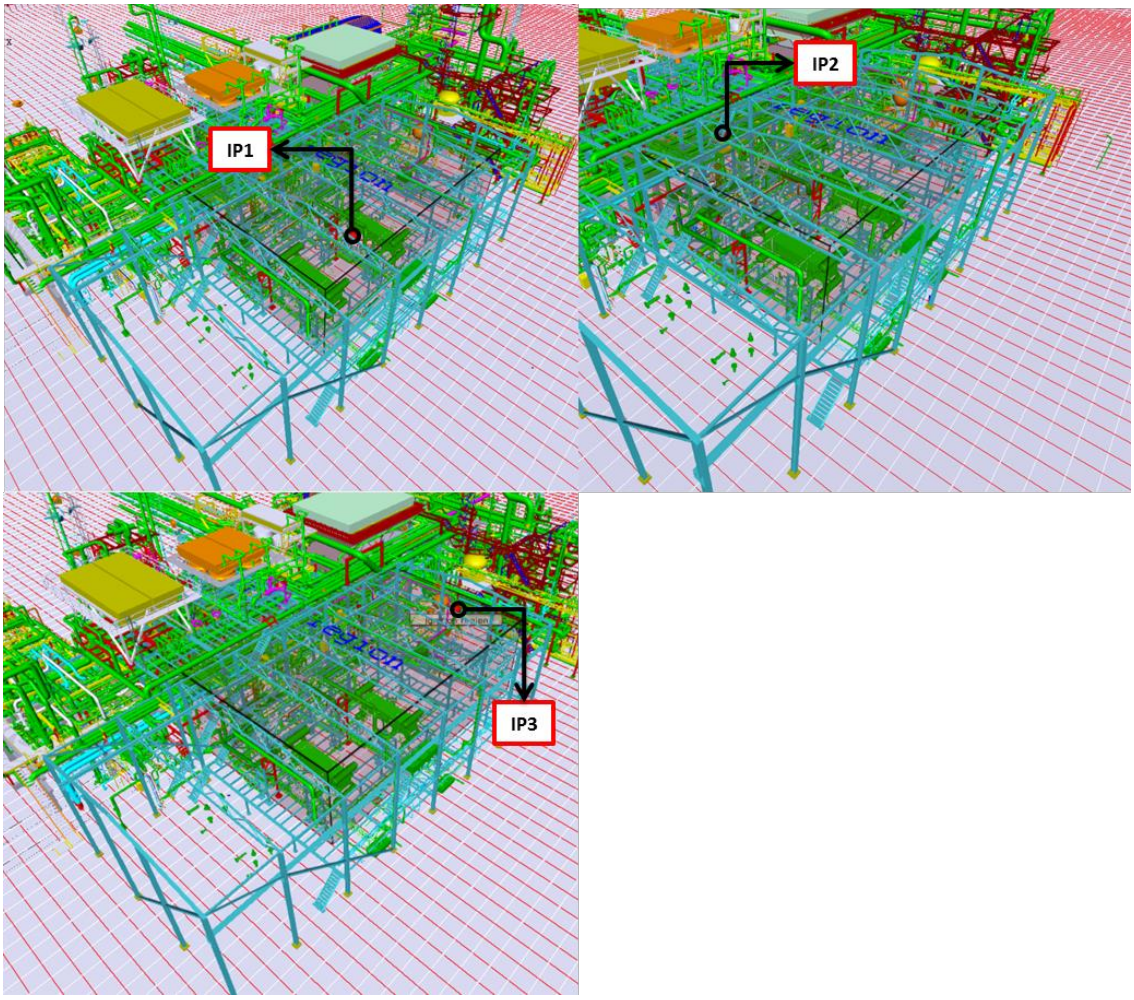

Figure 8. Location of ignition points (IP) in Model2 and Model3.

The IP2 and IP3 locations were outside the compressor shelter: the IP2 in the congested pipeline area and the IP3 at the column. The location of IP1 was inside the compressor shelter and was the same as the IP1 of Model1. The effect of the ignition point locations in Model2 and Model3 is seen in the measured overpressures as shown in Figure 9.

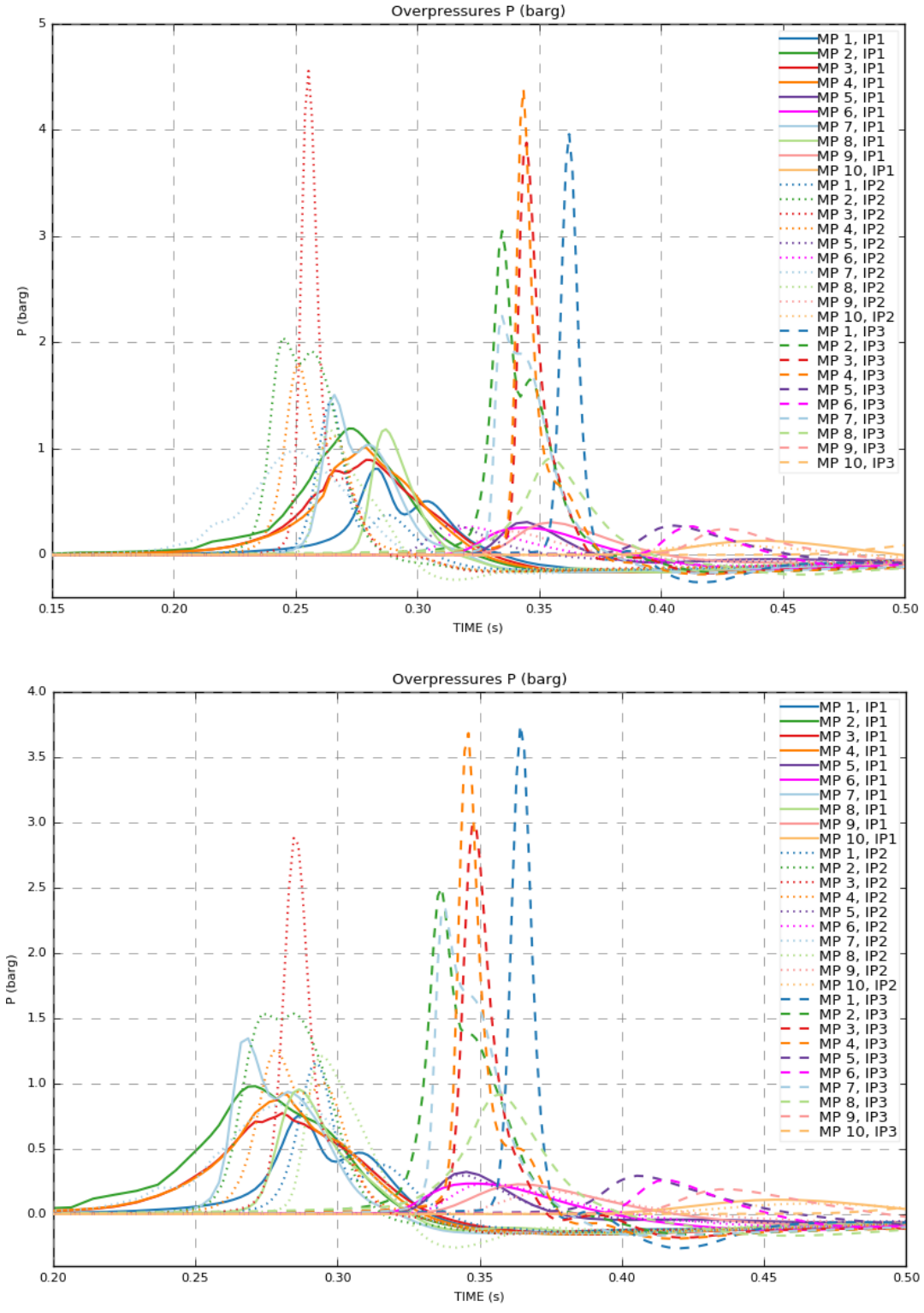

Figure 9. Overpressures for different monitor points in different ignition points (IP), Model2 (a) and Model3 (b). IP1= solid line, IP2 = dotted line and IP3 = dashed line.

For Model2 and Model3, it is seen that the overpressures formed in IP3 are greater than the overpressures formed in IP1 and IP2. The location of IP3 gives the strongest overpressure, as it is ideally located not in the most congested area, but is still surrounded by many objects that increase turbulence and give very high flame acceleration. The location of IP2 is in an 'over-congested' area where the distance is negligible, and the so-called “pocked” of unburned mixture formed between the objects is too small to cause flame acceleration. For IP1, located inside the compressor shelter, the distance between objects is too “wide” (in this context) and therefore continuous flame acceleration is high enough. For both Model2 and Model3 the IP3 was chosen to be for worst case scenario.